Synthesis of Long/Short Chain Branched Polyolefins

by

Metallocene/MAO Complexes

Dissertation

submitted to

Department of Chemistry

University of Hamburg

In partial fulfillment of the requirements

for the German academic degree

Dr. rer. nat.

Burçak Arıkan

Hamburg, 2008

1 TABLE OF CONTENTS

2 ABBREVIATION LIST

aPP	Atactic polypropylene
c	Concentration
Cp	Cyclopentadienyl
Cp*	Pentamethyl cyclopentadienyl
ChemG	Chemikaliengesetz
DEPT	Distorsionless Enhancement by Polarization Transfer
DSC	Differential scanning calorimetry
Flu	Fluorenyl
GefStoffV	Gefahrstoffverordnung
GPC	Gel permeation chromatography
h	Hour
IGated	Inverse Gated Decoupling
Ind	η^5-indenyl
iPP	Isotactic polypropylene
J	Coupling constant
K	Mark-Houwink constant
LDPE	Low Density Polyethylene
LLDPE	Linear Low Density Polyethylene
m	Mass
M	Metal
MAO	Methylaluminoxane
Me	Methyl
MMD	Molar mass distribution
M_η	Viscosimetric Molecular Weight
M_n	Number-Average Molecular Weight
M_w	Weight-Average Molecular Weight
M_w/M_n	Polydispersity
n	Mol
NMR	Nuclear Magnetic Resonance
NOE	Nuclear Overhaus Effect
P	Polymer chain

p	Pressure
PE	Polyethylene
ppm	Parts per million
Ph	Phenyl
PP	Polypropylene
R	Alkyl
sec	Secondary
sPP	Syndiotactic polypropylene
*t*Bu	Tertiary butyl
T	Polymerization temperature
T_g	Glass transition temperature
TCB	1, 2, 4-Trichlorobenzene
TEA	Triethylaluminium
T_m	Melting temperature
Tp`	Hydrotrispyrazolylborate
Tp*	Hydrotris(3,5-dimethylpyrazol-1-yl)borate
TpMe	Hydrotris(3-methylpyrazol-1-yl)borate
t_{Pol}	Polymerization time
x_E	Molar fraction of ethylene in the feed
X_E	Molar fraction of ethylene in the polymer
X_p	Molar fraction of propylene in the feed
x_p	Molar fraction of propylene in the polymer
δ	Chemical shift
η	Hapticity
α	Mark-Houwink-Constant

The Catalysts Used

3
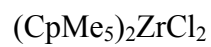
$(CpMe_5)_2ZrCl_2$

[Bis(1-η^5-pentamethyl cyclopentadienyl]-zirconiumdichloride

4

[Ph$_2$C(2,7-di-^{ter}BuFlu)(Cp)]ZrCl$_2$
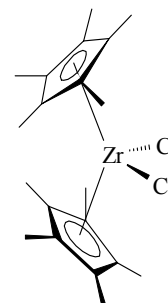
[Diphenylmethylen(2,7-bis(1,1-di-methylethyl)-9-η^5-fluorenyl)(η5-cyclopentadienyl)] zirconiumdichloride

5

Tp^{Me}CpZrCl$_2$
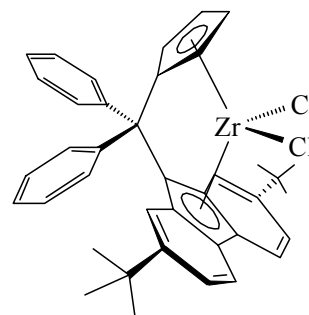
[Hydrotris(3-methylpyrazolyl)boratodichloro]cyclopentadienyl-zirconium(IV)
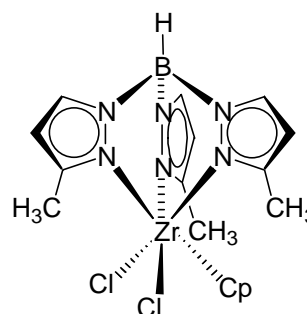
6

Tp*CpZrCl₂

[Hydrotris(3,5-dimethylpyrazolyl)boratodichloro]cyclopentadienyl-zirconium(IV)
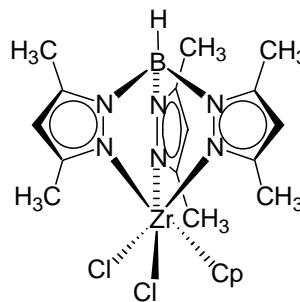
3   SUMMARY

The main focus of this work is on the synthesis of long chain branched polyolefins with MAO activated metallocene catalysts. Two different methods were applied; the first method was copolymerization of ethylene with comonomers, refered to as ethylene-graft-ethylene/propylene copolymerization. The second method was the direct generation and insertion of long chain branches in syndiotactic polypropylene by using vinyl chloride as a chain transfer reagent.

For the first method, it was essential to synthesize ethylene/propylene-comonomers to produce LCB-PE. The required properties of the EP-comonomer were low crystallinity, good solubility, and a high level of vinyl end groups. EP-comonomers were synthesized in the presence of MAO activated $(Cp^*)_2ZrCl_2$ were partially crystalline. The molar mass was is a range of 8000 to 25000 $g \cdot mol^{-1}$ containing greater than 70% vinyl end groups when synthesized at 45°C. The structure and properties were investigated by ^{13}C NMR.

EP-comonomers were used in ethylene-graft-ethylene/propylene copolymerization by using MAO activated $[Ph_2C(2,7$-di-$^{ter}BuFlu)(Cp)]ZrCl_2$ to obtain LCB-PEs. The materials were purified by washing the LCB-PE with toluene through Soxhlet extraction to remove residual EP-comonomer. The branches were detected by using ^{13}C NMR, melt rheology and, SEC-MALLS. The melting point of PE was reduced from 136 to 121°C by introduction low amounts of LCBs. The content of comonomer in the copolymer was determined indirectly by ^{13}C NMR. The existences of branches were confirmed by SEC-MALLS and melt rheology measurements. Due to coil contraction, decrease in the radius of gyration was observed relative to linear standards. An increase in activation energy, E_a, and a decrease in phase angle, δ, proved long chain branching in the polymer.

By the second method, the long chain branches were generated and directly inserted into syndiotactic polypropylene by using vinyl chloride as a chain transfer reagent. The presence of tiny amount of vinyl chloride in the propylene polymerization caused β-chloride elimination following insertion of one vinyl chloride unit, generating a vinyl terminated polypropylene chain. These vinyl terminated chains were capable of re-insertion into the main chain to form long branches.

The branches were detected using melt rheology and SEC-MALLS. The sparse amount of LCB was determined. The materials showed thermocomplexity in the melt rhelogy compared to the linear reference.

The last section of this thesis entails the synthesis of a new class zirconium complex containing both Cp and Tp ligands, and the studies of their behavior in homo- and copolymerization of olefins and their reaction mechanism. The role of the Cp ligand was enhancement of rigidity in the catalyst system, as well as prevention of the formation of more than one active species in the polymerization. The major chain transfer mechanism in Tp´MCl$_3$ complexes is chain transfer to MAO and AlMe$_3$, replacing Cl with Cp ligands resulted chain transfer by β-hydride elimination determined by NMR studies.

4   ZUSAMMENFASSUNG

Das Hauptaugenmerk der vorliegenden Arbeit lag auf der Synthese von langketten-verzweigten Polyolefinen mittels Metallocen/MAO Katalysatoren. Hierzu wurden zwei Methoden angewendet; zum Einen die Copolymerisation von Ethen mit verschiedenen Comonomeren, auch bekannt als „ethylene-graft-ethylene/propylene copolymerization" und zum Anderen die direkte Generierung und Insertion von Langkettenverzweigungen in sPP, mittels Vinylchlorid als Kettentransferreagenz.

Bei der ersten Methode war die Synthese von Ethen/Propen-Copolymeren unerlässlich für die Darstellung von LCB-PE. Die gewünschten Eigenschaften der EP-Copolymere waren eine geringe Kristallinität, gute Löslichkeit, sowie ein hoher Grad an Vinyl-Endgruppen. Um diesen Anforderungen zu genügen wurde für die Synthese der teilkristallinen EP-Copolymere bei 45°C mit einem $(Cp^*)_2ZrCl_2$/MAO-System durchgeführt. Die Molarenmassen befanden sich im Bereich von 8000 – 25 000 $g \cdot mol^{-1}$, wobei der durchschnittliche Anteil an gewünschten Vinyl-Endgruppen über 70 % betrug. Struktur und Eigenschaften wurden mittels ^{13}C NMR Spektroskopie charakterisiert.

Die EP-Copolymere dienten wiederum zur Darstellung von LCB-PE, indem sie in einer „ethylene-graft-ethylene/propylene copolymerization" in Gegenwart von Ethen mit $[Ph_2C(2,7-di-^{ter}BuFlu)(Cp)]ZrCl_2$/MAO umgesetzt wurden. Das erhaltene Gemisch wurde gewaschen und durch Soxlet-Extraktion von überschüssigem, nicht-eingebauten EP-Polymer befreit.

Die Verzeigungen mit ^{13}C NMR, Schmelzrheologie und SEC-MALLS untersucht.Es konnte gezeigt werden, dass bereits geringe Verzweigungsraten zu einer Herabsetzung des Schmelzpunkts, von 136°C für reines PE auf 121°C für LCB-PE, führen. Der Comonomergehalt wurde indirekt mit ^{13}C NMR bestimmt, während die Existenz von Verzweigungen sowohl durch SEC-MALLS, als auch durch rheologische Messungen bestätigt werden konnten: Es konnte eine Knäuel-kontraktion, als eine Abnahme des hydrodynamischen Radius bei LCB-PE gegenüber einem linearem Standard beobachtet werden. Die rheologischen Messungen bestätigten die LCB-Existenz, aufgrund einer Erhöhung von E_A, bei gleichzeitiger Verkleinerung des Phasenwinkels (δ) gegenüber den linearen Standards.

Bei der zweiten Methode wurden die Langkettenverzweigungen *in-situ* generiert und direkt, über das Kettentransferreagenz, Vinylchlorid, in eine sPP-Hauptkette eingebaut. Während der Polymerisation von Propen verursachte bereits die Gegenwart geringster Mengen an Vinylchlorid eine *β*-Chlorid-Eliminierung, was wiederum zur Entstehung von kurzen PP-Ketten mit endständigen Vinylgruppen führte, welche ihrerseits die Fähigkeit besaßen in die Hauptkette re-insertieren und somit Langkettenverzweigungen zu bilden. Die Verzweigungen wurden wie bei Methode Eins schmelzrheologisch und mit SEC-MALLS detektiert. Bei den, durch die zweite Methode, hergestellten Materialien konnten nur vereinzelte LCB nachgewiesen werden. Die Polymere zeigten bei den rheologischen Messungen gegenüber der linearen Referenz eine erhöhte Thermokomplexität.

Der dritte und letzte Teil der vorliegenden Arbeit befasste sich mit der Synthese einer neuen, sowohl Cp, als auch Tp Liganden aufweisenden, Klasse von Zirkonium-Komplexen. Untersucht wurde ihr Verhalten in Homo- und Copolymerisationen von Olefinen, insbesondere in Bezug auf mögliche Abbruchmechanismen. Während bei Katalysatorsystemen ohne Cp-Liganden häufig die Bildung mehrere aktiver Spezies beobachtet wurde, bewirkte die Einführung eines Cp-Liganden eine Stabilisierung der Ligandengeometrie um das Zentralatom und verhinderte somit die Bildung von bi-modalem Polymer. Darüber hinaus wurde der Kettentransfer auf MAO und AlMe$_3$ bei Tp´MCl$_3$ basierenden Systemen als Hauptursache für Abbruchreaktionen bestimmt. Nach der Substitution von Cl durch einen Cp-Liganden konnte durch NMR-Untersuchungen eine Änderung im Abbruchmechanismus festgestellt werden. Bei Tp´CpMCl$_2$ Systemen scheint die *β*-Hydrid Eliminierung der maßgebliche Abbruchmechanismus zu sein.

5   INTRODUCTION

5.1   Background

Industrial polyethylene was first developed by Fawcett and Gibson and produced under extremely high pressures (500 – 1200 atm) and high temperatures (200 – 400 °C) by the Imperial Chemical Industries, Ltd. (ICI), in 1933. The polymerization reaction was radical in nature and initiated by trace amounts of oxygen. The product was low-density polyethylene (LDPE, ~ 0.915-0.935 g·cm^{-3}) with low crystallinity (~ 40-50%).[1]

Later, Robert Banks and John Hogan developed a chromium trioxide based catalyst for polyethylene synthesis at Philips Petroleum, which has been used for the commercial production of polyethylene. However, the heterogenous system developed by Ziegler in 1953 was a breakthrough for the industrialization of polyolefins, recognized by the Nobel Prize for Chemistry in 1963.

Some of the largest breakthroughs in this field were developed by Walter Kaminsky and Hansjörg Sinn. They were able to develop homogeneous single-site metallocene catalysts activated by the cocatalyst methylaluminoxane (MAO).[2] Using metallocene and Ziegler-Natta systems today, it is possible to copolymerize ethylene with higher olefins, which opened the way to obtain materials with superior mechanical properties and controlled molecular architecture.

5.2   Ziegler-Natta Catalysts

The catalytic polymerization of ethylene at room temperature and low pressures (5 – 100 atm) in the presence of a heterogeneous organometallic catalyst system, discovered by Karl Ziegler, leads to the production of high molar mass polymers.[3] Ziegler developed catalyst/co-catalyst pairs based on titanium halides (TiCl$_4$) and aluminium alkyls, usually diethylaluminium chloride (Et$_2$AlCl).[4, 5]

The polyethylene produced from these systems was composed of highly linear chains with higher crystalinity and density, very different from LDPE. Therefore, it was called as a high-density (linear) polyethylene (HDPE). Following this discovery, Giulio Natta and co-workers used the same system for the regiospecific polymerization of propylene and other α-olefins. [6,7]

The first polypropylene obtained was a mixture of polymer fractions with different microstructures, due to the heterogeneous nature of the catalyst system. The first fraction was an amorphous, low molar mass atactic polypropylene. The second fraction was highly crystalline, high molar mass isotactic polypropylene. However, the complexity required for separation of the different polypropylene fractions made an industrial use diffucult for these materials.[7] The stereoselectivity could be increased by the reduction of $TiCl_4$ to $TiCl_3$, yielding isotactic polypropylene as the major fraction and the supporting of $TiCl_4$ on $MgCl_2$ domain was the success of the industrial polypropylene.

5.3   Metallocene Catalysts

The low level of control derived from the heterogenous Ziegler-Natta catalysts gave a great need for more control of the polymerization catalyst system. Metallocene-based catalysts were developed due to the homogeneous character of these systems. Initially, these catalyst systems were not singularly active, but required a cocatalyst. Consequently, development of metallocene based olefin polymerization was directly connected to the discovery and use of cocatalysts.

Just after the development of the Ziegler-Natta system, Natta and Breslow reported the first soluble catalyst systems.[8-11] These metallocene based mixture of titanocene dichloride (Cp_2TiCl_2) with triethylaluminum (TEA) or diethylaluminum chloride (DEAC) polymerized ethylene with very low activity. This system was found to be inactive for propylene polymerization. The advantage of this metallocene system was the only one active center (single-site) which creates polymers with uniform structure and narrow polydispersity, in contrast to Ziegler-Natta catalysts.

In 1973 Reichert found that addition of water improves the olefin polymerization activity of the $Cp_2TiEtCl/EtAlCl_2$ catalyst system.[12] A similar observation was also made by Breslow for the Cp_2TiCl_2/Et_2AlCl system.[13]

A major breakthrough in metallocene based polymerization occurred in the early 1980s when Sinn and Kaminsky discovered the great enhancement in the activity of the metallocene/alkylaluminum system with the addition of water at University of Hamburg. The partially hydrolyzed Me_3Al activated Group(IV) metallocenes for the polymerization of ethylene and α-olefins in this system.[14,15] The partially hydrolyzed Me_3Al was called methylaluminoxane (MAO).

13

After the discovery of metallocene/MAO, the interest in stereoselective propylene polymerization became very high. Depending on the symmetry of metallocene system, it is possible to obtain three different structural variations of polypropylene. The configuration resulting when all the substituents are in the same spherical orientation is called *isotactic*. If substituent groups are arranged alternately, the configuration is called *syndiotactic*, whereas a random sequence of positions gives the *atactic* configuration (Figure 5.1).
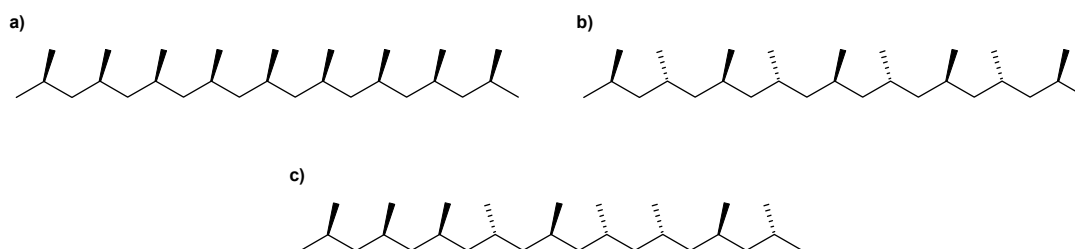
Figure 5.1   Primary microstructures of polypropylenes: a) isotactic, b) syndiatactic, c) atactic

However, the synthesis of stereoselective polypropylene by catalytic polymerization was dependent on the development of chiral, stereorigid metallocenes. Britzinger developed *ansa*-titanocene derivatives with bridged tetrahydroindenyl ligands, used in the polymerization of propylene.[16] Later, Ewen reported that the *rac-/meso*-[C_2H_4(4,5,6,7-H_4Ind)$_2$]TiCl$_2$ activated by MAO produces a mixture of isotactic and atactic polypropylene.[17] The *rac*-form produced isotactic polypropylene and achiral *meso*-form produced atactic polypropylene.

The work of Britzinger and Kaminsky showed that the *ansa*-zirconocene analog with MAO activation was able to polymerize propylene with high tacticity and narrow polydispersity (Figure 5.2).[18] New metallocene-based catalysts were developed with different chirality to yield polypropylenes with various tacticities.
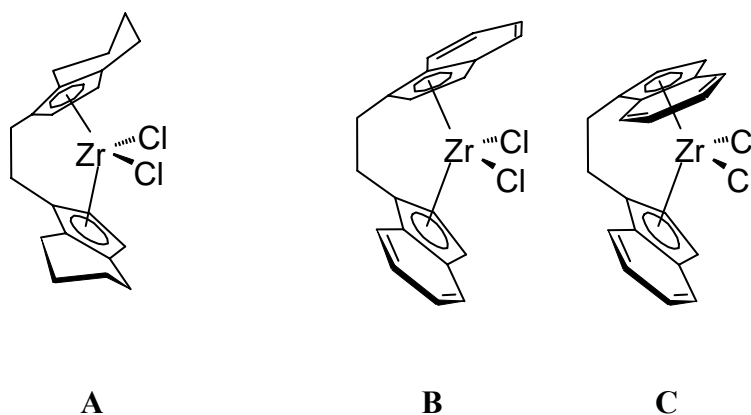
Figure 5.2   Single-site systems studied first for propylene polymerization

Ewen and Razavi developed the C_s-symmetric ansa-metallocene [Isopropyliedene(1-cyclopentadienyl-9-fluorenyl)] zirconiumdichloride (Figure 5.3) activated with MAO, which were used in synthesis of syndiotactic polypropylene.[19]
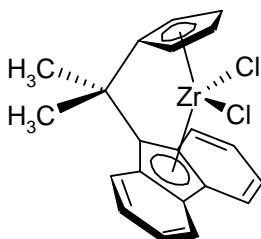
Figure 5.3 C_s-symmetric ansa-metallocene [Me$_2$C(Cp)(Flu)]ZrCl$_2$[19]

5.3.1 Methylaluminoxane (MAO)

One of the most commonly used cocatalyts in olefin polymerization by metallocene systems is methyaluminoxane (MAO). MAO can be synthesized by partial hydrolysis of trimethyl aluminium[2]. The affect of MAO on activity of the olefin polymerisation was first recognized by Sinn and Kaminsky. [20] Despite the importance of MAO, the structure and the role of MAO in the polymerization are still not well understood. The work of Barron characterized isolated *tert*-butylaluminoxane cluster structures which contained bulkier substituents than MAO. The structure of MAO was proposed as a mixture of linear or cyclic oligomers of MeAlO units (Figure 5.4).[21-23] According to cryoscopic and ebullioscopic measurements, the molar mass of MAO is in a range of 1000 and 1500 g·mol^{-1}.
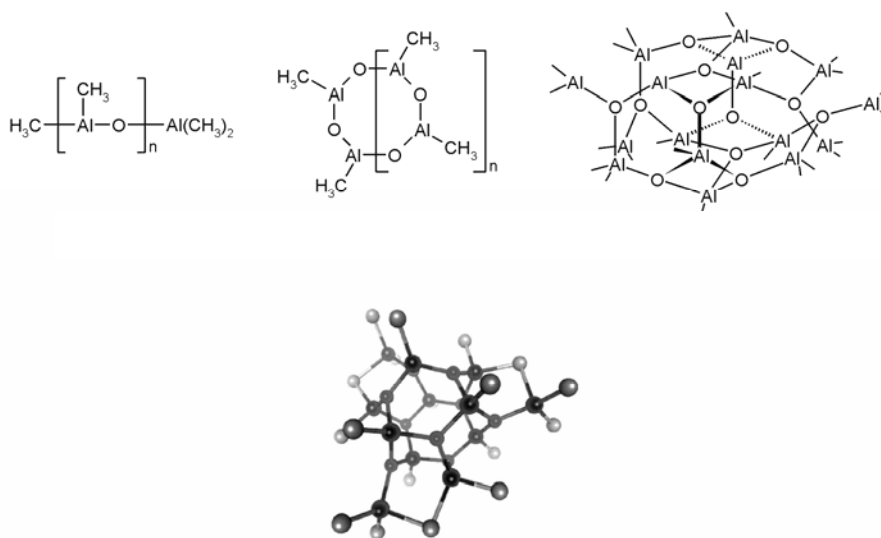
Figure 5.4   The possible structure elements of methylaluminoxanes (MAO), chain structure, ring structure, three dimensional structure according to Sinn, C_{3h}-symmetric structure according to Eilertsen

Detailed studies were undertaken to find the active center and the exact mechanism of metallocene-based polymerization, but neither is entirely understood. The accepted active species is a cationic methyl substituted metallocene. MAO first makes the dimethyl substituted complex by abstracting the halogen from the metallocene twice. Later, the equilibrium forms between methyl substituted metallocene and methylalumoxane as a contact ion pair (Figure 5.4).[24-26] MAO acts as noncoordinating anion. The formation of metallocene chloromethyl- and metallocenedimethyl complexes with MAO was proved by NMR studies.[27,28]
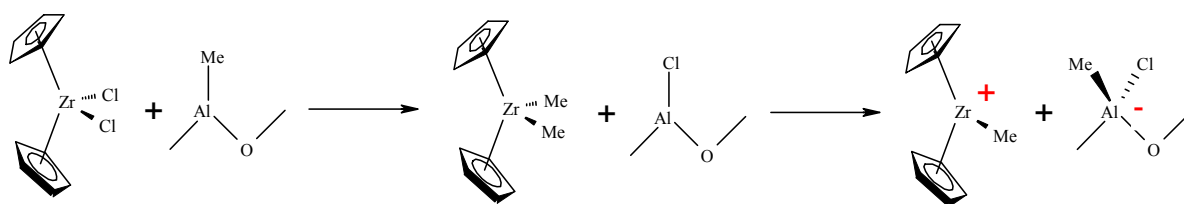
Figure 5.4   the accepted mechanism for the formation of the catalytically active species activated by MAO

Jordan and co-workers were able to isolate [Cp$_2$Zr(Me)THF]$^+$ and [Cp$_2$Zr(Bn)(MeCN)]$^+$ and reported their X-ray structures. Both are active species in ethylene polymerization.[29]

In addition to MAO, other cocatalyts were also developed including such as perfluoroaryl boranes or trityl and ammonium borates.[30]

17

5.3.2 Polymerization Mechanism

The exact insertion mechanism for the metallocene system is not completely unserstood. The accepted insertion mechanism was postulated by Cossée and Arlman in the 1960s (Figure 5.5). This system was first suggested for Ziegler-Natta catalyst system, but applies for olefin polymerization by metallocene system as well.[31-34]
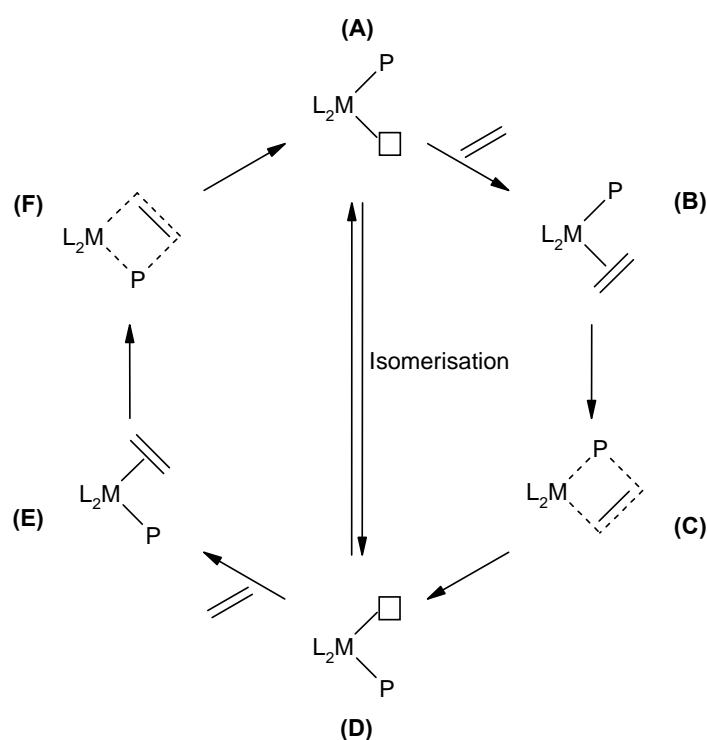
Figure 5.5 Direct-insertion mechanisms according to Cossée-Arlman

According to this mechanism, the olefin approaches the free side of the activated 14-electron metallocene catalyst (**A**) and coordinates at the vacant coordination site to generate **B**. The polymer chain inserts, involving a four-centred transition state (**C**), to give **D**. Isomerisation can occur to regenerate **A**, or propagation through **E** and **F** could take place. Brookhart and Green have suggested a slightly more complex mechanism, involving formation of β-CH agostic interactions in **A** and **D**.[35,36]

The insertion process shown above is terminated by chain transfer mechanisms. In metallocene systems, chain transfer can occur through multiple pathways. The most common chain transfer mechanisms are shown in Figure 5.6.

1. Alkyl group transfer

2. ß-hydride elimination

3. Hydrogen transfer

4. ß-methyl elimination

5. Bond metatheses
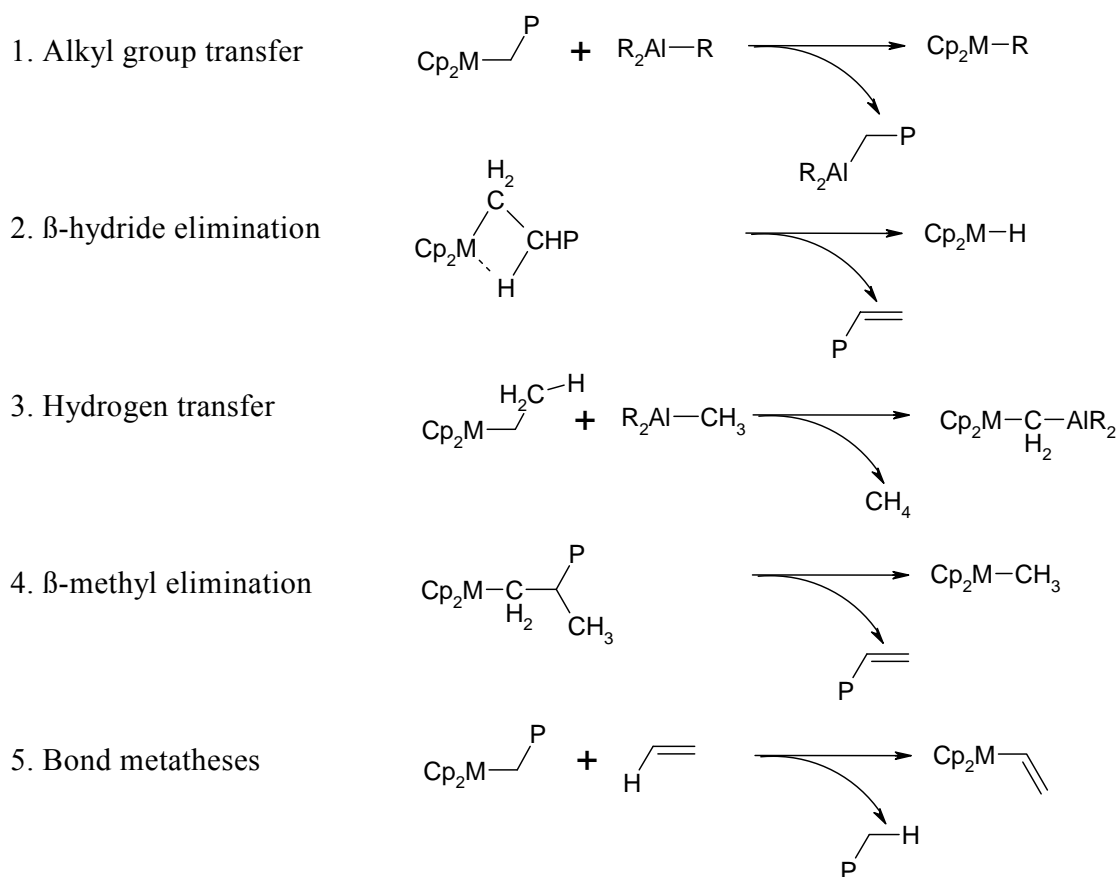
Figure 5.6   Possible termination reactions with metallocene catalyst

End group analysis allows determination of the chain transfer mechanism. The most common pathway is β-hydride transfer to the metal, or directly to the monomer. β-hydride transfer occurs in homopolymerization of higher α-olefins or in the copolymerization of ethylene with α-olefins resulting in polymer chains with sterically hindered end groups, such as vinylidenes. β-methyl transfer in propylene polymerization leads to the formation of vinyl end groups.

Chain transfer to aluminium, which must be considered when using alkyl aluminums as a cocatalyst, generates a highly reactive aluminium-alkyl bond, which can be hydrolyzed. The resulting polymers contain saturated endgroups.[37]

5.3.3 Regioselectivity and Stereochemistry

The insertion of propylene and higher olefins typically occurs with high regioselectivity, prefering primarily 1,2-insertion under many reaction conditions (Figure 5.7). The high regioselectivity observed for metallocene catalysts controls the microstructure of polyolefins produced. Regioselectivity can be changed based on the polymerization conditions. For example, 2,1-insertion becomes kinetically preferred at high polymerization temperatures (Figure 5.7).[38]
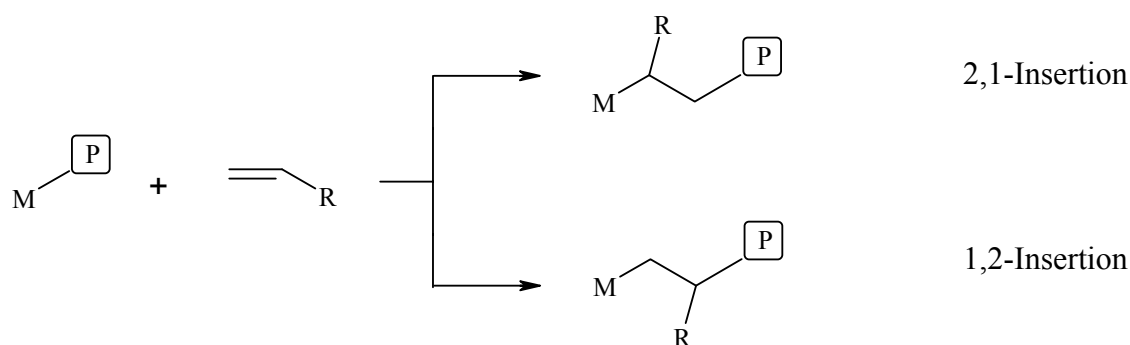
Figure 5.7   Regioselectivity of metallocenes: 2, 1- and 1, 2- insertion

An advantage of metallocene systems is the control of the polymer microstructure by either stereochemistry (enantiomorphic site control) of the catalyst or the stereospecifity of the last inserted monomer (chain-end control).[39] The work of Ewen observed and isolated irregular sequences by ^{13}C-NMR method.[40] The types of irregular sequences observed for entiomorphic site conrol are "mrrm," and for chain end control are "mmrm" (Figure 5.8).

m   *m*   *m*   *m*   *m*   *r*   *m*   *m*   *m*   *m*   *m*
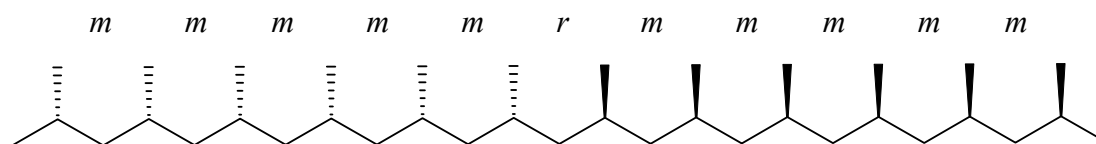
Chain-End Control: *mrmm*

m   *m*   *m*   *m*   *r*   *r*   *m*   *m*   *m*   *m*   *m*
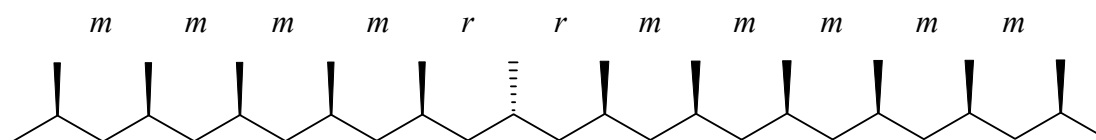
Enantiomorphic Site Control: *mrrm*

Figure 5.8   Stereoerrors for isotactic polypropylene by chain-end control and site control.

5.4   Classification of Polyethylene – Today and Future Potential

5.4.1 Classification of Polyethylenes

Polyethylenes are classified according to their density as well as the amount and form of branches in the substance, which gives polyethylenes with different mechanical properties (Figure 5.9).
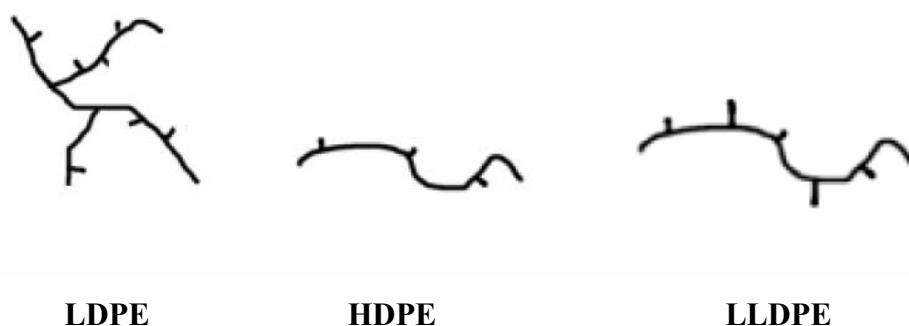
LDPE   **HDPE**   **LLDPE**

Figure 5.9   Representation of various polyethylenes: LDPE, HDPE, LLDPE

Low Density Polyethylene (LDPE), produced by free radical polymerization, contains many branches. This hyperbranched structure diminishes the intermolecular interactions between chains and leads to a decrease in crystallinity, toughness, and density of the polymer. As a result of these features, LDPE is widely used in the production of films, squeeze bottles, or table clothes, as examples.

High density polyethylene (HDPE) has a small number of short-chain branching and thus stronger intermolecular forces and tensile strength. The material is harder, stronger and more chemically resistant than LDPE. HDPE is prepared by a catalytic process (e.g. Ziegler-Natta, Phillips or metallocene catalysts), therefore the branching can be controlled by the appropriate choice of catalyst and reaction conditions.

The high affinity of metallocenes incorporates higher α-olefins giving LLDPE, polymeric materials with significant numbers of short chains. In addition, these materials showed narrow molar mass distributions[43], higher tensile strength, impact and puncture resistance. For these reasons metallocene based polyolefins with controlled branches have become a focus for industrial applications.[44]

5.4.2 Material Properties and Future

The synthesis and industrial application of polyolefins by metallocene catalysts have been growing in recent years because this system leads to materials with superior properties compared to those produced by Ziegler-Natta systems. Due to single site behavior the materials with narrow molecular weight distributions with variable molar mass are obtained. In addition, the polymerization of higher α-olefins can be obtained with high tacticity. The high tacticity and tailored microstructure of these polymers results in materials with superior mechanical properties. They are stronger and tougher than conventional polymers giving improved sealing properties and increased elasticity.[41]

Recent research in this field focuses on the improvement of material properties for specific applications, and modifying the material properties for easier processability. For example, *in-situ* polymerization with nanocomposites offers materials with enhanced mechanical and thermal properties important for the future materials desired for use in the automotive industry.[42] Using these methods it is possible to arrive the desired material properties with very low incorporation of nanocomposites.

Recent catalytic systems that reach beyond simple olefin co-/homopolymerizations has been achieved by Dow Chemicals. This system involves the catalytic production of olefin block copolymers consisting of hard/soft domains using a chain shuttling agent (CSA). With the help of a CSA, two separate catalysts selectively polymerize different monomers in the same reactor. This process gives a new class of polymers which resemble thermoplastic elastomers with high selectivity.[45]

5.4.3 Polyethylene with Long and Short Chain Branches

The molten properties of polymers differ significantly depending on their molecular weight and microstructure. The important mechanical properties are the toughness and stiffness of the materials. Focus has been directed to the design of new polyolefins combining good mechanical and physical properties with easy processability.[46] One approach to these types of polyolefins is the controlled introduction of branches into the polymer main chain.

The effects of chain branches on the material properties of polyethylene have been recognized for a long time[47]. Although the HDPE or LLDPE produced contain superior mechanical properties, LDPE still takes a large piece of the market because of the easy processability of this material.[47] This enhanced processability of LDPE is caused by the presence of long chain branches. However, LDPE is randomly and highly branched, making this target very challenging to improve. The lack of good physical properties and microstructure control for LDPE, compared to HDPE or LLDPE, motivated research in this field.

The significant amount of short chain branches in metallocene-based LLDPE enables the production of a new class of materials by making thermoplastics increasingly elastomeric. Thus, metallocene-based copolymers show excellent physical properties by disturbing the crystallization kinetics and the melting points resulting in materials with enhanced toughness, sealability, and lucidity[48]. In addition, these materials exhibit narrow polydispersity and a random distribution of comonomers.

Long chain branches (LCB) in the polymers induce drastic effects on the properties of the molten polymers. Incorporation of LCB increases the viscosity, involving the onset of shear thinning at much lower shear rate and is the cause of strain hardening in elongation.[49] Materials with improved elasticity are obtained, compared to their highly linear analogs.

The advanced works have been published on the melt rheology of these new polymeric materials. Especially, polyethylenes with defined linear or long-chain branched topography were synthesized in order to find relationships between catalyst structure, polymerization conditions, and branch incorporation.[50,51]

The half-metallocene single-site catalyst developed by Dow Chemicals with constrained geometry (CGC) such as $[CpMe_4(SiMe_2N^tBu)]TiCl_2/MAO$ was first reported to produce LCB-polyethylene.[52-55]

Later, it was reported that sterically more hindered Cp_2ZrMe_2 activated with MAO or $B(C_6F_4)_3$ is also able to produce LCB-PEs.[55-57]

The exact mechanism for LCB formation is not known but the copolymerization route is accepted for this system as well. It was also found out that the catalysts generating chains with sterically open vinyl end groups have a higher tendency to produce LCB. However, the formation of LCB depends on many other features. For example, α-olefin comonomers decrease the amount of LCB, as they tend to terminate the growing chain.[58] The incorporation of LCB is hindered due to the short-chain branches in the growing chain and as a consequence the degree of LCB tends to decrease with increasing comonomer content.

5.4.4 Polyolefins in the Market

Roughly one third of the plastic industry is devoted to the production of polyethlyene. Polypropylene production follows polyethylene by taking 20% of world plastic production (Figure 5.10). Most polyethylene and polypropylene are produced by using low-pressure Ziegler-Natta or Chrome catalysts in gas and slurry phases.
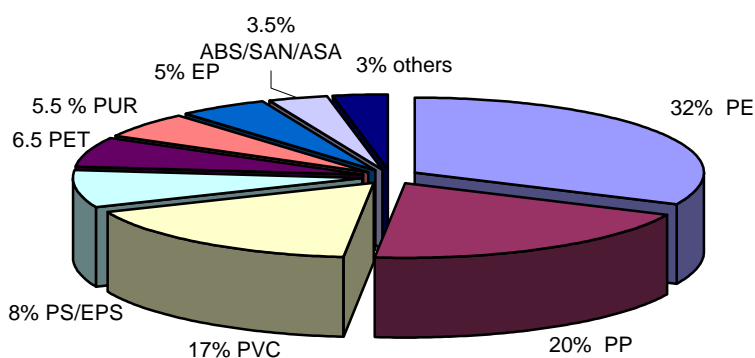
Figure 5.10   World plastic production in 2004 Source (PlasticsEurope Deutschland, WG Statistics and Market Research) [Define your abbreviations here, ie. PP = polypropylene, etc

Although demand for alternative materials to polyolefins has been rising, the demand for polyolefins are still growing. The need for linear low density polyethylene and polypropylene will increase because of the advantages in material properties compared to conventional materials (Figure 5.11).
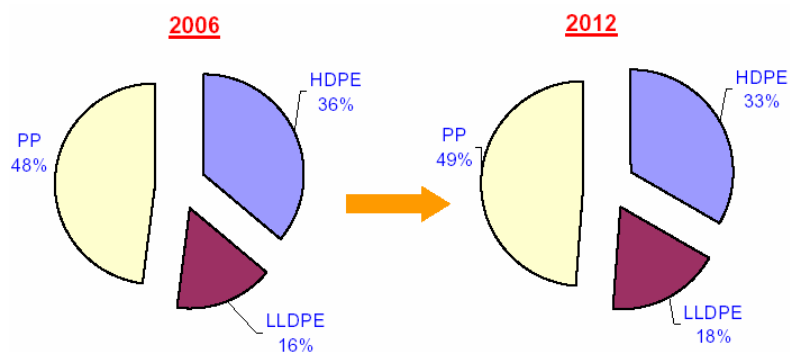
Figure 5.11   Polyolefin catalyst market outlook: 2006 – 2012 (Chemical Market Resources, Inc.)

Even though the commercialization of metallocene and single-site polymers has been met with many difficulties, the cost-effective production and superior properties of the materials obtained grew interest in the marketable production of these polymers. In 1991, Exxon started the first commercial metallocene-based HDPE. Metallocene-based polyethylenes are expected to take 9% of total polyolefin market by 2009 (Global Information Inc.).

6   LONG AND SHORT CHAIN BRANCHED POLYOLEFINS

6.1   Introduction

This work focuses on using different methods for the synthesis of long and short chain branched polyolefins in metallocene/MAO-catalyzed systems. Polyolefins with defined long/short chain branches were synthesized and the relation between material properties and branched structure were investigated. In order to obtain long and short chain branched materials, two different methods were applied; first was the copolymerization of ethylene with comonomers, which is called ethylene-graft-ethylene/propylene copolymerization. The second method was the direct generation and insertion of long chain branches by using a chain transfer reagent.

The materials obtained were characterized to investigate their properties. Long and short chain branches in the polymer were identified by using ^{13}C NMR, size exclusion chromatography with coupled multi angle laser light scattering (SEC-MALLS), and rheological measurements. Using these methods the following parameters were determined for each material, which show deviation from the linear references when branching is present:

1.   the η_0-M_w-relation.[59,62]

2.   change of viscosity ($|\eta^*(\omega)|$), the complex moduli ($G'(\omega)$, $G''(\omega)$), and the $\delta(|G^*|)$-plot.[50,59-61]

3.   characterization of strain hardening.[62-64]

4.   change in activation energy.[65-68]

The major advantage of combining different analytical methods is the successful assessment of material topography and rheological behavior. The interpretations of these parameters were explained in more detail in the results section.

Several precedents to characterize long-chain branches in polyolefins in linear viscoelasticity were present in the literature. The relationship between shear-rate viscosities and mass average molar mass is one way to detect the influence of the branches in the polymer. Normally the influence of branches on the shear flow of the materials are similar to the broadening the molar mass distribution or molar mass (M_w) of the material. The known effect of the introduction of a low degree of long-chain branching is the higher shear-rate viscosities (η_0) compared to the linear polymer with the same M_w.[50,59,66,69-70] This deviation can be formulated by obtaining a ratio of η_0/η_0^{lin}, where η_0^{lin} is the zero shear-rate viscosity expected from the η_0-M_w relationship. According to previous studies, it was found that η_0 decreases with high amounts of LCBs in the polymer, giving a ratio of η_0/η_0^{lin} of less than 1. Additionally, low M_w polymers with small amounts of LCBs might also show a decrease in η_0.[7]

The introduction of branches in metallocene based polymers leads to an increase in the activation energy (E_a). E_a is independent of M_w and the molar mass distribution of the polymer, and is used to determine the construction of the materials. Even though the relationship between short chain branches and E_a were developed previously[71-73], the effect of LCBs thermorheological behavior of the material still needs further investigation. The activation energies of highly LCB-LDPE have been reported in the range of 55-75 kJ/mol.[74-76]

In this work we present results on the synthesis and characterization of a class of graft-copolymers obtained by the copolymerization of ethylene/propylene comonomers and ethylene. The direct generation and insertion of LCB-sPP in a presence of vinyl chloride as a chain transfer reagent is also discussed.

6.2   Long and Short Chain Branched Polyethylene by Copolymerization

6.2.1 Introduction to Comonomers

The insertion of long and short chains can take place by using comonomers in copolymerization. All the main works in this field are based on synthesis of LCB-polymers with ethylene based comonomers due to the efficient incorporation of sterically open vinyl end groups, which are able to re-insert to the polymer chains forming long branches.[77]

Long chain branches were obtained in continuous solution copolymerization of ethylene with low pressure propylene by using constrained geometry catalysts.[78] Kokko and Seppala synthesized LCB-PEs by copolymerization of ethylene with higher α-olefins like 1,7-octadiene.[79] Dekmezien and his co-workers were able to obtain LCB-PPs by the incorporation of pre-formed vinyl terminated ethylene-based comonomers.[80]

Sparse amounts of LCBs were obtained by copolymerization of ethylene with higher α-olefins such as propene, 1-butene, 1-pentene and etc. However, this was not the most efficient method to modify new LCB-polymers because insertion of short branches into the polymer chain is a limiting factor for the formation of long chain branches.

Copolymerization of olefins with ethylene based comonomers was a preferable technique to synthesize new polymers with LCBs because ethylene based comonomers contain re-insertable vinyl end groups to form LCBs.

A major problem with ethylene based comonomers was their similarities with the resulting LCB materials such as crystallinity, solubility, and density which caused purification problems of the comonomer residue at the end.

Propylene or other higher α-olefin based comonomers was considered as challenging due to the ß-hydride chain transfer mechanism, which gives sterically hindered chain ends such as vinyl, vinylidene, and vinylene (Figure 6.1).

| Vinyl | Vinylidene | Trisubstituted | Vinylene |
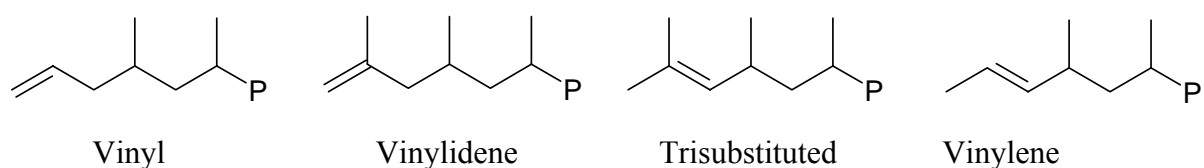
Figure 6.1   Possible olefinic chain ends in polypropylene

Resconi and Repo obtained oligomeric polypropylene with vinyl end groups.[81,82] Depending on the catalyst structure and reaction conditions ß-methyl elimination is favored instead of ß-hydride elimination. Nevertheless, the resulting PPs with vinyl end groups were not promising for the LCB formation, because their low molar mass considered them as short chains.

Dekmezian postulated several pathways to form polypropylene with vinyl terminal groups. According to his study, β-methyl elimination is the major pathway to observe vinyl end groups and the chain growth by 1, 2 insertion of propylene is favored (Figure 6.2, path A). It was postulated in pathway B that vinyl end groups can be obtained after β-hydride elimination as well, but in this case termination occurs after a 2,1-misinsertion of propylene. In pathway D, chain termination occurs after C-H bond activation which gives vinyl end group as well.
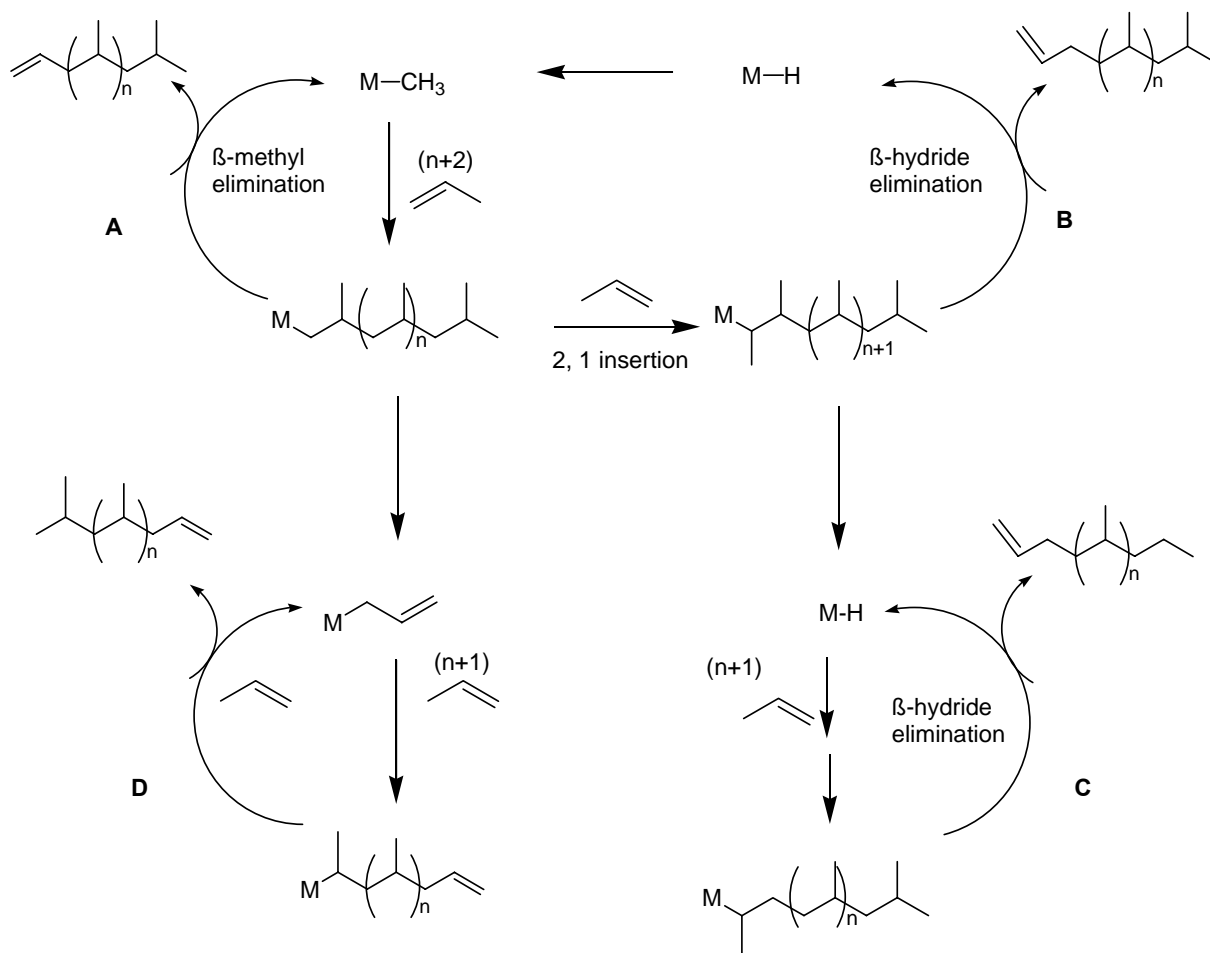
Figure 6.2   Postulated pathways by Dekmezian that could lead to vinyl end groups by propylene polymerization

The main motivation behind using ethylene/higher-α-olefines comonomers was to obtain comonomers consisting of vinyl end groups with distorted crytallinity and better solubility, which causes easy separation of excess amount of comonomers from the LCB-polymer fraction. In addition, the polymers containing two domains, a crystalline main chain and an amorphous side chain, were potentially interesting to study for their melt behavior.

The challenge of synthesizing ethylene/higher-α-olefines comonomers is incorporation of sterically open end groups which are able to incorporate to the growing chain. Depending on the chain termination reaction, ethylene/propylene-comonomers (EP) can form either vinylidene or vinyl end groups. Zhu and his co-workers studied the formation of long chain branches in ethylene/propylene copolymerization by using MAO activated CGC catalysts. They studied possible pathways for the formation of probable end groups.[78] Four different end groups were observed: vinyl, terminal vinylidene, internal vinylidene, and trans-vinylene end group (Figure 6.3). The vinyl and vinylidene end groups were obtained by the CGS system. They also hypothesized that the chains containing vinyl end groups were the reason for the formation of long chain branches in the EP-copolymers.
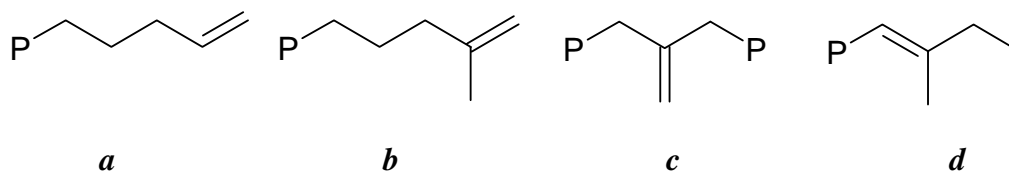
Figure 6.3   The end groups Zhu and his co-workers observed in EP-copolymers: *a) vinyl b) terminal vinylidene c) internal vinylidene d) vinylene*

EP-comonomers were examined for the synthesis of LCB-polymers in our previous work.[83] The catalyst system of $[(CH_3)_2M(Cp)_2]ZrCl_2/MAO$ (M: Si, C) was screened to produce low molar mass EP-comonomers at different ethylene/propylene monomer ratios by varying the temperature (see Figure 6.4).
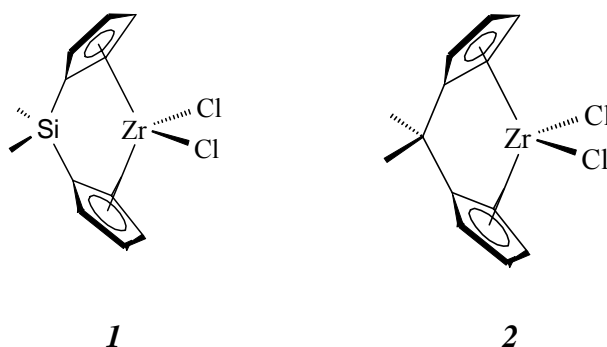
Figure 6.4 Metallocenes used in the synthesis of ethylene/propylene comonomers:

1) [Me$_2$Si(Cp)$_2$]ZrCl$_2$ *2)* [Me$_2$C(Cp)$_2$]ZrCl$_2$

Despite the similar structure of both metallocenes, **1** showed only vinylidene selectivity, where **2** gave both vinyl and vinylidene end groups. The content of vinylidene end groups generated by metallocene-**1** was between 48.7 and 67.3%. The content of vinylidene groups was from 30 to 44% whereas the degree of vinyl groups was between 6.8 and 17%.

The objective focuses on the development of new types of partially amorphous EP-comonomers with enhanced vinyl selectivity compared to other well known EP- comonomers. These types of comonomers are attractive for the controlled synthesis of long chain branched polyolefins. They are easy to insert into the growing chain and easy to purify.

In the following section, EP-comonomers were synthesized and then studied in copolymerization with ethylene to give long chain branched polymers.

6.2.2 Ethylene/Propylene Comonomers

Cp*$_2$ZrCl$_2$ (Cp* = C$_5$Me$_5$) was used to obtain low molar mass, partially amorphous EP-comonomers with enhanced amounts of sterically open vinyl end groups. The reactions were investigated to obtain the desired materials, where ethylene concentration is low at various molar fractions of the comonomers. EP-comonomers with the desired properties were attained with M$_w$ in a range of 8000 – 25000 g/mol. Their monomer incorporation, material structure and end groups were analysed.

6.2.2.1 Materials

Copolymerization of ethylene and propylene has been studied in detail using metallocene systems. Cp*$_2$ZrCl$_2$ is known to produce high molar mass polyethylene in the homopolymerization of ethylene, but produces low molar mass amorphous atactic polypropylene containing vinyl end groups.[81] The chain transfer mechanism for Cp*$_2$ZrCl$_2$ catalyzed polypropylene polymerization favors β-methyl elimination instead of β-hydride elimination. This behaviour of the MAO activated Cp*$_2$ZrCl$_2$ system made it a very attractive candidate for synthesis of the targeted EP-comonomer.
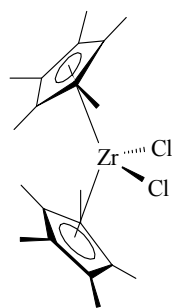
Cp*$_2$ZrCl$_2$

3

Figure 6.5   Metallocenes used in the synthesis of ethylene/propylene comonomers:
3) Cp*$_2$ZrCl$_2$

The EP-comonomers were synthesized under low ethylene concentration using Cp*$_2$ZrCl$_2$/MAO at 45 °C. In order to obtain EP-comonomers containing both amorphous and crystalline domains with low molar mass, the amount of propylene in the feed was kept very high, because the catalyst shows high incorporations of ethylene even at low ethylene content in the feed.

The total amount of monomer concentration in the feed was kept to 2 mol/l (Table 6.1). The percentage of propylene in the feed was varied from 97.5 to 100 mol%. The total pressure of the monomers was in the range of 4.1 to 4.5 bar. The MAO concentration and the injected amount of catalyst were kept constant, and the polymerizations were run for two hours after injection. The molar mass, crystallinity, and propylene incorporation of the resulting comonomers were controlled with small adjustments of propylene in the feed.

Table 6.1 Reaction conditions of ethylene/propylene comonomers synthesized in 200 mL toluene by metallocene **3** activated by MAO [1mg·ml^{-1}] at 45°C

Reaction Parameters

Comonomer	n_{Zr}	c_{total}	$c_{propylene}$	$c_{ethylene}$	$p_{propylene}$	$p_{ethylene}$	Propylene feed	Ethylene feed
	[mol]	[mol/l]	[mol/l]	[mol/l]	[bar]	[bar]	[mol-%]	[mol-%]
EP1	1.57·10^{-6}	2	1.95	0.05	3.98	0.54	97.5	2.5
EP2	1.57·10^{-6}	2	1.96	0.04	4.00	0.40	98.0	2.0
EP3	1.57·10^{-6}	2	1.97	0.03	4.02	0.32	98.5	1.5
EP4	1.57·10^{-6}	2	1.98	0.02	4.03	0.20	99.0	1
-	1.57·10^{-6}	2	2.00	-	4.10	-	100	0

Polymerization time: 2h

The EP-comonomers were characterized by various analytical methods such as GPC and ^{13}C NMR measurements. The properties of these materials are summarized in Table 6.2. The materials did not have any melting point using DSC, because of the incorporated propylene.

Table 6.2 Polymerization results of ethylene/propylene comonomers

Reaction Results					
Comonomer	$M_w{}^a$	$X_{propylene}{}^b$	$X_{ethylene}{}^b$	$X_{propylene}{}^c$	$X_{ethylene}{}^c$
	[g/mol]	[mol-%]	[mol-%]	[mol-%]	[mol-%]
EP1	25500	97.5	2.5	13	87
EP2	15000	98.0	2.0	17	83
EP3	12800	98.5	1.5	19	81
EP4	8000	99.0	1	23	77
-	180	100	0	100	-

^{a}Molar mass by GPC; ^{b}Molar fraction of monomers in the feed; ^{c}Molar fraction of monomers in the polymer determined by ^{13}C NMR; yield: 2 to 10 g comonomer

6.2.2.1.1 Molar Mass

The molar mass of the EP-comonomers decreased when increasing the propylene feed. The highest molar mass was about 25500 g·mol^{-1} where the propylene in the feed was 97.5 mol-% (Figure 6.6). At higher propylene concentrations, the rate of chain transfer increased giving a reduction in the molar mass, to 8000 g·mol^{-1}.
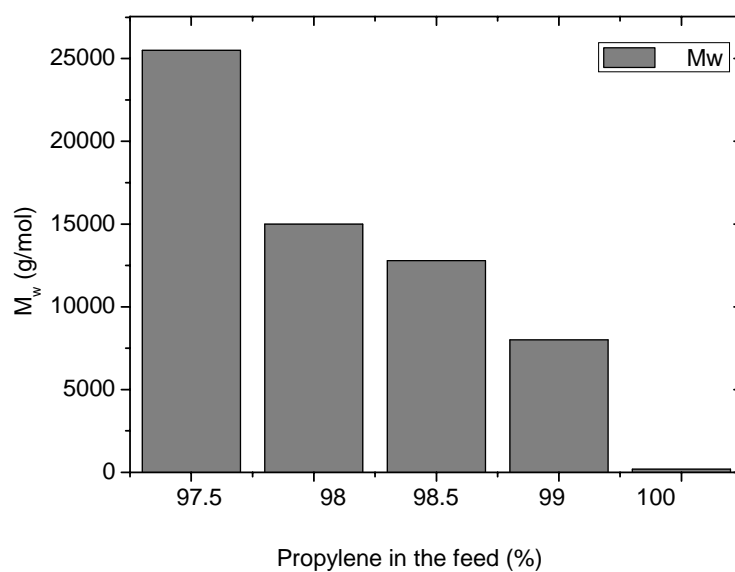
Figure 6.6   Molar mass of EP-comonomers as a function of a propylene amount in the feed

6.2.2.2.2   Propylene Incorporation

The microstructure of the EP-comonomers main chain as well as the molar fraction of ethylene and propylene were examined by inverse gated decoupled ^{13}C NMR, for quantitative integration. In order to calculate and determine the microstructure of the copolymer, ^{13}C NMR spectra were split into the eight areas shown, as described by Randall (Figure 6.7).[84] The copolymer triads were determined accordingly and their expected chemical shifts are reported in Table 6.3.
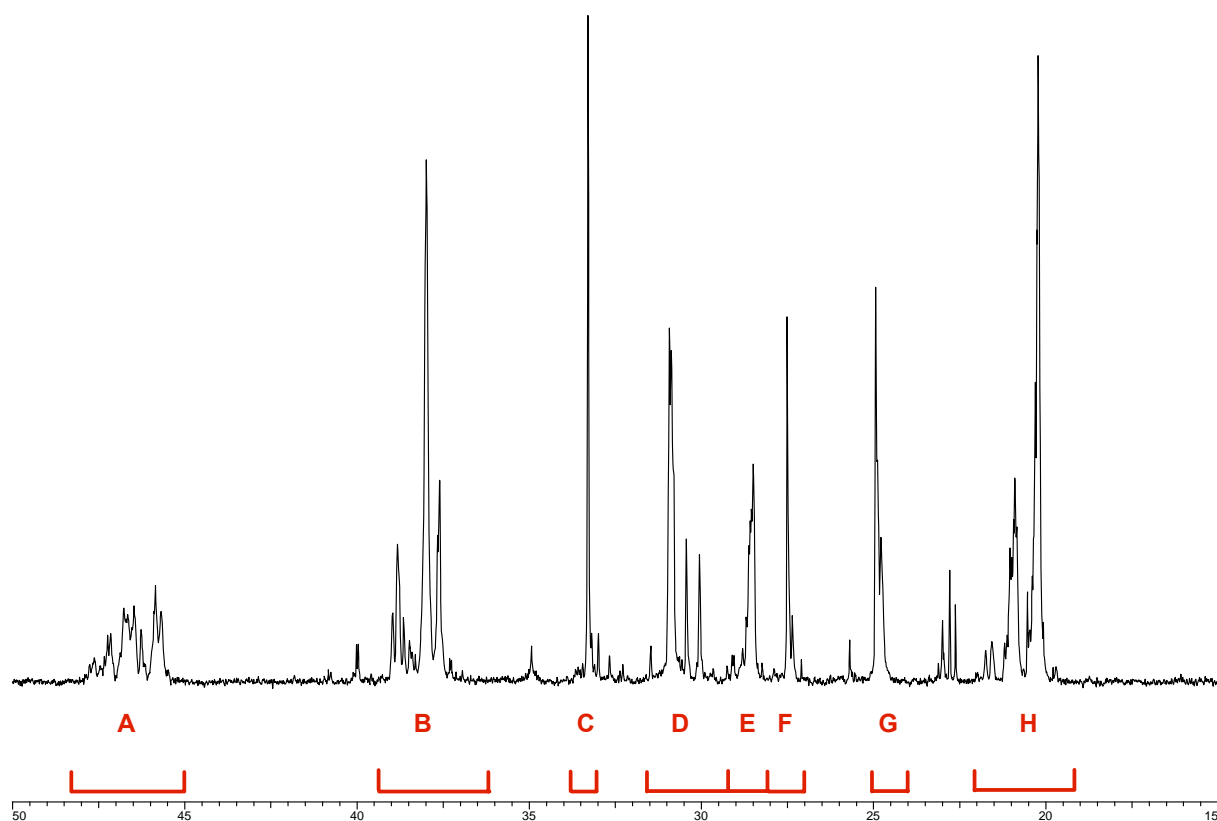
Figure 6.7   ^{13}C NMR spectrum of ethylene/propylene comonomers and integrated areas according to Randall

39

Table 6.3   Chemicals shifts of triads according to Randall

Area	Chemical shift (δ)	Triads
A	45.0-48.0	PPP (1); (PPE+EPP) (1)
B	36.0-39.0	(PPE+EPP) (1); (EEP+PEE) (1); EPE (1); PEP (1)
C	33.0-33.5	EPE (1)
D	29.1-31.5	(PPE+EPP); (EEP+PEE) (1); EEE (2)
E	28.0-29.5	PPP (1)
F	27.0-28.0	(EEP+PEE) (2)
G	24.0-25.0	PEP (1)
H	19.0- 22.0	PPP (1); (PPE+EPP) (2); EPE (1)

Intensity data from each of the eight spectral regions was measured by integration (Table 6.4). The factor k is the NMR proportionality constant which describes the observed resonance intensities, proportional to the number of contributing molecular species.

Table 6.4   Triad equations and intensities calculated from integration of triblock fractions

Intensities	Relation between integrals and triads
I_A	k·(PPP + 0.5· (PPE + EPP))
I_B	k·(EPE + 0.5·(EEP + PEE) + EPE + 0.5·(PPE + EPP))
I_C	k·(EPE)
I_D	k·(2·EEE + (PPE+EPP) + (0.5·(EEP + PEE))
I_E	k·(PPP)
I_F	k·(EEP+PEE)
I_G	k·(PEP)
I_H	k·(PPP + (PPE + EPP) + EPE)

Table 6.5   Calculation of triad parts from the integrals in ^{13}C NMR spectrum

Triad equation	Relation between integrals and data regions
EEE	$0.5 \cdot (I_D + I_E + I_F + I_A + I_C + 3 \cdot I_G - I_B - 2 \cdot I_H)$
EEP + PEE	$I_H + 0.5 \cdot I_B - I_A - 2 \cdot I_G$
PEP	I_G
EPE	I_C
PPE + EPP	$0.5 \cdot (2 \cdot I_H + I_B - 2 \cdot I_A - 4 \cdot I_C)$
PPP	$0.5 \cdot (3 \cdot I_A + 2 \cdot I_C - 0.5 \cdot I_B - I_H)$

The molar fractions of propylene in the chain for the EP-comonomers are summarized in Table 6.2. The incorporation of propylene increases at higher amounts of propylene in the feed. The maximum incorporation of propylene was about 23 mol-% with 99 mol% of propylene in the feed.

Figure 6.8 shows the relationship between M_w and propylene incorporation relative to the propylene feed. The molar mass of the EP-comonomers decreases by increasing concentration of propylene in the feed. Increasing the feed of propylene increases the amount of propylene in the comonomer, the catalyst incorporates 13 % propylene with a 97.5 % feed of propylene, and 23% with a 99% feed of propylene. With the lower 13% incoporation of propylene the molar mass-M_w is 25000 g/mol, while the molar mass-M_w decreases to 8000 g/mol when the propylene incorporation increases to 23%.
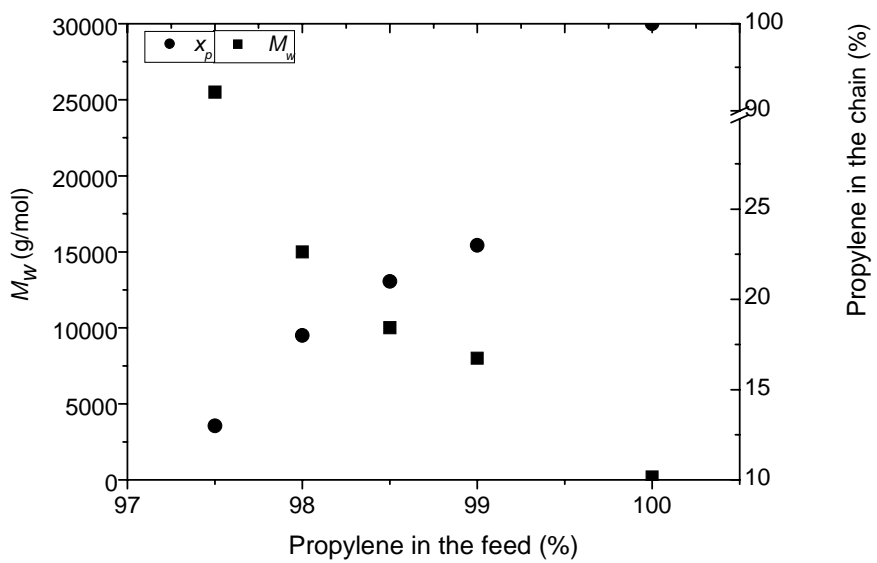
Figure 6.8   The relation between molar mass and content of propene in the chain based on content of propene in the feed

6.2.2.2.3 End Groups

The terminal end groups of the EP-comonomers were determined by ^{13}C-NMR for materials having low molar mass. End group analysis is the best method to find the mechanism of the chain termination process. Polyolefins produced by metallocene catalysis contain various end groups due to the different chain termination reactions in the polymerization. For ethylene polymerization vinyl or alkyl groups are typically obtained. In case of propylene polymerization a variety of olefinic end groups are possible, depending on the chain termination reaction (Figure. 6.9).
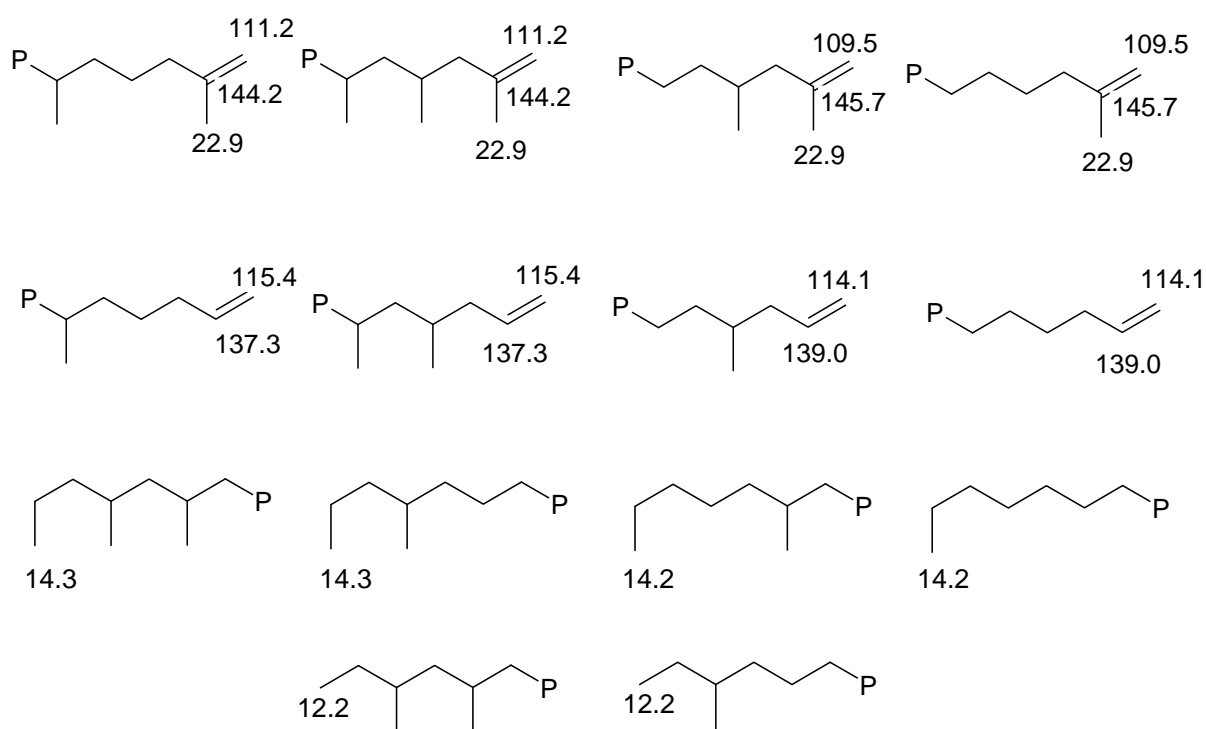
Figure 6.9   Possible olefinic and aliphatic terminal groups of ethylene/propylene comonomers with their approximate chemical shifts in ^{13}C NMR

Synthesis of propylene polymers with vinyl end groups is a challenging problem since the common chain transfer process occurs by insertion of propylene followed by β-H elimination.[85] The vinyl end groups were observed for the EP-comonomers when catalyzed by **3**, indicating the main chain transfer process is β-CH$_3$ elimination.[81] Accordingly, the main chain transfer mechanism for **3** is expected to be 1,2 insertion of propylene followed by β-CH$_3$ elimination (Figure 6.10).
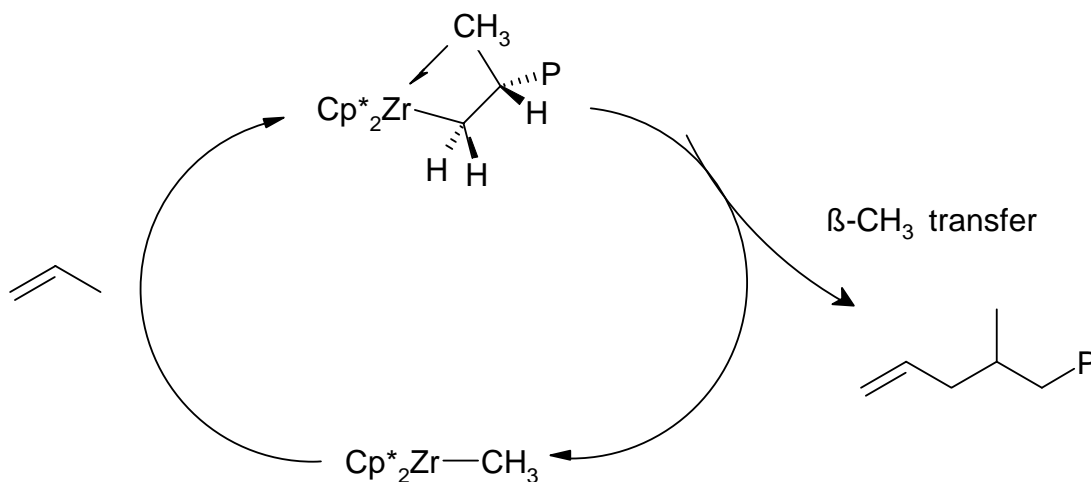
Figure 6.10 The major chain transfer mechanism for the synthesis of ethylene/propylene comonomers with **3**

The high selectivity of β-CH$_3$ elimination, instead of β-H elimination, is based on steric reasons. The proposed transitions state by Resconi shows the sterically crowded methyl groups on the Cp* ring disfavor β-hydride elimination, therefore **3** prefers to β-methyl elimination (Figure 6.11).

A   *B*
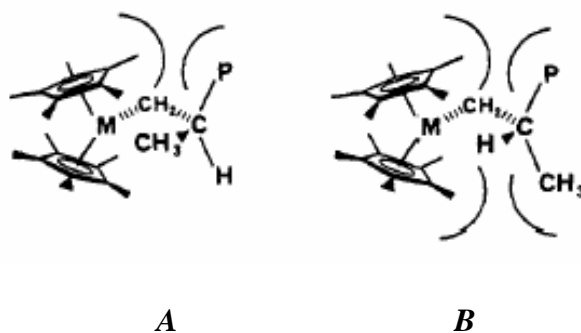
Figure 6.11 Proposed transition states β-CH$_3$ elimination (*A*) and β-H elimination (*B*)

The degree of vinyl group enhancement was from 54.8 to 88.4% by increasing the content of propylene, and no vinylidene groups were detected in the ^{13}C NMR spectra of EP-comonomers. A small amount of methylene signals from vinylidene groups was observed at δ 111.9 in atactic polypropylene fractions. This signal, assigned to the -CH$_2$, indicates that a small portion of β-hydride elimination occurs after 1,2 insertion of propylene into the chain. The signal at δ 144, corresponding to the quaternary carbon was not observed due to the low intensity relative to the –CH$_2$.

The signals assigned to the vinyl end groups were found at δ 115 and 114, respectively. EP-comonomers did not exhibit any ^{13}C NMR resonances for carbon atoms belonging to vinylidene end groups. Therefore, the major termination pathway occurs selectively by 1,2 insertion of the monomer, followed by β-CH$_3$ elimination. The end group analysis for respective EP-comonomers is listed in table 6.6, and representative spectra are shown in Figure 6.12.

Table 6.6   Content of end groups in EP-comonomers produced by metallocene-**3**

Comon.	$X_p{}^a$	$X_E{}^a$	$x_p{}^b$	$x_E{}^b$	Vinylidene % (111/109 ppm)	Vinyl % (114 /115 ppm)	Alkyl % (14.7/11.6 ppm)
EP1	97.5	2.5	13	87	n.d	n.d	n.d
EP2	98.0	2.0	17	83	n.d	54.8	45.2
EP3	98.5	1.5	19	81	n.d	67.7	23.3
EP4	99.0	1	23	77	n.d	88.4	11.6
-	100	0	100	-	10.1	82.9	7.0

^{a} fraction of monomers in the feed;^{b}Molar fraction of monomers in the polymer determined by ^{13}C NMR
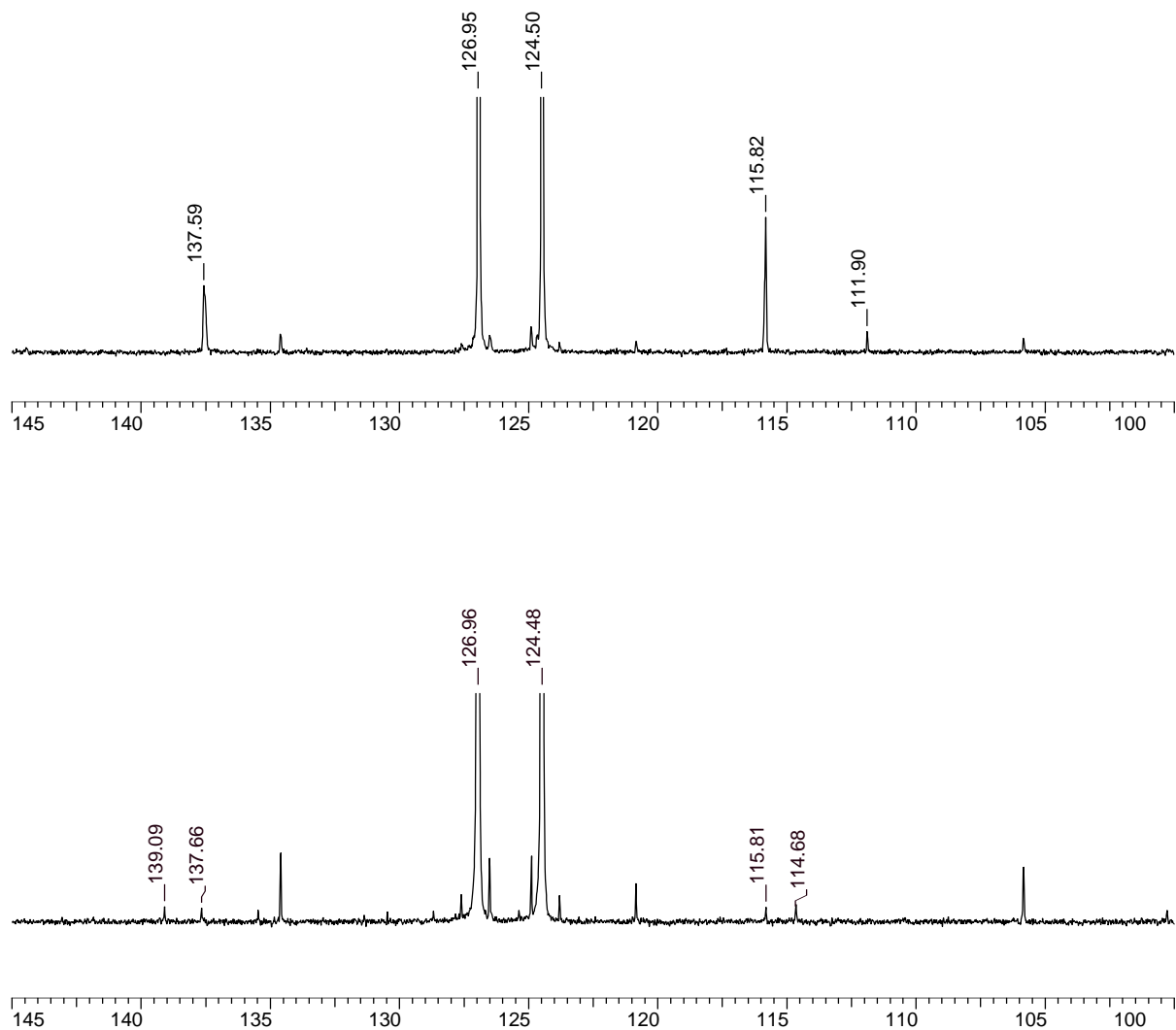
Figure 6.12 Olefinic region of polypropylene (top) and ethylene/propylene-comonomer prepared by MAO activated **3**

6.2.3 Ethylene-graft-ethylene/propylene Copolymerization

Various long chain branched polyethylenes (LCB-PEs) were synthesized by the copolymerization of ethylene with EP-comonomers, as explained in the previous sections. The aim of this study was to understand the relation between material behaviors and the branches structures.

LCB-PEs were synthesized in two steps. First the EP-comonomers were generated, then copolymerizations were run using a MAO activated fluorenyl catalyst **4** (Figure 6.13). **4** has been shown to be a very successful catalyst for comonomer incorporation in LLDPEs.[86] Also, fluorenyl based catalysts produces PEs with extremely high molar mass ($>1x10^6$ kg/mol), which creates problems in rheological measurements due to long relaxation times. Molar mass of the materials were regulated by addition of hydrogen explained later in this section.

EP-comonomers with 8000 g/mol M_w were used to generate LCB-PEs due to their higher solubility, and the higher content of propylene in the chain relative to higher M_w EP-comonomers. Polymerizations were performed for two hours, and ethylene consumption was monitored by a mass flow control system. The bimodal copolymer fractions were purified by washing with hot toluene and Soxhlet extraction. This method resulted in the synthesis of LCB-PEs with novel material properties by controlled insertion of comonomers with easy purification.
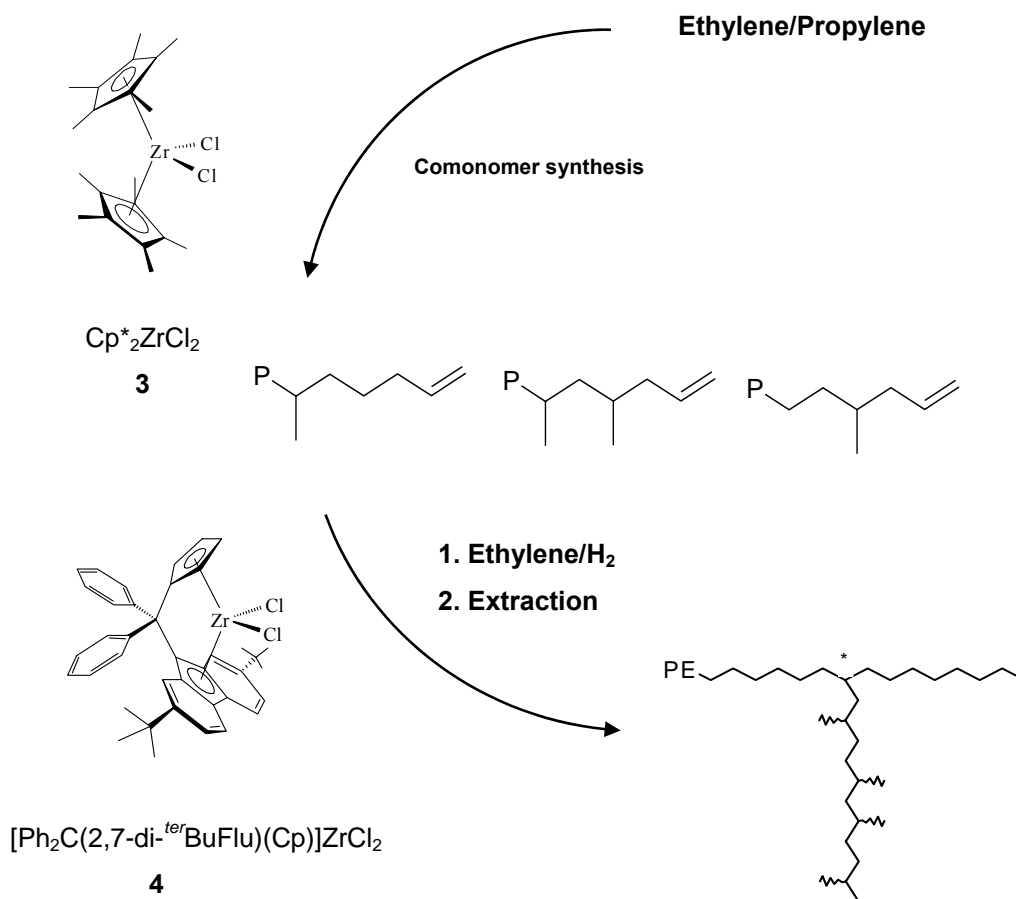
Figure 6.13 Reaction scheme for ethylene-graft-ethylene/propylene copolymers

6.2.3.1 Materials

The LCB-PEs were synthesized by ethylene-graft-ethylene/propylene copolymerization, which differ in the content of EP-comonomer (0 to 5 %), by **4** activated with MAO. Molar mass of the resulting materials were regulated by the addition of 0.2 bar hydrogen gas as explained in the following section. The polymerization conditions are written in Table 6.7.

Table 6.7   Reaction conditions for ethylene-graft-ethylene/propylene copolymers synthesized with EP-comonomers at 60°C

Polymerization Parameters							
Run	c_{total} [mol/l]	$p_{ethylene}$ [bar]	EP-comon. [g/mol]	H_2 [bar]	ethylene [mol-%]	comon. feed [mol-%]	comon. feed [g]
1	0.1	1.2	-	-	100	-	-
2					100	0	0
3					99.5	0.5	1.7
4	0.1	1.2	8000	0.2	99	1	3.4
5					98	2	6.4
6					95	5	16
7					100	0	0
8					99.5	0.5	0.85
9	0.05	0.6	8000	0.2	99	1	1.7
10					98	2	3.4
11					95	5	8

Constant conditions: 400 ml toluene, c_{MAO} = 1mg/ml, polymerization time = 2 h, $n_{catalyst}$ = 1.98·10^{-7} mol, the obtained material was between 5 to 10 g before purification

6.2.3.2   Extraction

The main difficulty in the characterization of ethylene-graft-ethylene/propylene copolymers is the purification of LCB-polymer fraction from excess comonomers in the bimodal material mixture. Previously, LCB-polyolefins were synthesized with ethylene based comonomers. [87] However, the similarities between ethylene based comonomer fractions and LCB-polyolefins such as melting point and solubility caused severe purification problems. The bimodal LCB-PEs were separated from excess ethylene comonomers by Kumagawa extraction. Even though this method was applied succesfully to obtain a monomodal LCB-PEs fraction, the yield of the pure fraction was low.

Rulhoff and Kaminsky then synthesized LCB-PPs with ethylene based comonomers. These materials were purifed by the extraction method of Kong, Fan and Xia.[88] Using this method, it was possible to separate polymer fractions depending on their molar mass, solubility, density, and crystallinity. The mixture of different polymer fractions are dissolved in p-xylene at 120 °C and 2,6-di-^{tert}buyl-4-methyl-phenol (BHT) is added dropwise until one fraction appears in the solution. The ratio of p-xylene to BHT is 1:1 at completion. This method is successful in separating polymer mixtures, but the yield of the pure LCB-fraction is still too low, especially if the material requires a second or third extraction.

An important feature of these LCB-materials is the inserted propylene in the comonomer chain distorts crytallinity and improves solubility. This allowed the excess EP-comonomers to be separated from the bimodal LCB-PE fraction easily using Soxhlet extraction.

A representative example of purified an unpurified LCB-polymer is shown in fig 6.14. Before Soxhlet extraction (lighter curve), the material consists of both low molar mass EP-comonomer and LCB-PE, after the extraction the material is monomodal LCB-PE which is ready for further analytical investigations.
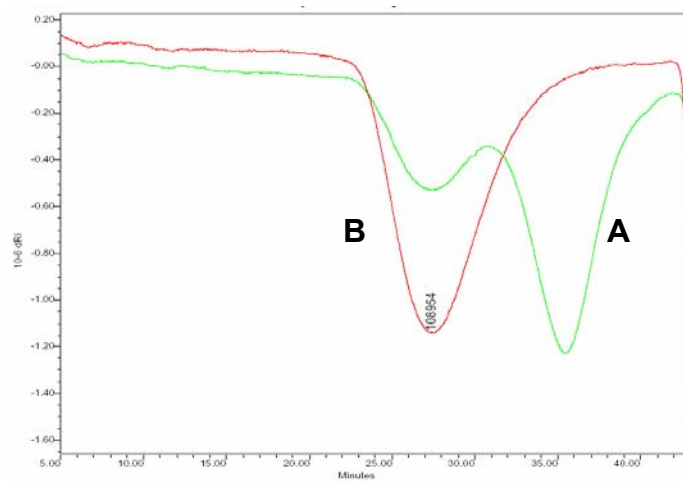
Figure 6.14 LCB-PE before soxhlet extraction bimodal product (**A**) and after soxhlet extraction monomodal LCB-PE (**B**)

6.2.3.3   Material Properties

The obtained LCB-PEs were characterized in detail using multiple analytical method. The general copolymerization results are summarized in Table 6.8. The melt behavior of the copolymers was studied by rheology as well. These results are going to be discussed in the following sections.

Table 6.8   Properties of LCB-PEs synthesized by MAO activated **4** at 60°C in toluene

Polymer Characteristics							
Run	$M_w{}^a$ [g/mol]	M_w/M_n	$n_{comonomer}{}^b$ [mol-%]	$w_{comomer}{}^b$ [g-%]	$T_m{}^c$ [°C]	η_0 [Pas]	E_a [kJ/mol]
1	1500000	1.6	0	0	136	n.d	n.d
2	101000	2	0	0	136	3.0×10^4	n.d.
3	105000	1.8	0.16	31.4	134	$>2.8 \times 10^6$	60-70
4	120000	1.8	0.17	32.7	132	$\gg 2.3 \times 10^7$	n.d.
5	78000	2.1	0.31	47.1	130	3.5×10^5	80
6	122000	2.7	0.58	60.4	126	$\gg 1.3 \times 10^7$	n.d.
7	42000	2.0	0	0	136	142	28.8
8	30500	1.7	0.20	36.4	134	n.d	n.d
9	32700	1.7	0.26	42.7	131	n.d	n.d
10	34000	2.0	0.35	50.4	129	538	49.2

[a] Determined by GPC, [b] Determined by ^{13}C NMR, [c] Determined by DSC, n.d: not determined

6.2.3.3.1 Molar Mass

Molar mass of the materials were determined by GPC. The molar mass of ethylene-graft-ethylene/propylene copolymers were reduced by the addition of hydrogen to the reaction system.

Previous studies have shown that addition of hydrogen to metallocene catalyzed polymerization decreases the activity of the catalyst and molar mass of the materials. Most probably hydrogen coordinates to the metal center and forms an intermediate η^2-hydrogen complex. The η^2-hydrogen complex supports the termination reaction, probably through σ-bond metathesis, to release a Zr-H species for further propagation (Figure 6.15). In addition, Penlidis reported that the bimodal polymers were obtained catalyst by Et[Ind]$_2$ZrCl$_2$ and Cp$_2$ZrCl$_2$ in a presence of hydrogen since the metal centre of a catalyst is coordinated by hydrogen and a new coordination site is produced.[89]
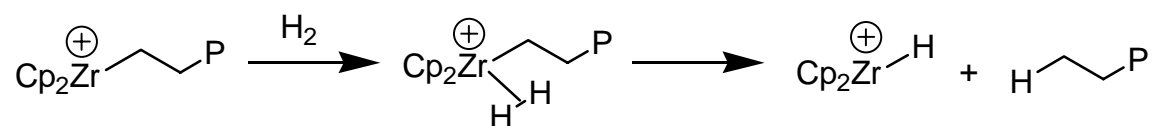
Figure 6.15 Coordination of hydrogen to the metal center

The molar mass of these polyolefins must be regulated in a range for successful rheological measurements. The effect of hydrogen on molar mass of ethylene homopolymerization was studied by varying the hydrogen in the feed. The polymerization temperature and the content of ethylene were kept constant. The reactions were performed where the ethylene pressure was low (0.6 and 1.2 bar).

GPC measurements showed that at low ethylene concentration (0.05 mol/l, 0.6 bar), the molar mass of resulting materials is about 30000 g/mol, and at higher ethylene concentration (0.1 mol/l, 1.2 bar) is in range of 70000 to 110000 g/mol (Figure 6.16). Due to the high sensitivity of the catalyst to hydrogen, the variation in molar mass was observed. There is no direct influence of the EP-comonomer on the molar mass. Polydispertiy of the resulting materials were around 2 as expected for single site behaviour.
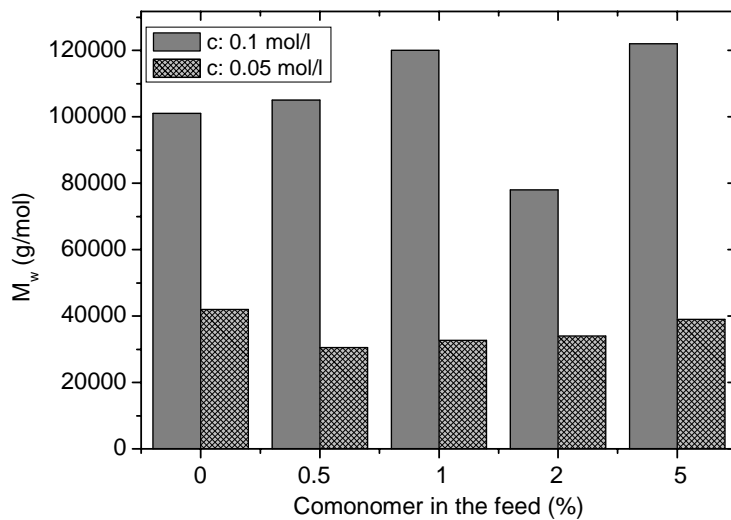
Figure 6.16 Molar mass of LCB-PE at high and low ethylene concentration

6.2.3.3.2 Comonomer Incorporation

One way to determine long chain content in ethylene-graft-ethylene/propylene copolymers is ^{13}C-NMR, but NMR is unable to determine branch length longer than 6 carbons.

The materials synthesized in this work were measured using inverse gated decoupled ^{13}C for quantification of the branches. The branching carbon atom of the side chain could not be detected directly in LCB-PEs by ^{13}C NMR measurements. This could be due to overlap of the branching carbon signal with other signals, or the very low effective concentration of this branching carbon. Another signal in the EP-comonomer (δ 33.3) was taken as a reference for this carbon (Figure 6.17).
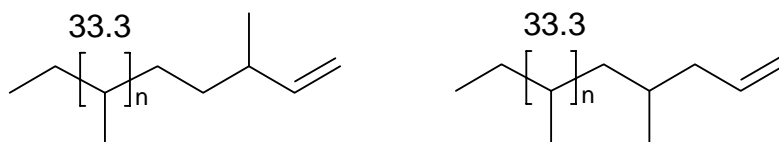
Figure 6.17   The signal correlated to the vinyl carbon atom in EP-comonomer

In addition, the main chain signal of the CH$_2$-chain both in LCB-PE and EP-comonomer is around δ 30, the signal overlapping coming from EP-comonomer was extracted from the main LCB-PE signal. The equation for the calculation of comonomer incorporation was modified according to this system. The ^{13}C NMR spectrum of HDPE and LCB-PE are shown in Figure 6.18. The signals coming from EP-comonomer are clearly observed.
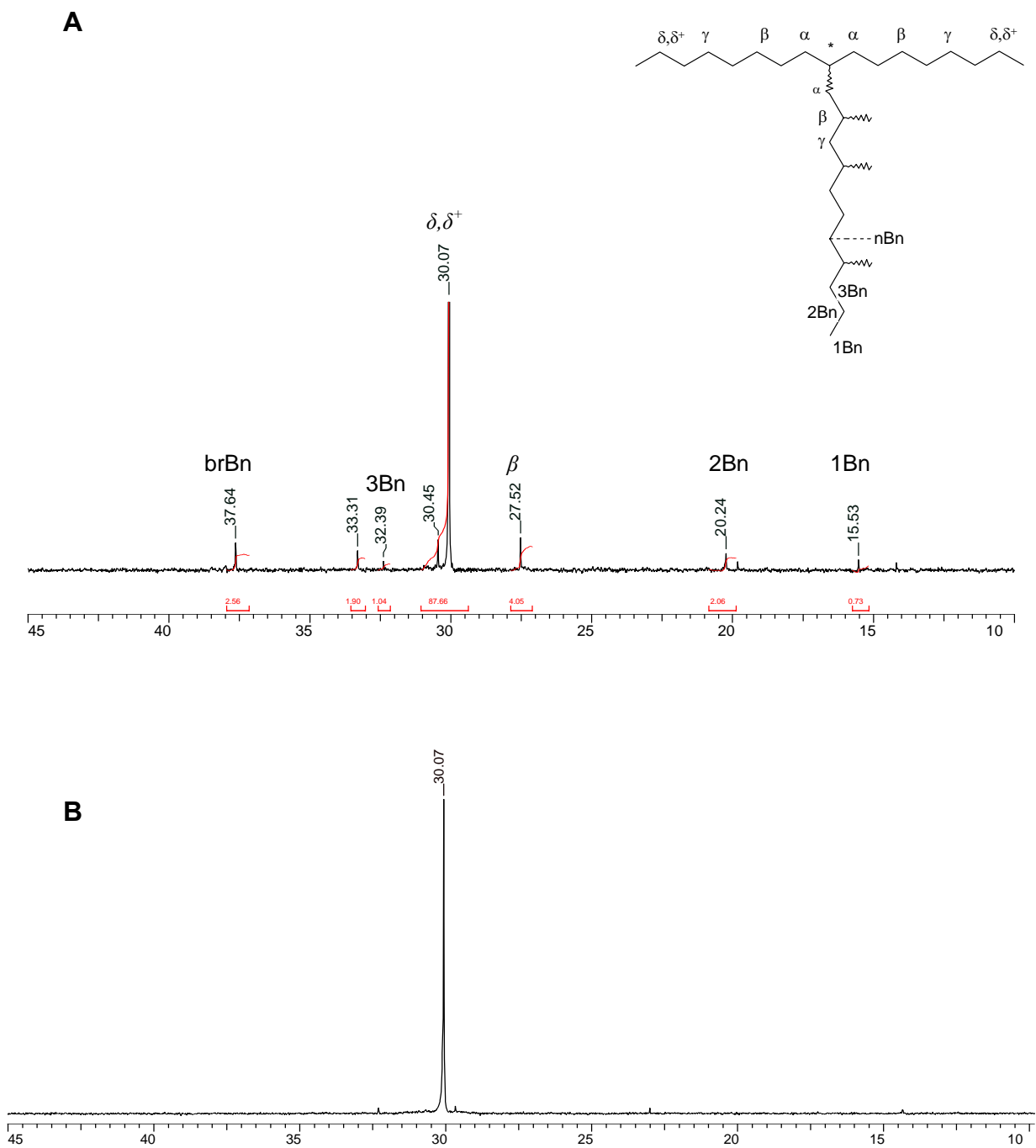
Figure 6.18 ^{13}C NMR spectra of LCB-PE (**A**) and Homo PE (**B**) obtained by **4**

56

The comonomer content was calculated with the equations below without including number of carbon atoms. I(*) is the integration area of the branching carbon signal, and $I(\delta,\delta^+)$ is the integration of the main signal of CH_2-chain at δ 30.0, n_c is the incorporation of comonomer in mol-% (eq. 2), and w_c is the incorporation of the comonomer in weight-% (eq. 3). The average molar mass m_c of EP-comonomer was taken to be 8000 g/mol.

$$c* = \frac{\left(\dfrac{I(vinyl)}{I(33.3\,ppm)}\right)_{comonomer} \quad xI(33.31\,ppm)_{polymer}}{\left(I(\delta,\delta*) - \left(\dfrac{I(30.0)_{comon.}}{I(33.3)_{comon.}}\right) \times I(33.3)_{polymer}\right)} \tag{1}$$

$$n_c* = c* \times 1000 \times 0.2 \tag{2}$$

$$w_c = \frac{n_c \cdot m_c}{n_c \cdot m_c + (100 - n_c) \cdot 28} \cdot 100 \quad [wt.-\%] \tag{3}$$

Even though this method is not an exact determinatination of comonomer incorporation, the estimate obtained was supported by comonomer feed amount, SEC-MALLS, and melt rheology.

The EP-comonomer incorporation in wt-% and mol-% is shown in figure 6.19. The branch incorporation increases by increasing comonomer content in the feed. The maximum incorporation was about 60 wt-% and 0.51 mol-% at high monomer concentration. There is no strong influence of ethylene concentration on comonomer incorporation.
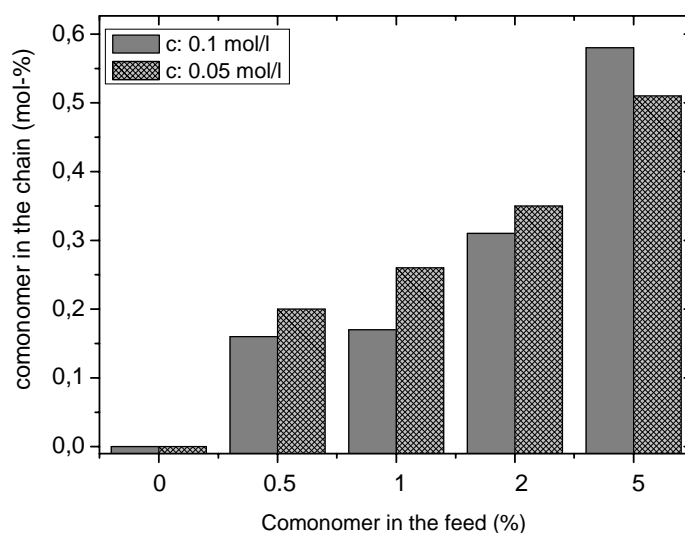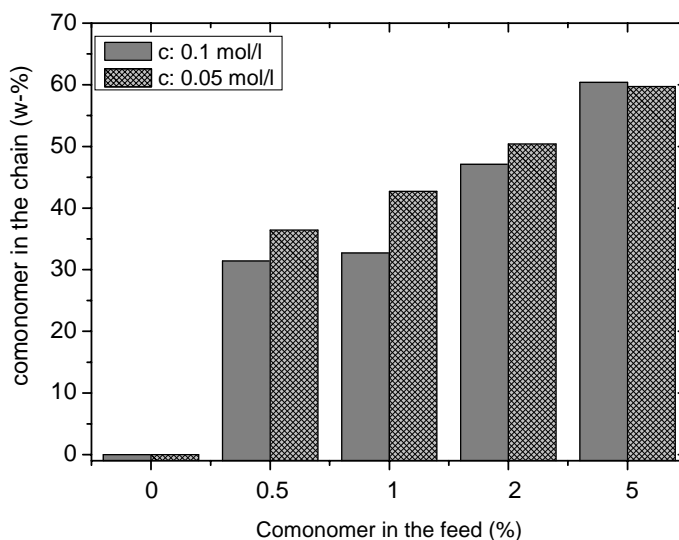
Figure 6.19   Comonomer incorporation in wt% (top) and mol% (bottom) relative to concentration

6.2.3.3.3 Melting Point

The melting point of the LCB-PEs was investigated by DSC. Comparison of melting points shows thermal dissimilarity between homo polyethylene and long chain branched samples. The melting point reduces from 136 °C to 121 °C even at very low incorporated comonomer content (Figure 6.20). At high comonomer loading the melting point is dramatically decreased at low ethylene concentration compared to higher ethylene concentration.
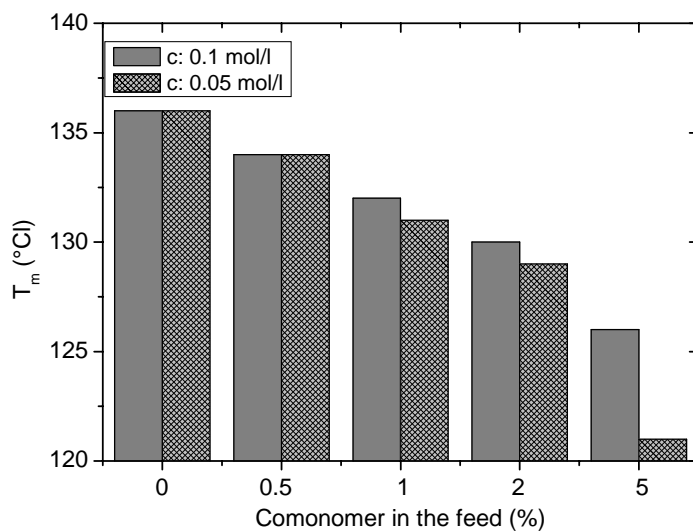
Figure 6.20   Dependency of melting point of LCB-PE at high and low ethylene concentration on the content of comonomer in the feed

6.2.3.3.4 SEC-MALLS

Broad molar mass distiribution and long chain branches have a similar effect on the rhelogical behaviour of the materials. In order to observe this effect coming from long chain branches, the materials were measured by Size Exclusion Chromotography coupled to Multi Angle Laser Light Scattering (SEC-MALLS). [90]

The Multi Angle Light Scattering (MALLS) detector measures the radius of gyration. The presence of long-chain branches leads to a decrease in the radius of gyration $<r^2>^{0.5}$. The long-chain branches can be analysed by employing the Zimm-Stockmayer long chain branching equation, which can be calculated as the ratio of squared radii of gyration of linear and branched material (eqn 1). [91]

$$g = \frac{\left\langle r_{branch}^2 \right\rangle}{\left\langle r_{linear}^2 \right\rangle} \qquad g < 1 \qquad \text{if the sample is branched} \qquad \textbf{(1)}$$

$$g = 1 \qquad \text{if the sample is linear}$$

According to Zimm-Stockmayer, the number of branches per molecule of polyethylene can be calculated from equation 2, when assuming a statistical branching distribution and three functional branch points where m is the number of branches per molecule

$$g = \left[\left(1 + \frac{m}{7}\right)^{0.5} + \frac{4 \cdot m}{9 \cdot \pi} \right]^{-0.5}, \qquad \textbf{(2)}$$

The molar mass distribution (MMD) as well as their $<r^2>^{0.5}$, as a function of the molar mass M_{LS} for materials prepared at low ethylene pressures (0.6 bar) and different comonomer amounts in the feed are given as SEC-MALLS results (Fig 6.21). Using the molar mass distribution, it is possible to determine $<r^2>^{0.5}$, if the samples are monomodal, and if the purification step was successful in removing the comonomer. Typical metallocene based PE has a MMD M_w/M_n at around 2. The materials shown in Figure 6.21 have the MMD approximately 2 (see Table 6.8), indicating these materials do not contain any residue of EP-comonomers. Due to the quite low molar mass of the materials the relationship between $<r^2>^{0.5}$ and long chain branches could not be determined properly.
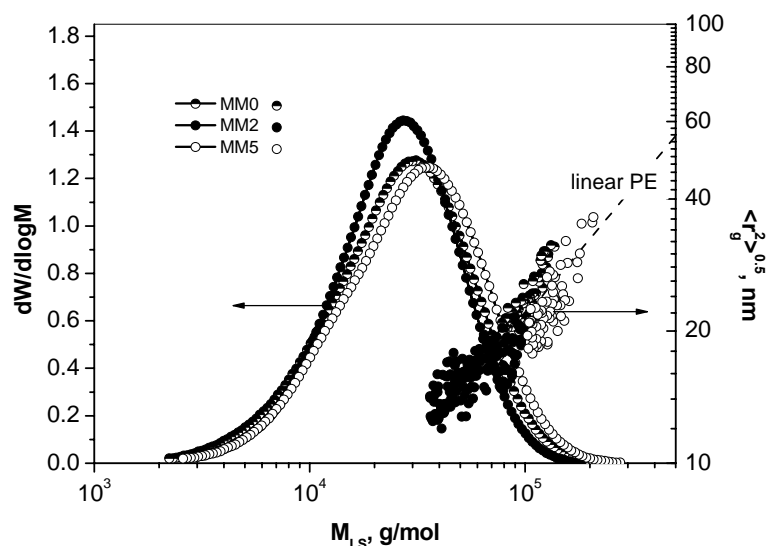
Figure 6.21   Molar mass distribution of the products prepared at low ethylene pressure (MM0: no comonomer, MM2: 2% comonomer MM5: 5% comonomer in the feed) and the radius of gyration as a function of absolute molar mass M_{LS}

The amount of comonomer incorporation as long chain branches was calculated by NMR spectroscopy, and the effect of incorporated comonomers on the melting point was determined by DSC. According to the NMR results, comonomer incorporation for MM2 is 0.354 mol-% which means that 50 % of molar mass stems from the comonomers incorporated as LCBs with narrow polydispersity at around 2. In addition, MM5 is even more branched than MM2 showing comb-like branching topography. The molecular structure of the materials prepared at low ethylene concentration were further analysed by rhelogical measurements.

The materials prepared at higher ethylene pressure (1.2 bar) and different comonomer feeds were also analysed by SEC-MALLS. The MMD of material with 2 % comonomer in the feed is unimodal and the material does not contain any residual EP-comonomers. In addition, a significant contraction of $<r^2>^{0.5}$ was found for this sample (Figure 6.22).
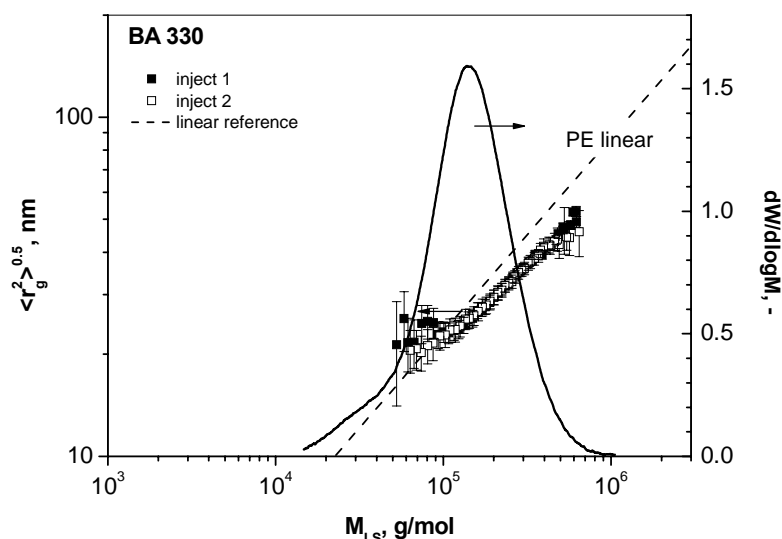
Figure 6.22   Molar mass distribution of the products prepared at high ethylene pressure (MM2: 2% comonomer) and the radius of gyration as a function of absolute molar mass M_{LS}

These measurements were also performed for the other materials prepared at higher ethylene pressure with varying comonomer feeds. The $<r^2>^{0.5}$ of all the materials deviates from the linear reference, and significant contraction is found for all the samples (Figure 6.23). These SEC-MALLS measurements indicates the materials prepared with 1, 2 and 5 % of comonomer are long chain branched. In addition, the degree of branching was determined according to the Zimm-Stockmayer-theory.[91]

The comparison between the data of the LCB-PEs shows that the $<r^2>^{0.5}$ of the materials deviates more strongly from the linear reference by introducing higher amounts of comonomers. This provides evidence that the sample with 5 % comonomer in the feed possesses more long chain branches than the sample with 2% comonomer in the feed.
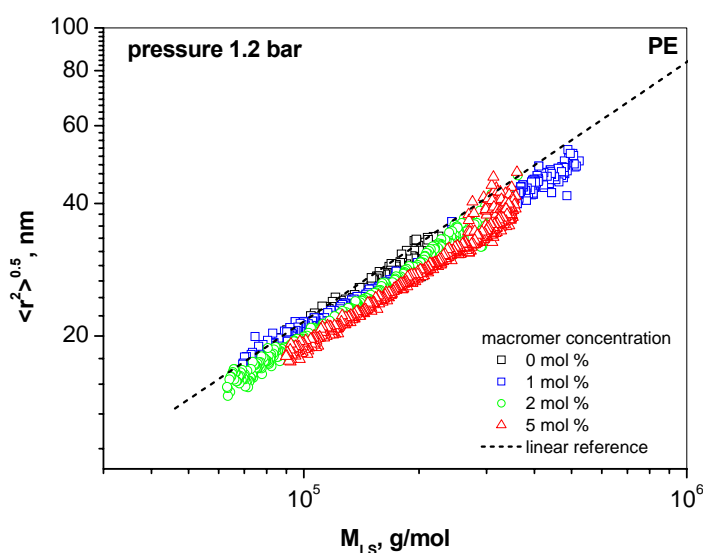
Figure 6.23 The radius of gyration as a function of absolute molar mass M_{LS} of the products prepared at high ethylene pressure and different comonomer amount in the feed (from 0 to 5 % comonomer in the feed)

6.2.3.3.5 Melt Rheology

Melt rheology is one of the best methods for long-chain branch detection, even at very low branch concentrations in the chain. It is much more sensitive than NMR spectroscopy especially for branches longer than six carbon atoms.

Long chain branching has a strong influence on the rheological properties of the materials. Due to the regulated molar mass and narrow MMD, the materials were able to be investigated in melt rheology. This study gives detailed information of activation energy, zero shear-rate viscosity and phase angle of the obtained LCB-PEs by ethylene-graft-ethylene/propylene copolymerization.

Activation Energy

The calculation of Arhenius-type flow activation energy (E_a) is another way to determine the branching architecture of polymers. In contrast to other rhelological values, it is independent of the molar mass and molar mass distribution. It is determined by plotting the zero shear-rate viscosity as a function of the inverse absolute temperature 1000/T. The E_a typically increases with the amount or length of LCBs in the material[92-94]. The Arrhenius-type equation (eqn **3**) gives the activation energy of linear polyethylene as about 28 kJ/mol, and LCB-PE is in the range of 35 to 50 kJ/mol.

$$E_a = \log a_T\,(T, T_0)\,2.3 \cdot R\left[\frac{1}{T} - \frac{1}{T_0} \right] \qquad\qquad\qquad\textbf{(3)}$$

E_a = activation energy   R = gas constant $a_T(T,\,T_0)$ =shift factor

T = temperature of the measurements

T_0 = reference temperature

The E_a of materials prepared at low ethylene pressure (0.6 bar) and different comonomer feeds was calculated, and the E_a of three samples are noticeably different from each other (Figure. 6.25). The E_a of the polymer prepared without any comonomer is 28.8 kJ/mol, very close to the E_a of the linear HDPE reference. The other materials prepared with 2 and 5 % comonomer were found to have approximately 50 kJ/mol E_a relative to the linear reference. However, different concentrations of comonomer have similar activation energies. The similar E_a for each sample can be explained by comparable branch architecture and by the finding that the difference between a star-like polymer and a highly branched system is not very large with respect to the thermorheological properties.
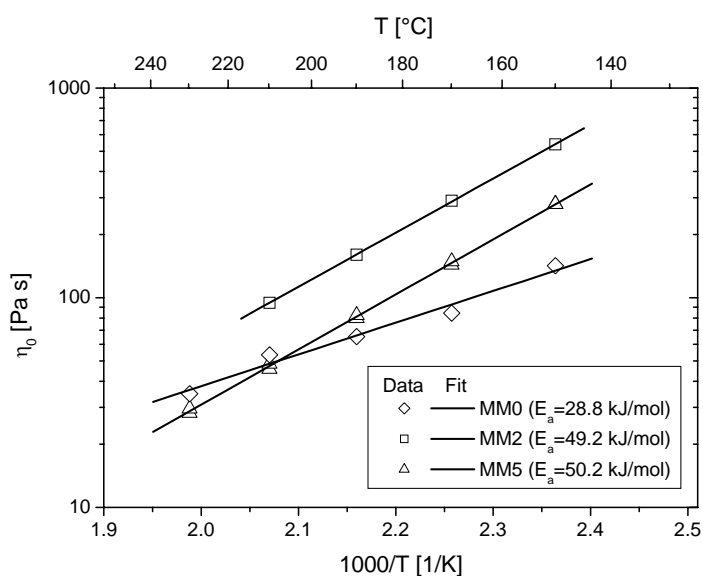
Figure 6.24   Arhenius plots of the zero shear-rate viscosity of the products prepared at low ethylene pressure (MM0: no comonomer, MM2: 2% comonomer MM5: 5% comonomer in the feed

Zero Shear-Rate Viscosity

The rheological characterization was carried out by Dr. F. Stadler at University of Erlangen. The combination of zero shear-rate with the M_w of the materials was examined due to probe the branching structure.

For many linear polymers the well known correlation for the dependence of the zero shear rate viscosity on the molar mass is described by equation 4, where η_0 is zero shear rate viscosity, K_1 is a material which is a temperature dependent constant, and α is an exponent with a value between 3.4 and 3.6.

$$\eta_0 = K_1 \cdot M_w{}^{\alpha} \tag{4}$$

This correlation is valid if $M_w > M_c$. M_c is the critical molar mass and it is typically two times the entanglement molar mass (M_e). M_c is between 2900 and 3800 g/mol for polyethylene.[95] For small molar masses ($M_w < M_c$)

$$\eta_0 = K_2 \cdot M_w \tag{5}$$

K_1 and K_2 are the parameters dependent on the polymer type, temperature, and M_c. This correlation is found to be MMD independent.

However, the zero shear rate viscosity depends not only on the molar mass of the polymers but also on the LCB-topography of the materials. Therefore, eqn 4 can not be directly used for LCB-systems, but the deviation of η_0 from the linear reference given by eqn.4 can be used as an indicator of LCBs.

LCBs show strong influences in the viscosity function. Generally, zero shear rate viscosity increases by introducing small amounts of LCBs, but high amount of LCBs leads to decrease in zero shear rate viscosity.[92,96-98] Therefore, the behavior of linear standard polymer must be known.

The η_0 of the materials shows a very distinct deviation from η_0-M_w correlation established for linear PE[99], and is noticeably above η_0-M_w line (Figure 6.25). The gray area indicates the range where LCB-PEs were found in previous studies.
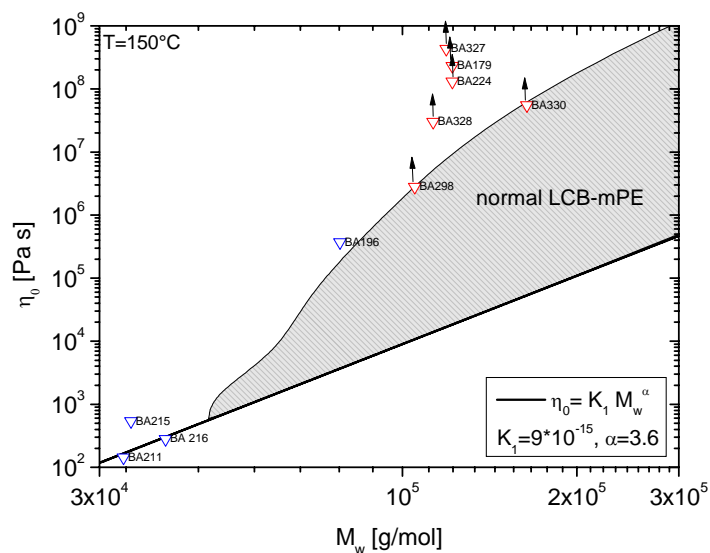
Figure 6.25 Correlation between zero shear-rate viscosity η_0 and molar mass M_w. The gray area indicates the range, where LCB-PEs were found previously[50,59,100]

Phase Angle

The phase angle (δ) as a function of complex modulus ($|G^*|$) can be used as another way to determine the possible presence the LCBs in the materials. However, one has to consider that the same effects can be caused by high molecular tails, thus requiring a thorough *SEC*-analysis.

Therefore, the characterization of the MMD of polymers is essential for a better understanding of viscoelastic behavior of the materials. The influence of the molar mass distribution can be disregarded, as all the materials investigated here have polydispersity of around 2.

The phase angle of viscoelastic fluids is in a range of 0 to 90° and determined by

$tan\ \delta = G``/G`$ $\qquad\qquad\qquad$ $G`` =$ Loss modulus

$\qquad\qquad\qquad\qquad\qquad\qquad$ $G`\ \ =$ Storage modulus

The complex viscosity

$$|\eta^*| = \sqrt{\eta^{`2} + i\eta^{``2}} = |G^*|/\omega \qquad\qquad \omega = \text{frequency}$$

where $\eta` = G`/\omega$ and $\eta`` = G``/\omega$.

It is assumed that for $\omega \rightarrow 0$

$$\lim_{\omega \rightarrow 0} G``/\omega = \lim_{\omega \rightarrow 0} |\eta^*| = \eta_0$$

Figure 6.26 shows the plot of $\delta(|G^*|)$ for the materials prepared with comonomers and other linear references high ethylene pressure. These materials clearly deviate from the linear standard, supporting the finding that they are actually long-chain branched. The comparison of other materials with various comonomer feeds supports this effect. These plots are very similar to LDPE, which are known to have a tree-like branching structure and also a very broad MMD.

According to the topology map established by Trinkle *et al*[101], the characteristic point in the $\delta(|G^*|)$-plot corresponds to highly entangled structures such as asymmetric stars and combs. This is another strong indicator that comb-like structures were synthesized.
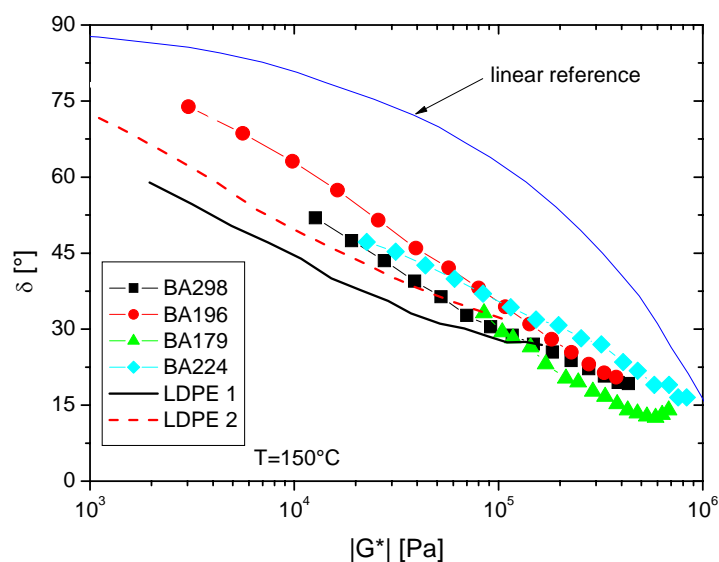
Figure 6.26   Phase angle as a function of complex modulus for the LCB-PEs from the linear references was established elsewhere for PE with $M_w/M_n \approx 2$ [102]

Fig. 6.27 shows the complex modulus $G'(\omega)$ and $G''(\omega)$ and the viscosity functions $|\eta^*(\omega)|$ as a function of frequency. The data are atypical for long-chain branched mPE, which would rather show two separated relaxation times. The shape is typical for LDPE, which has a much broader molar mass distribution. This can be interpreted as the shape of the viscosity function of LDPEs is not dominated by the broad *MMD*, but by the long-chain branching structure.

It is also interesting to note that for none of the polymers examined, neither the terminal nor the rubbery regime could be accessed in dynamic- mechanical tests. This is the consequence of the large frequency range the relaxation processes occupy – leading to the LDPE-like data.
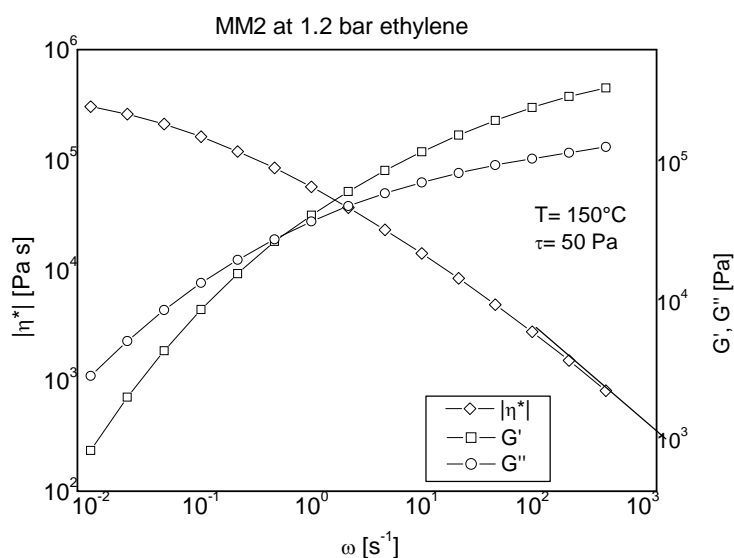
Figure 6.27   the complex modulus $G'(\omega)$ and $G''(\omega)$ and the viscosity functions $|\eta^*(\omega)|$ as a function of frequency.

70

6.3 Direct Synthesis of Long Chain Branched sPP by using Vinyl Chloride as a Chain Transfer Reagent

6.3.1 Introduction

Metallocene systems give polymeric materials with unique properties such as high tacticty, stereoregularity, and narrow polydispersity. Polydipersity of metallocene-based polypropylenes are very low, about 2 to 2.5, which are highly desirable in fine fiber production. The use of these materials in the medical and food containers are highly desirable because of no wax fraction.

The poor melt strength and highly linear structure are the main barriers to the expansion of metallocene-based polypropylene production. Recent studies in this field are focused on the modification of viscoelastic properties of polymers by the insertion of long and short branches as explained in the previous sections.

Although it is very interesting to synthesize long/short branched polyolefins to affect the viscoelastic properties using a tandem system, or by copolymerization methods with varying macromers, the main challenge is multiple reactions and purification steps as mentioned in the previous chapter.

The ideal method is the direct insertion of long chain branches into the main polyolefin chain by a metallocene system to optimise processability and properties of these materials. However, developing an easy synthetic method to arrive at such materials is a difficult problem.

This chapter describes studies of the direct synthesis of syndiotactic polypropene containing long chain branches by metallocene/MAO system where trace amounts of vinyl chloride were present as a chain transfer reagent. Even though using chain transfer reagent for the synthesis of branched polyolefins was studied before, the affect of chain transfer reagent on the material properties were not investigated in detail as in the current study.

Gaynor reported using vinyl chloride as a chain transfer agent to prepare branched polyolefins.[103] Four different MAO activated metallocene cataysts were used in the homo and co-polymerization of ethylene, and in the homopolymerization of propylene. The molar mass, viscosity, and the content of vinyl end groups in the polymeric materials were investigated. The role of vinyl chloride in this system in Gaynor work and this current study are very important and based on β-chloride elimination reported previously Stockland and Jordan.

Figure 6.28 shows the propylene polymerization with and without vinyl chloride. The presence of tiny amount of vinyl chloride in the propylene polymerization causes β-chloride elimination following insertion of one vinyl chloride unit, which gives a vinyl terminated polypropylene chain.[104]
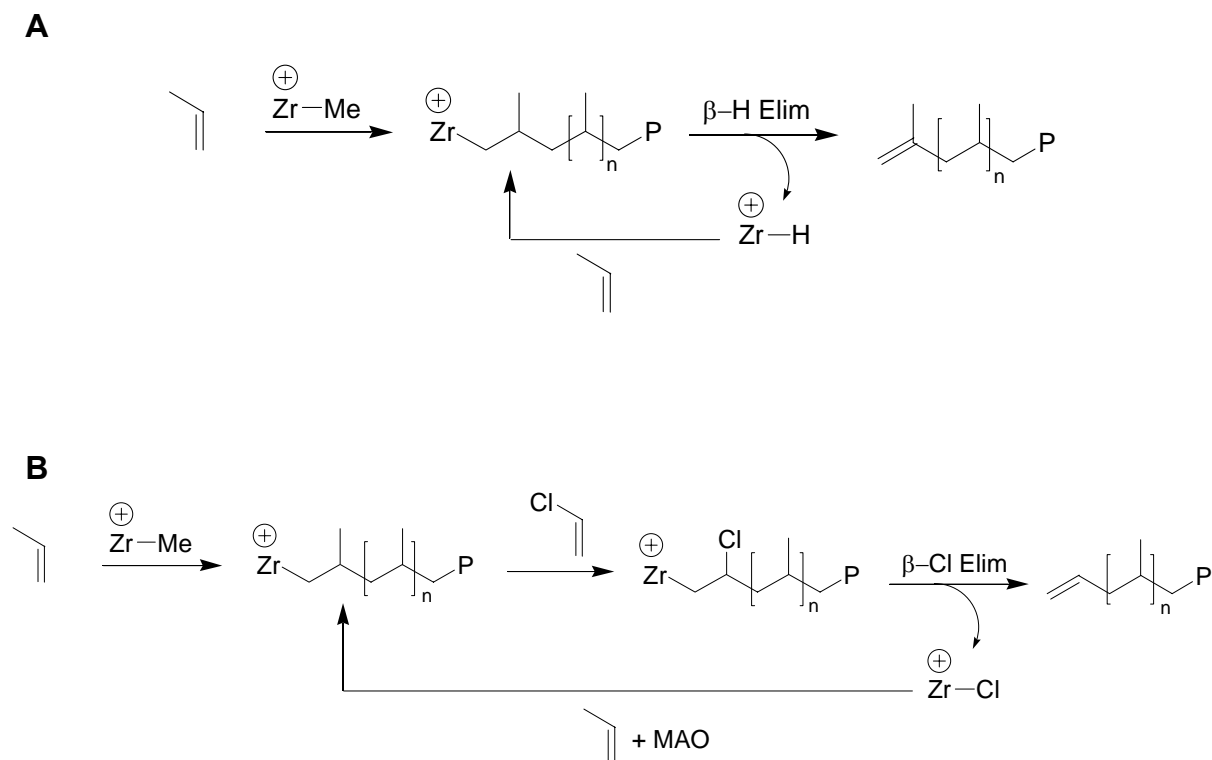
A

B

Figure 6.28   Propylene polymerization without vinyl chloride (**A**) and with vinyl chloride (**B**)

The main aim is the re-insertion of chains containing vinyl terminal groups into the polypropylene chain, allowing long chain branched polypropylenes to be obtained directly in one-pot by a metallocene system.

6.3.2 Materials

A series of syndiotactic polypropylene in the presence of a trace amount of vinyl chloride by metallocene/MAO system was prepared in order to obtain long chain branching materials. The reaction conditions and some of the polymer properties are listed in Table 9. The reactions were performed in the presence of [Ph$_2$C(2,7-di-*tert*-Bu$_2$Flu)(Cp)]ZrCl$_2$/MAO at 30°C. The amount of vinyl chloride in the feed was varied from 0 to 1 g while propylene pressure was supplied continuously by pressure control at 1.54 bar.

Due to the fact that vinyl chloride supports chain termination, the activity of catalyst decreased notably from 1260 to 480 kg$_{poly}$/(mol$_{Zr}$·h·c$_{mon}$) at higher contents of vinyl chloride in the feed. Therefore, the reactions were not able to run VC higher that 1 g in the feed.

Different analytical methods were used to determine long chain branching. The detailed description of the properties of obtained sPP is given in the following sections.

.

Table 6.9   Polymerization conditions and properties of sPP prepared with vinyl chloride as a chain transfer reagent by [Ph$_2$C(2,7-di-*tert*-Bu$_2$Flu)(Cp)]ZrCl$_2$ activated with MAO (1 mg/ml) at 30 °C

Reaction Parameters							Properties		
Art	$n_{catalyst}$	c_{mon} [a]	p_{mon} [a]	m_{VC}	n_{VC}	VC/Zr	T_m [b]	M_w [c]	Activity [d]
	[mol]	[mol/l]	[bar]	[g]	[mol]		[°C]	[kg/mol]	
PP	$1.18 \cdot 10^{-6}$	1	1.54	0	0	0	141	311	1260
PP/VC	$1.18 \cdot 10^{-6}$	1	1.54	0.25	0.004	33898	141	210	660
PP/VC	$1.18 \cdot 10^{-6}$	1	1.54	0.50	0.008	67796	141	175	520
PP/VC	$1.18 \cdot 10^{-6}$	1	1.54	1.00	0.016	135593	142	128	480

[a]propylene, [b]melting point determined by DSC, [c] molar mass determined by GPC, [d] Activity: kg$_{poly}$/(mol$_{Zr}$·h·c$_{mon}$), yield: 1 to 3 g, V$_{toluene}$: 200 mL

6.3.2.1   SEC-MALLS

Figure 6.29 shows the molar mass distribution curves of the polymer synthesized without VC and of those produced with traces of VC. Table 2 displays the absolute molar mass values determined by coupled GPC-MALLS. Figure 6.29 and table 6.10 clearly show that the weight average molar mass is decreased when the synthesis is performed in the presence of VC, due to the chain transfer behavior of VC. The width of the molar mass distribution characterized by the ratio M_w/M_n remains unchanged.
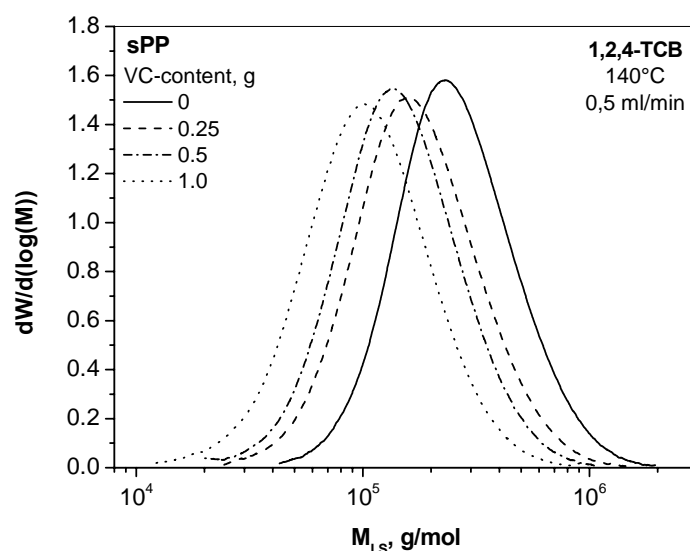
Figure 6.29   Molar mass distribution curves as a function of absolute molar mass for sPP synthesized in the presence of different small amounts of VC.

Table 10 Absolute molar masses determined by GPC-MALLS for the polymers synthesized using different VC-concentrations during synthesis

Poly. Type	VC-content [g]	M_w [kg/mol]	M_n [kg/mol]	M_w/M_n [-]
sPP-0	0	311	155	2.0
VC-sPP-0.25	0.25	210	104	2.0
VC-sPP-0.5	0.5	175	90	1.9
VC-sPP-1	1.0	128	65	2.0

Figure 6.30 depicts the coil dimensions as a function of the absolute molar mass for the polymer synthesized without VC and that with 1.0g VC. The radius of gyration for the sPP without VC gives the well known power-law dependence indicating linear molecule topography. The power law exponent for the material is 0.60 which is close to the value of 0.58 reported for syndiotatic polypropylene.[105]
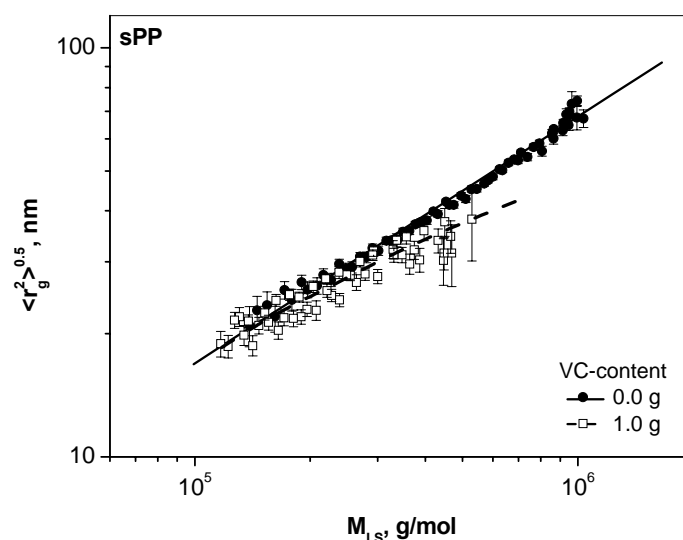
Figure 6.30   Conformation plot for the polymer produced without and with 1.0 g VC

For the polymer synthesized in the presence of 1.0g VC a slightly different dependence of the radius of gyration on the molar is found. At low molar masses the radius of gyration lies on the scaling law for the linear sPP. At molar masses above 300,000 g/mol a subtle deviation towards smaller radii is found indicating a slight coil contraction which is a hint to the formation of long chain branches during synthesis. The radii of gyration of the polymers produced with the lower amounts of VC are within the experimental error identical with the linear reference polymer. Thus, the concentration of long-chain branched species is so small that it cannot be resolved by *GPC-MALLS*.

6.3.2.2   Tacticity

The microstructure of polyolefins has a strong influence on the viscoelastic properties of the material such as melting point, crystallinity, stiffness which gives them different technical application possibilities.

The microstructure of polypropylenes produced with MAO activated *Cs*-symmetric fluorenyl catalysts in a presence of vinyl chloride were investigated by ^{13}C-NMR measurement. The effect of vinyl chloride on the tacticity of the resulting materials was analysed in order to detect differences in the material properties. Shown in Figure 6.31 is the possible pentads in syndiotactic polypropylene.[106] The signals of rmmr- and mrmm-pentads overlap to each other so they are calculated together.
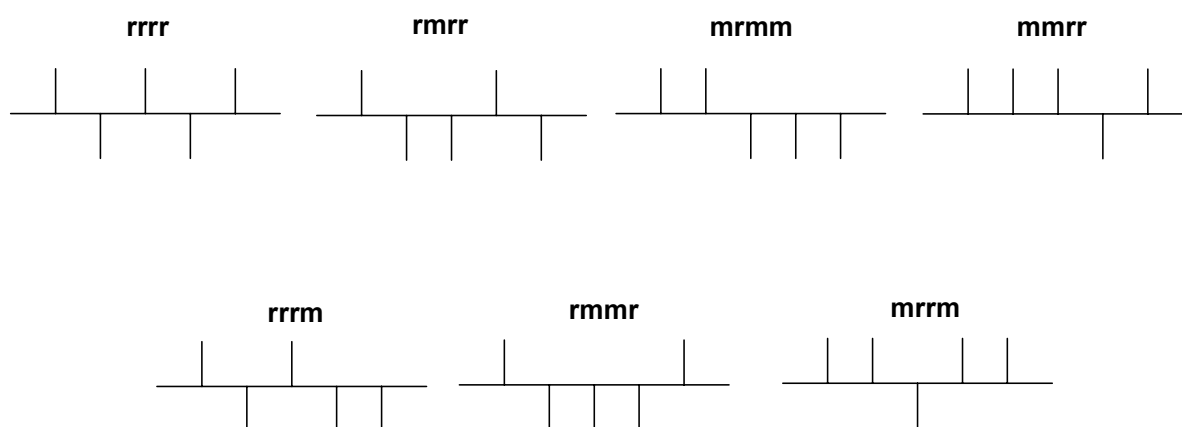
Figure 6.31   Syndiotactic polypropylene pentads observed in the polymers

Table 11 lists the pentads of syndiotactic polypropylene materials prepared. There was no influence of vinyl chloride on the stereoregular rrr-pentaden observed. The tacticity was approximately 91%. The NMR-data indicates that the syndiotacticity stays approximately unaffected by the introduction of VC at 91-92%.

Tabel 11   Determination of pentads distribution and tacticity of the materials at different amount of VC in the feed

Pentaden [%]

Art	m$_{VC}$	*rmmr*	*mrmm + rmrr*	*mmrr*	*rmrr*	*mrrm*	*rrrm*	*rrrr*
	[g]	[21.43]	[20.89]	[21.09]	[20.76]	[20.19]	[20.24]	[20.36]
PP	0	1.03	1.41	2.05	-	3.7	-	91.82
PP/VC	0.25	1.41	1.14	1.45	-	4.19	-	91.72
PP/VC	0.50	-	1.62	1.89	-	5.44	-	91.09
PP/VC	1.00	0.82	1.43	1.21	-	5.16	-	91.40

6.3.2.3   Melt Rheology

Because of the small amount of sample available only rheological measurements in the linear viscoelastic regime could be performed. The syndiotacticity of the samples is not influenced by the VC (see NMR-data), and this factor can be safely ignored in the forthcoming discussions.

Figure 6.32 shows the master curves of the samples synthesized without VC, with 0.5 g, and with 1 g of vinyl chloride (*sPP-0, VC-sPP-0.5,* and *VC-sPP-1*, respectively). VC *sPP-0* was found to behave thermorheologically simple. The sample *VC-sPP-0.5* did not behave similarly in the strict sense, as $G'(\omega)$ at low ω frequencies cannot be properly included in the master curve. Also $G'(\omega)$ and $G''(\omega)$ run almost parallel at the low frequency.

The viscosity function $|\eta^*(\omega)|$ also has a constant slope (even with a very small tendency for becoming steeper around 0.1 s^{-1}), which is commonly referred to as S-shape and associated with long-chain branches. The observation that the quality of the "master curve" of this sample is of inferior quality around this frequency ω is also an indicator of long-chain branches, (and the non-matching $G'(\omega)$-data) corresponding to a thermorheological complexity usually found for miscible blends and slightly branched systems such as LCB-mPE. This was also recently affirmed for PP.[2] The linear viscoelastic data of VC-PP-0.25 are very similar to VC-PP-0.5 and are not shown here.

Due to the significantly lower M_w of VC-PP-1, the terminal regime could be reached in $G''(\omega)$ and η_0, while the constant slope of 2 in $G'(a_T\times\omega)$ is not reached yet. This is typical for narrowly polydisperse polymers – the terminal relaxation times of the viscous and elastic parts of the deformation differ distinctly. But also in this sample a clear mismatch of $G'(a_T\times\omega)$ is observed between $a_T\times\omega=1$ and 0.01 s^{-1} – again indicating a thermorheological complexity. It was not possible to obtain correct values for $G'(a_T\times\omega)$ below 0.01 s^{-1}, due artifacts induced by the low storage modulus and the resulting high tanδ. Both findings are an indicator of long-chain branches, although the parallelism of $G'(\omega)$ and $G''(\omega)$ can also be caused by atypical molar mass distributions (high molecular tails), which was not observed in GPC for any of the samples examined.
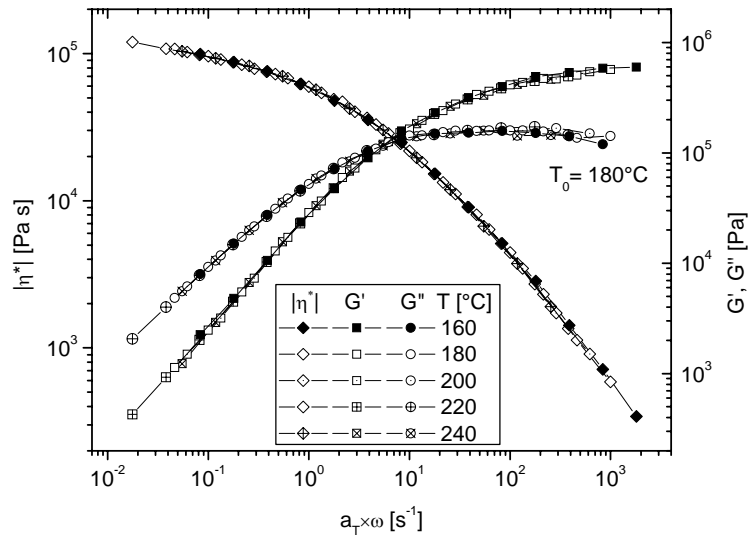
A)
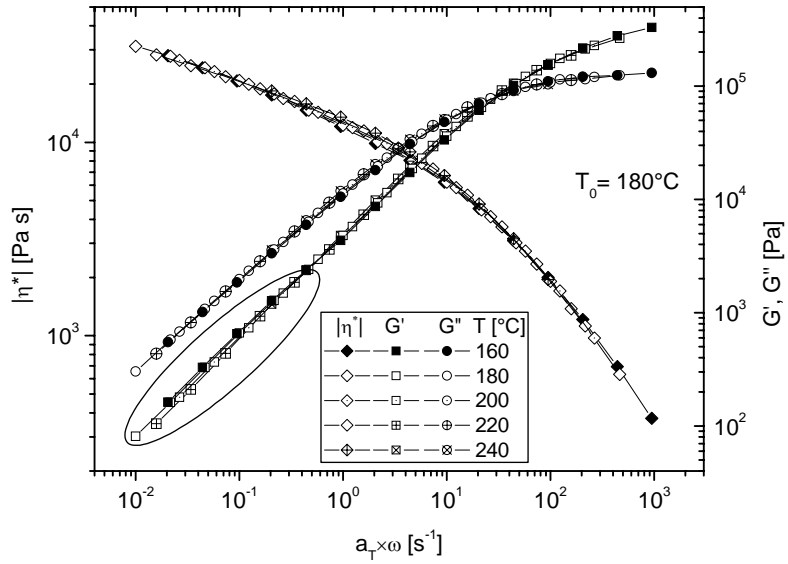
B)
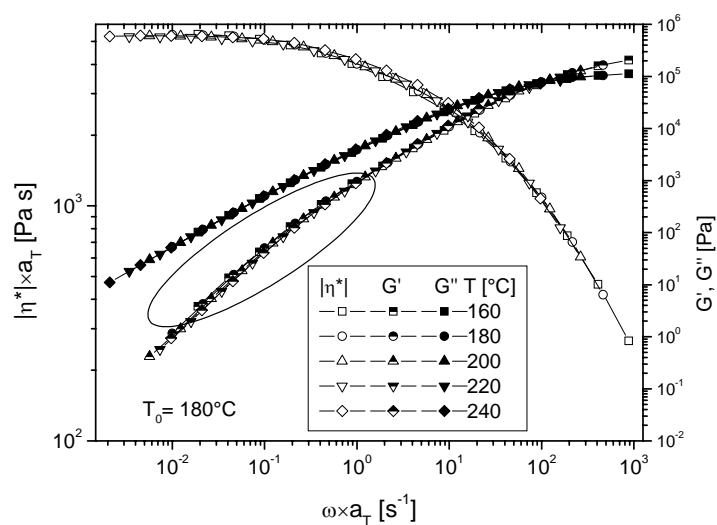
C)

Figure 6.32   Master curves of the samples with **A)** 0g VC, **B)** 0.5g VC, **C)** 1 g VC

The plot $\delta(|G^*|)$ was reported to be very successful in the detection of even very sparse degrees of long-chain branching.[100,107-108] Also this is the best plot for assessing the presence of any thermorheological complexity. Figure 6.33 shows that the $\delta(|G^*|)$-plots of the samples with different VC-contents do not have an obvious tendency. Usually a reduction of $\delta(|G^*|)$ – a deviation from the linear reference – is associated with a higher degree of long-chain branching (or a high molecular tail). While the reduction of $\delta(|G^*|)$ in the range around $|G^*|=10^4$ Pa with increasing VC-content is immediately obvious for the samples with 0, 0.25, and 0.5 g VC-feed, the $\delta(|G^*|)$-plot of VC-PP-1 seems to strongly disagree with this trend, indicating initially the LCB-content of VC-PP-1 is lower than that of VC-PP-0.5. However, one has to be aware that the $\delta(|G^*|)$-plot is highly molar mass dependent for sparsely branched systems.

It was previously shown for LCB-mPE that halving the LCB-content (in terms of LCB/10000 C), but increasing the molar mass M_w by 70%, will lead to a significantly larger reduction of $\delta(|G^*|)$.[102] To understand this feature is is necessary to know that in sparsely branched samples – consisting basically of linear chains and stars – the reduction of $\delta(|G^*|)$ is governed by several factors. The most obvious factor is the LCB-concentration, but also arm length plays a significant role, which roughly corresponds to M_n.[109-110] As M_w/M_n is found to be around 2, a dependence of the $\delta(|G^*|)$-plot on the molar mass M_w is found here. For this reason the reduction of $\delta(|G^*|)$ always has to be assessed keeping the differences in molar

mass in mind.

The significantly lower molar mass of VC-PP-1 (128 kg/mol vs. 175 kg/mol for VC-PP-0.5) is the reason for this apparent disagreement. While the samples VC-PP-0.25 and VC-PP-0.5 show similar behavior to LCB-mPE with sparse long-chain branching around $M_w \approx 150$ kg/mol, the shape of the $\delta(|G^*|)$-plot of VC-PP is typical for samples with $M_w \approx 70$ kg/mol.

A comparison between the $\delta(|G^*|)$-data of the samples (fig. 6.33) shows that the sample without any VC is mildly deviating from the shape of the linear reference for PE, which could be a consequence of its relatively high molar mass M_w (It was found that an increase of the M_w of a sample leads to a broader transition zone between the elastic ($\delta \rightarrow 0°$) and the viscous regime ($\delta \rightarrow 90°$)[111]. This finding does not mean that it contains long-chain branching, but rather that the very small deviation from the linear reference could be either attributed to the molar mass dependence of the width of the transition between the shear thinning and the terminal regime,[99, 111] or an extremely small degree of long-chain branching – too small to be safely detected by any means available today.
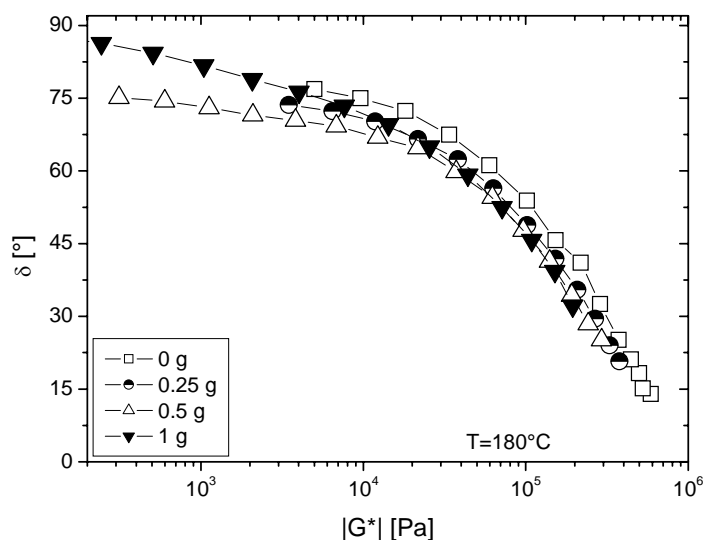
Figure 6.33 $|G^*|$-δ-plots for the samples with different VC-contents

The curves obtained at different temperatures for the sPP-0 sample are found to match very well, which implies that this sample is thermorheologically simple. This indicates the validity of the master curve constructed for this polymer (fig. 6.32A). The sample with 1g VC, however, shows a distinct and systematic disagreement between the data obtained at different temperatures, a strong indicator of long-chain branching. The sample *VC-sPP-0.5* shows the same feature but is less pronounced. This is an indicator of a lower degree of long-chain branching in the latter sample.

A)

B)

C)
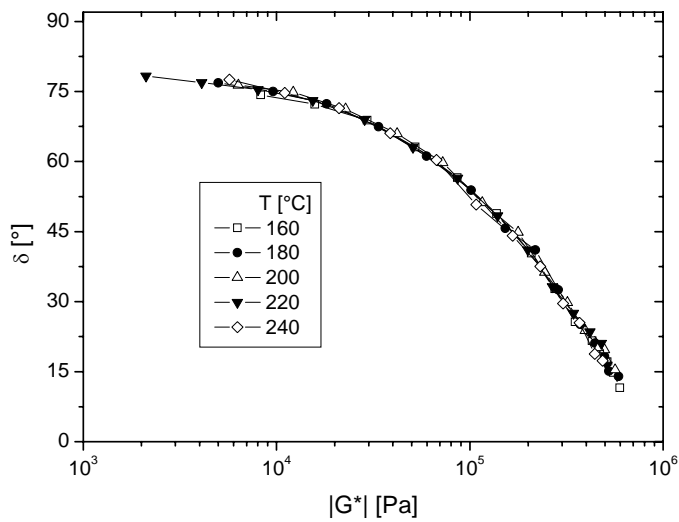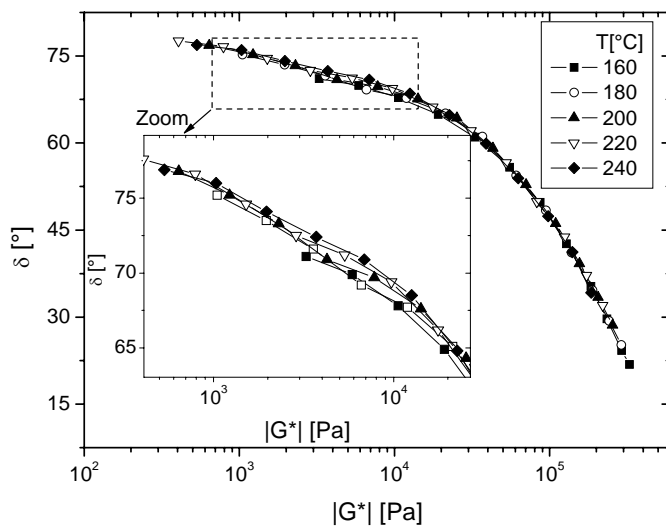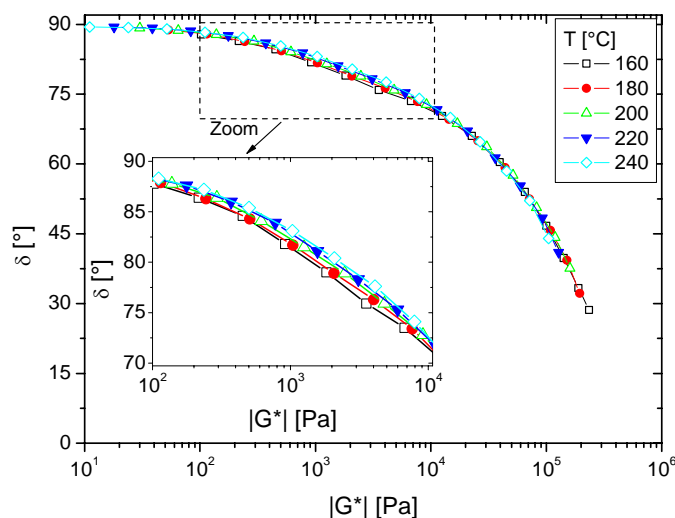
Figure 6.34 $|G^*|$-δ-plots of the samples with A) sPP-0, B) VC-sPP-0.5, C) VC-sPP-1.

When comparing the Arrhenius plots of the two samples (being aware of the thermorheological complexity of the sample with 0.5 g and 1g VC) it is clearly evident that the linear reference is less temperature sensitive than the sample synthesized in the presence of VC. An increase of the E_a with an increasing VC-feed is found (see insert in fig. 6.35), which is systematic but within the error margin usually given for E_a (±10%). The increase of activation energy E_a is usually associated with the introduction of side-chains into the main polymer chain.[67, 112-114] Both the introduction of short and long-chain branches leads to an increase of E_a, but since there are no short-chain branches supplied in the reactor, this possibility can be excluded. The increased E_a is a strong indicator of the incorporation of long-chain branches. The activation energy E_a of the linear sPP of 44.9 *kJ*/mol is somewhat higher than found for iPP (E_a≈41 *kJ*/mol).[115-117]
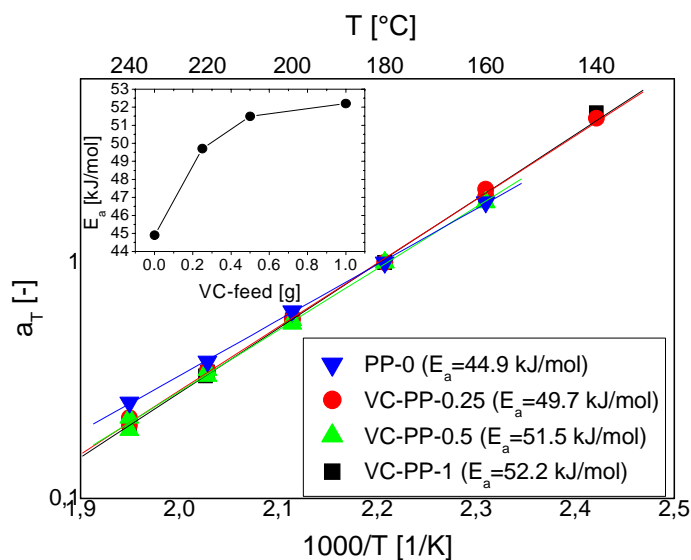
Figure 6.35   Arrhenius plots syndiotactic polypropylene synthesis without VC and with VC
(0.25, 0.5 and 1 g)

Another very useful quantity for the assessment of the presence of long-chain branches is the η-M_w-relation, which follows a 3.4-3.6 power law for linear polymers and is usually not fulfilled for long-chain branched samples.

To determine the zero shear-rate viscosity η, creep tests were used in the linear viscoelastic regime at 180°C (fig. 6.36). In the creep compliance J(t') reaching η corresponds to a double logarithmic slope of 1, which could be obtained for sPP-0, VC-sPP-0.25, and VC-sPP-1 at approximately J(t')>0.1. For VC-sPP-0.5, reaching the zero shear-rate viscosity η was not possible, the slope of J(t') decreases with increasing creep time. This behavior is the same as found for long-chain branched mHDPE with a very high molar mass and is caused by the onset of the significant influence of the sparse very long long-chain branches. Another possibility could also be that some change takes place in the chemical structure of VC-sPP-0.5, leading to an increase of η. This would mean that VC-sPP-0.5 would start cross linking, a behavior typically found for PE but not for PP, which usually decomposes before the cross linking sets in.[112] Figure 6.36 also clearly shows that (when disregarding VC-sPP-0.5) the introduction of VC leads to a clear decrease of the zero shear-rate viscosity η, indicated by the faster rise of the creep compliance J(t').
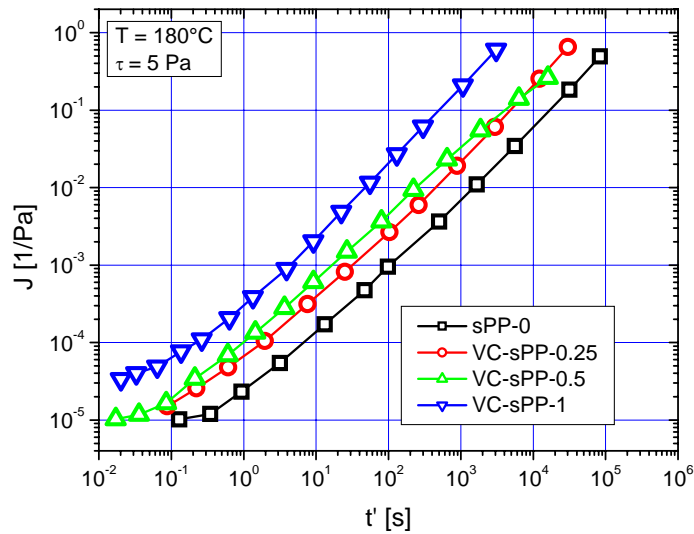
Figure 6.36   creep compliance. A slope of 1 indicates that η_0 has been reached.

Figure 6.37 shows the $\eta_0(M_w)$-correlation for the linear reference and the three VC-sPP samples. Although only one linear sPP-sample with the syndiotacticity of approximately 91% is available, a correlation between η_0 and M_w was laid through this sample using the slope of Auhl et al..[112] Thus this η_0-M_w-correlation can only be taken as an approximate reference.

The introduction of VC leads to a reduction of η_0 because of the reduction of M_w, but it becomes evident from Fig. 6.37 that a small amount of VC leads to an increase of η_0 in comparison to the linear reference, designated as η_0^{lin}. Thus η_0/η_0^{lin} is larger than 1 for VC-PP-0.25 and VC-PP-0.5. For VC-PP-1, however, η_0/η_0^{lin} is 0.66, as this sample lies below the linear η_0-M_w-reference.

While this might seem confusing, it is exactly what would be expected. Bersted[96] was the first to report that a low amount of long-chain branching leads to an increase of η_0, while a high amount decreases η_0. Although the "Bersted-model"[96] is only valid for constant M_w, it is qualitatively correct, if the molar mass changes. Auhl et al.[112] found a very similar behavior for electron beam irradiated iPP.
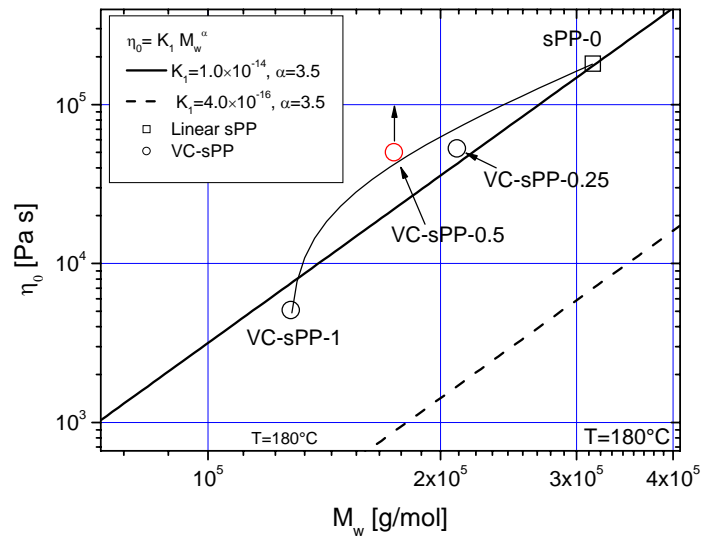
Figure 6.37   correlation between zero shear-rate viscosity η_0 and weight average molar mass M_w for different VC-contents. The line connecting the data was added to guide the eye according to the shape found elsewhere for comparable systems.[92,96, 112]

6.4 Conclusion

Different kinds of LCB-Polyolefins were synthesized by using two different methods in the presence of MAO activated metallocene based systems. In the first method, highly soluble EP-comonomers were synthesized and used in copolymerization with ethylene to form long chain branches. The branches were detected by using different analytical methods. The materials were analysed by SEC-MALLS. The MMD of materials was unimodal with M_w/M_n around 2 and the material does not contain any residual EP-comonomers. In addition, a significant contraction of $<r^2>^{0.5}$ was found for this sample proving branching structure. The incorporated comonomers showed significant influence of the melting temperature. The synthesized LCB-PEs showed very interesting rheological which is relatively similar to that of LDPE, which typically has a much broader *MMD*.

The high zero shear-rate viscosity made the elongational viscosity for most samples impossible. The LCB-PEs reported here are fairly complicated to synthesize and thus too expensive to be used in pure form in most applications.

In the second method, syndiotactic polypropylenes were synthesized in a presence of vinyl chloride. The different rheological indicators and the *GPC-MALLS* measurements point to the conclusion that the use of vinyl chloride gives the formation of long-chain branches. The shape of the viscosity and modulus functions and the $\delta(|G^*|)$-plots are a typical for LCB-, which is believed to have a similar LCB-formation mechanism.

The increase of E_a by 7 *kJ*/mol might not appear to be very large, but the increase of the activation energy of sparsely branched LCB-mPE is not much larger. The next question is how much the activation energy is simply the sum of the activation energy of a linear polymer and the contribution of the long-chain branching. But unfortunately there is neither a sufficient amount of data available for this material, nor can any conclusion be drawn with respect to the effect of different monomers on E_a of long-chain branched samples of a given topography.

For this reason, it can only be stated that the increase of E_a by the addition of VC is a clear indicator of long-chain branching, but the amount cannot be quantified. The fact that the samples are slightly thermorheologically complex is an indicator that they only contain sparse branching, as highly branched PE-samples were found to be thermorheologically simple.

The η_0-M_w-correlation clearly fails for all VC-sPPs indicating long-chain branching. The η_0-M_w-correlation indicates that all VC-sPP-samples are long-chain branched. Because of the different molar masses M_w, further quantification proves difficult. This transition from $\eta_0/\eta_0^{lin}>1$ to $\eta_0/\eta_0^{lin}<1$ was previously associated with a shift of the dominance of star-like chains to the higher branched chains, mostly tree-like chains.[92, 96, 125] Recently it was shown that this transition can also happen at quite low molar masses, if the degree of long-chain branching is very low, for example, if stars and linear chains dominate.[126] In the case of PE this requires M_w to be below approximately 50 kg/mol. As the entanglement molar mass M_e of sPP a little more than twice the value of PE,[125] this critical molar mass can be considered to be in the order of 120 kg/mol for sPP. Hence, the decrease of η_0/η_0^{lin} with increasing VC-content is also determined by the molar mass, which decreases the average arm length of the star molecules and thus leads to a decrease of the η_0/η_0^{lin}.

The polypropene sample synthesized without any VC does not contain sizable amounts of long-chain branches which were shown by the absence of thermorheological complexity and low activation energy. The use of VC in the polymer synthesis leads to slightly branched samples. These samples have higher activation energy and show signs of a thermorheological complexity, both of which are definitive indicators a slightly branched system.

7 SYNTHESIS OF POLYOLEFINS BY TRIS(PYRAZOLYL) BASED CATALYSIS

7.1 Introduction

Catalytic systems based on various metallocene/MAO are well known and have been studied for the polymerization of ethylene and higher olefines. The importance of early transition metal, non-metallocene catalysts has grown significantly because of the variability in structure which could cause different material properties in the polymer. One focus has been related to tris(pyrazolyl)borate ligands, shown in Figure 7.1, with titanium, zirconium, and hafnium metals because of their analogous properties to cyclopentadienyl (Cp) ligands. Both ligands are hard monomeric six-electron-donors, but tris(pyrazolyl)borate ligands (Tp) ligands differ from Cp ligands because they are able to form *fac*-octahedral complexes.
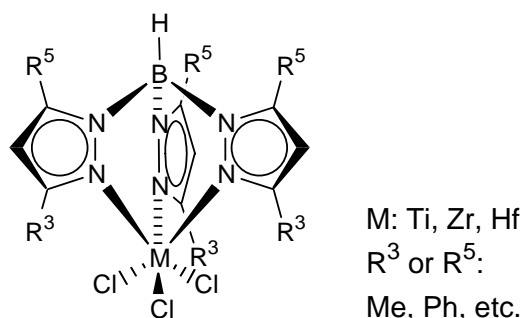

Figure 7.1   The general structure of tris(pyrazolyl)borate complexes

The combination of a Tp ligand with a Cp was first synthesized as (hydrotris(pyrazolyl)borato)dichlorocyclopentadienyl-zirconium(IV) [TpCpZrCl$_2$] and (hydrotris(3,5-Me$_2$-pyrazolyl)borato)dichlorocyclopentadienyl-zirconium(IV) [Tp*CpZrCl$_2$] complexes.[118] However, their behaviour in the olefin polymerization was not studied. Later, some of Tp and Cp based catalysts were studied very briefly in the polymerization of olefins but the detailed studies were performed on only Tp based catalyst system.[127-128]

Olefin polymerization study focused on tuning the Tp ligand with group (IV) metals and their behaviour in ethylene and ethylene/hexene polymerization were examined, as MAO activated species.[119-121] Depending on the size of the ligands at the 3- and 5-pyrazoyl positions it was possible to tune the material properties of the polymers. The Zr-Tp derivatives showed high activity, generating high M$_w$ and and narrow polydispersity polyethylene when the ligand had moderately bulky substituents. In addition, up to 26 mol% of 1-hexene incorporation was observed. Varying MAO amount in the reaction indicated that the chain transfer is alkyl exchange with aluminium instead of β-hydride elimination. Ti based Tp catalysts used in ethylene homopolymerization produced bimodal polymer fractions, which suggest more than one active polymerization species.

The objective of this work was to synthesize a new class of zirconium complexes containing both Cp and Tp ligands, and study their behaviour in ethylene and higher olefin copolymerizations. The role of the Cp ligand is enhancing rigidity in the catalyst system, as well as prevents formation of more than one active species in the polymerization.

The synthesis of new and known Tp ligands, and their zirconium based complexes, will be discussed. The properties of Tp catalysts are highly dependent on the ligand substituents at 3- and 5-pyrazoyl positions, therefore the synthesis of different CpTp complexes synthesized, and then their behaviour in the ethylene polymerization was explored. Shown in Figure 7.2 is the general structure of Tp′CpZrCl$_2$ complex.
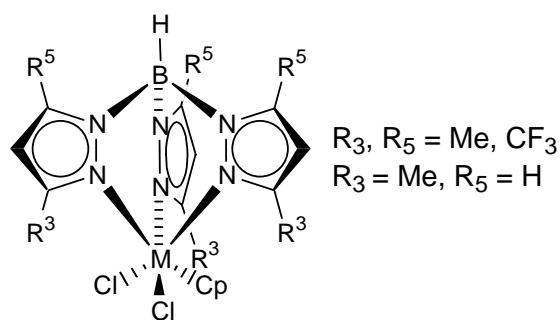
Figure 7.2 The various tris(pyrazolyl)borate complexes in this study

7.2   Synthesis of Pyrazol Ligands and Their Complexes

Three different Tp ligands were prepared according to known procedures, and their synthesis and characterization are explained in the experimental section. Alkali metal or Tl salts of the Tp ligand were used to metallate $CpZrCl_3$. These ligands were chosen as a systematic study of steric and electronic effects on the catalysts.
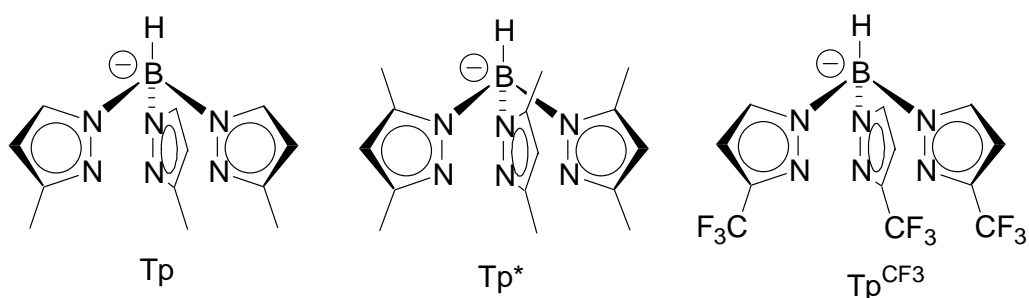
Figure 7.3   The various tris(pyrazolyl)borate complexes in this study

The general synthetic strategy for $TpCpZrCl_2$ complexes involves either salt metathesis using the alkali metal Tp derivate, or the Tl salt (Scheme 1). These procedures were based on those of Reger, but were modified as explained in the experimental section. $CpTp*ZrCl_2$ (**5**) was prepared by reacting $TlTp*$ with $CpZrCl_3$. The reaction of $NaTp^{CF3}$ and $TlTp^{CF3}$ with $CpZrCl_3$ in different solvents (THF and CH_2Cl_2) resulted in decomposition of the ligands, with little or no product formation. Coordination of the CF_3 based Tp ligand was probably inhibited due to the higher electonegativity of CF_3 group relative to CH_3 at the three positions on the ligand.
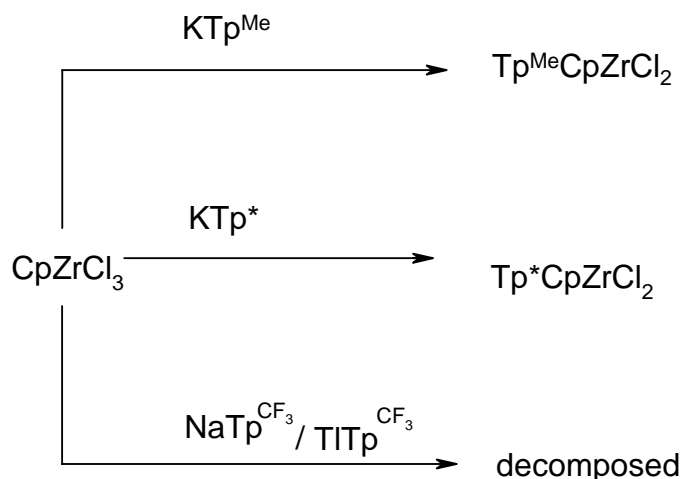
Scheme 1 The various tris(pyrazolyl)borate complexes in this study

5 and **6** were synthesized using the above strategy, but the CF_3 derivative was unstable for isolation (Figure 7.5). **5** contains methyl substituents at the 3-position of Tp ligand, and **6** has methyl substitution at the 3- and 5-positions.
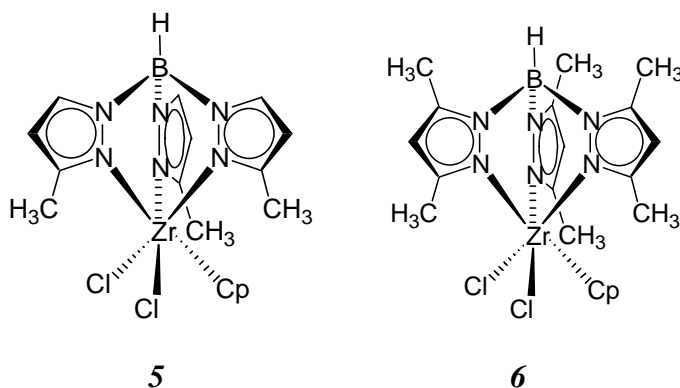
Figure 7.5 The Tp′CpZrCl$_2$catalysts used *5)* $Tp^{Me}CpZrCl_2$ *6)* $Tp^*CpZrCl_2$

Due to known isomerization of substitued Tp ligands, the relative positions of the methyl groups in **5** was explored by a 2D-NOESY. The replacement of the Cl with a Cp group the zirconium metal gives one inequivalent methyl group. The NOESY spectrum clearly contains an interaction between the two equivalent methyl groups and the Cp ligand, proving that the methyl groups are placed as shown in **5**.
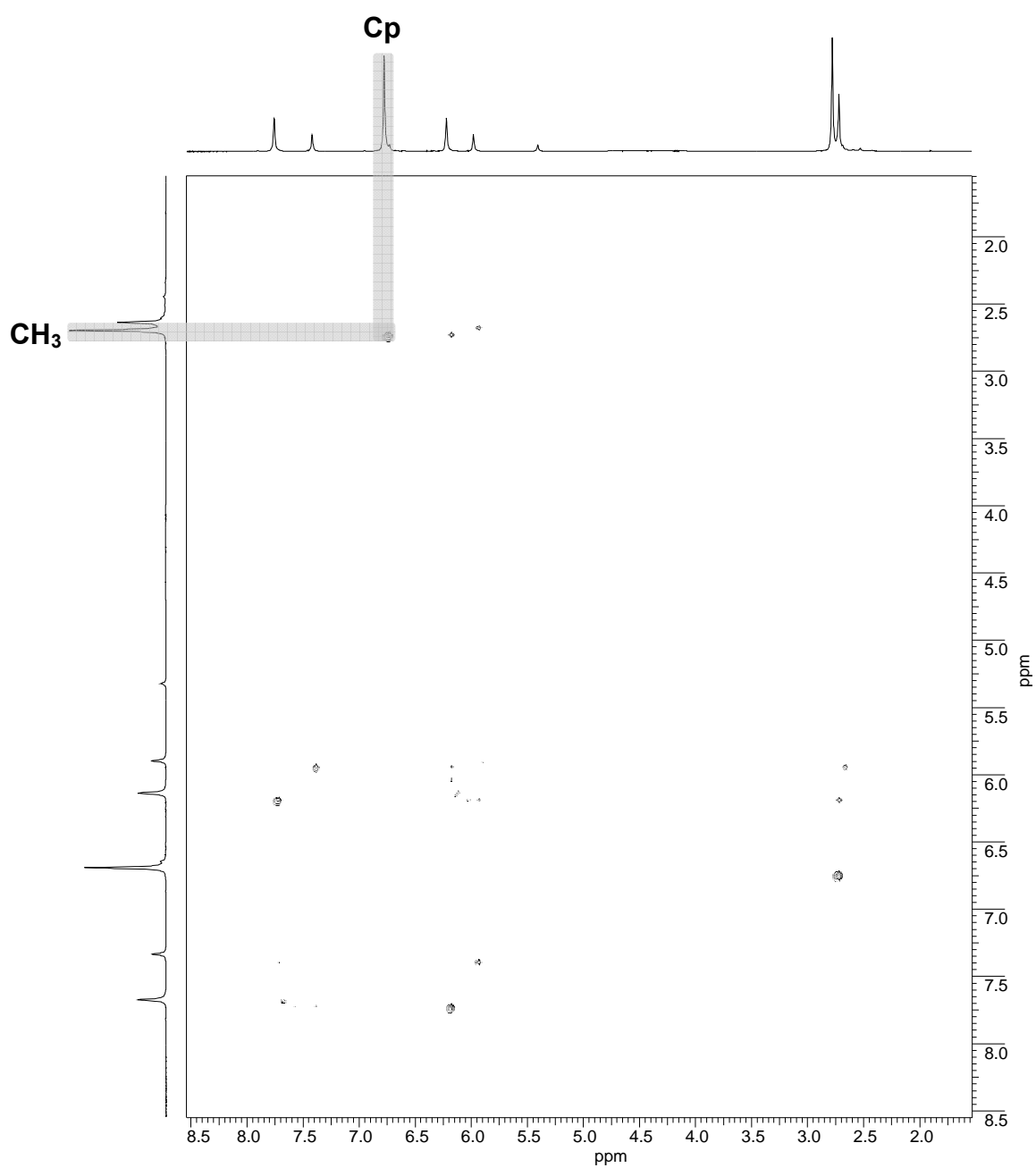
Figure 7.6   NOESY   spectrum   of   [hydrotris(3-methylpyrazolyl)boratodichloro] cyclopentadienyl-zirconium

7.3 Polymerization of Ethylene and 1-Hexene in the Presence of Tp´CpZrCl₂ Complexes Materials

The ethylene homopolymerization and ethylene/hexene copolymerizations were examined in the presence of MAO activated **5** and **6** (Figure. 7.7). The polymerizations were performed under low ethylene pressure in glass Fisher-Porter bottle at 60 °C, and parameters are summarized in Table 7.1.

$$Tp´CpZrCl_2 \quad + \quad 200/1000\ MAO \xrightarrow[\text{toluene}]{\qquad \qquad} \text{Homo-/Co-polymer}$$
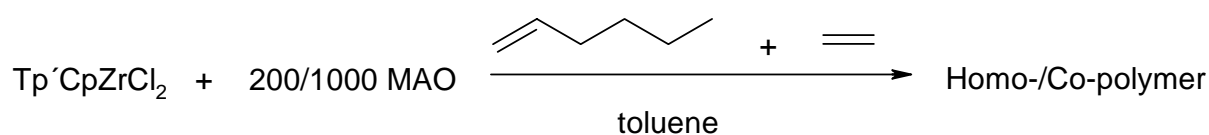
Figure 7.7   The Tp´CpZrCl₂catalysts used in this work *5)* $Tp^{Me}CpZrCl_2$ *6)* $Tp^{*}CpZrCl_2$

Table 7.1   Polymerization conditions prepared with MAO activated TpCp based catalysts in toluene (polymerization time: 1h, $V_{toluene}$: 50 ml)

Polymerization Parameters

Art	Cat.	$n_{catalyst}$ [mol]	$T_{poly.}$ [°C]	Al/Zr	$c_{ethylene}$ [mol·L⁻¹]	$p_{ethylene}$ [bar]	$X_{ethylene}$	X_{hexene}
Homo PE				200	0.1	1.2	1	-
Homo PE	5	$1·10^{-6}$	60	1000	0.1	1.2	1	-
PE/Hexene				200	0.1	1.2	0.9	0.10
PE/Hexene				1000	0.1	1.2	0.9	0.10
Homo PE				200	0.1	1.2	1	-
Homo PE	6	$1·10^{-6}$	60	1000	0.1	1.2	1	-
PE/Hexene				200	0.1	1.2	0.9	0.10
PE/Hexene				1000	0.1	1.2	0.9	0.10

7.3.1 Polymerization Results

The ethylene polymerization behaviour of sterically hindered and open Tp′MCl$_3$ complexes were studied under MAO activation conditions, and their ability to incorporate higher α-olefins and the major chain transfer mechanism were studied by varying Al/Zr ratio.[120, 122] The sterically crowded Tp′MCl$_3$ complexes showed higher activity and higher incorporation of hexene up to 26 mol %.[120, 122] The major chain transfer mechanism in both sterically crowded and open Tp′MCl$_3$ complexes is chain transfer to MAO and AlMe$_3$ (Figure 7.8) giving polyethylene with saturated chain ends.
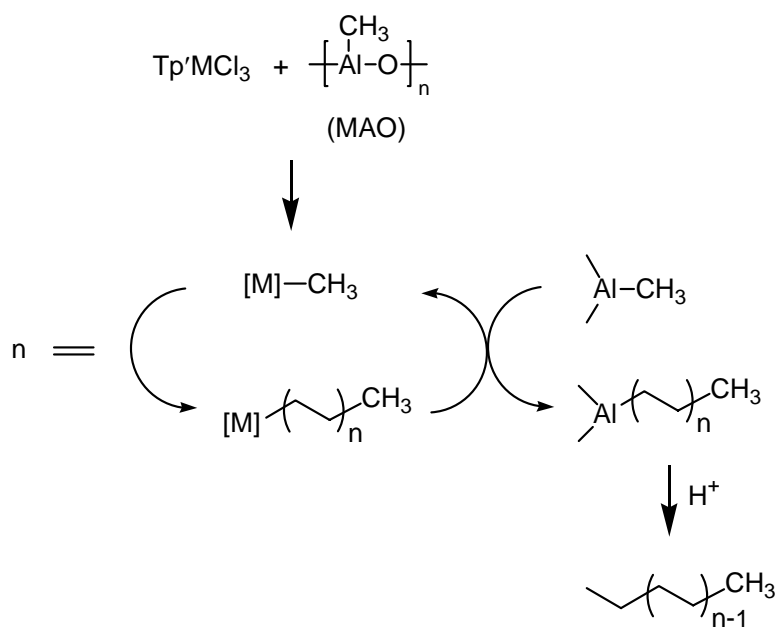
Figure 7.8   Major chain transfer mechanism of Tp′MCl$_3$ to MAO and the AlMe$_3$[120, 122]

MAO activated CpTp`ZrCl$_2$ were used in the homo and copolymerizations and the Al/Zr ratio was varied from 200 to 1000 in the both cases. The polymers were analyzed by ^{13}C NMR to explore material properties, and to obtain a better understanding of the chain transfer mechanism in this system. Polymerization results are summarized in Table 7.2

Table 7.2   Ethylene and ethylene/1-hexene copolymerization by **5**/MAO and **6**/MAO

Polymerization Results

Art	Cat.	Al/Zr	Activity[a] [kg$_{poly}$/(mol$_{Zr}$·h·c$_{mon}$)]	M$_w$[b] [g/mol]	MMD [M$_w$/ M$_n$]	hexene[c] [mol %]	T$_m$[d] [°C]
Homo PE		200	2060	184700	3.2	-	127.1
Homo PE	5	1000	3500	196200	3.1	-	139.5
PE/Hexene		200	1900	241100	3.4	n.d	125.4
PE/Hexene		1000	3700	325300	3.2	3.64	124.4
Homo PE		200	1220	n.d	n.d	-	134.6
Homo PE	6	1000	2340	483000	3.2	-	138.8
PE/Hexene		200	1100	216600	3.3	n.d	131.4
PE/Hexene		1000	2970	267800	2.6	1.79	126.8

^{a}[kg$_{poly}$/(mol$_{Zr}$·h·c$_{mon}$)], ^{b}Determined by GPC, ^{c}Determined by ^{13}C NMR, ^{d} determined by DSC

Highly linear polyethylenes were obtained by using **5/MAO** and **6/MAO** (Figure 7.9, top spectrum). The copolymers incorporated 1-hexene, observed as butyl side chains in the ^{13}C NMR spectum (Figure 7.9, middle spectrum). Side chains were assigned according to Galland (Table 7.3).[123-125] At low Al/Zr ratio, no branching carbon was detected because of low incorporation of hexene. In contrast to MAO activated Tp´MCl$_3$, olefinic end groups were detected in the TpCp based homo and copolymers, providing evidence that ß-H-elimination is involved in chain transfer (Figure7.9, bottom spectrum).
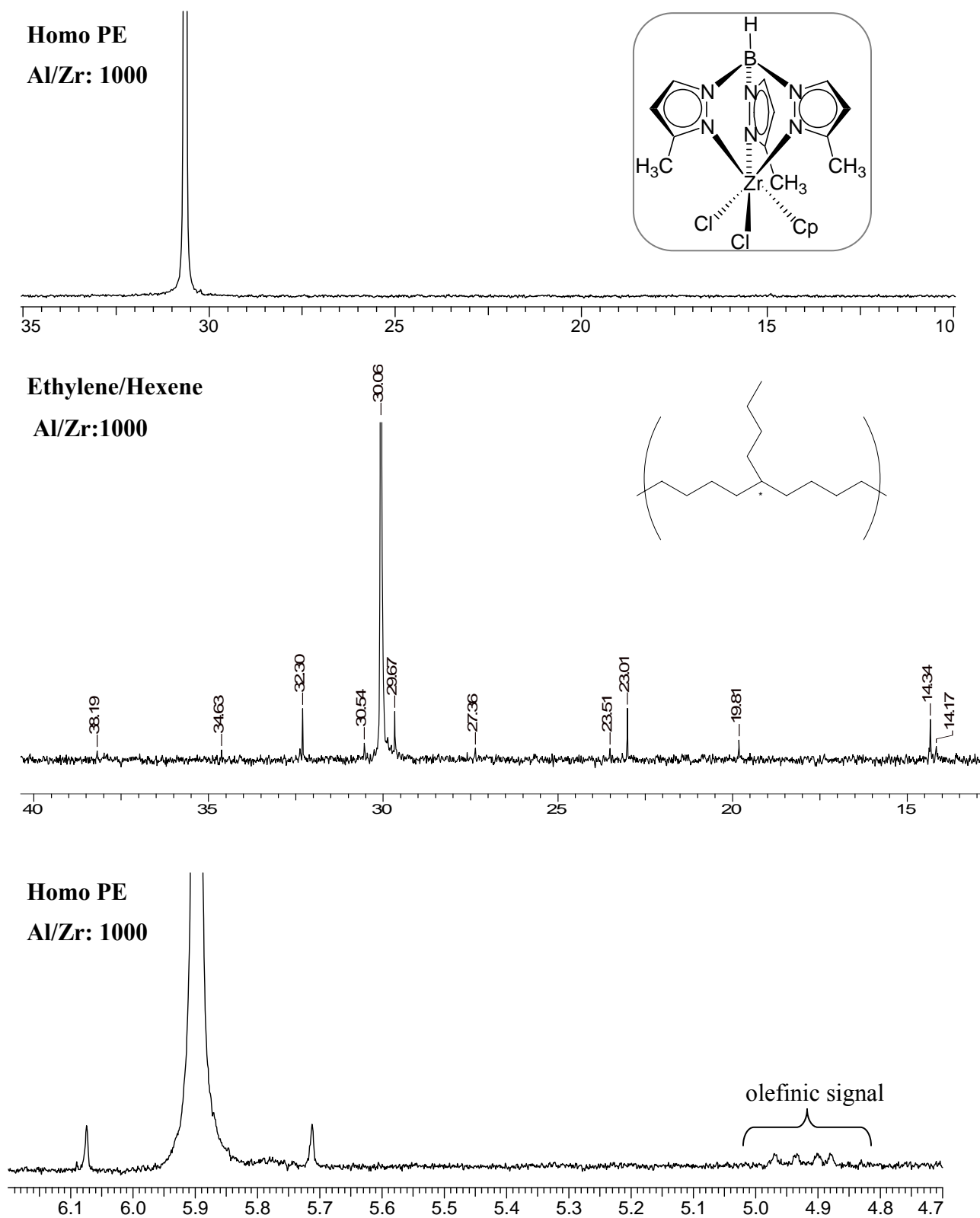
Figure 7.9 ^{13}C NMR of polyethylene (top), 13C NMR of ethylene/hexene copolymerization (middle), and 1H NMR of the olefinic region of polyethylene produced by 5 and 6.

Table 7.3   Chemical Shift Assignments in ^{13}C NMR Spectra

Carbon	Sequence	Chemical shifting (ppm)
brB$_4$	EHE	38.2
$\alpha\delta^+$	EHEE	34.6
4B$_4$	EHE	34.1
$\gamma\delta^+$	HEEE	30.5
$\delta\delta^+$	EEE	30.0
3B4	EHE	29.5
$\beta\delta^+$	EHEE	27.3
2B$_4$	EHE + HHE + HHH	23.4
1B$_4$	EHE + HHE+HHH	14.1

The T_m of the polymers was dependant on the Al/Zr ratio and the polymerization conditions, either homo- or copolymerization. The use of low Al/Zr ratio resulted lower T_m,127 to 134°C in PEs. Raising the Al/Zr ratio to 1000 resulted in a significant increase in T_m to 138 °C. Ethylene/1-hexene copolymerization gave the expected drop in T_m, especially at Al/Zr ratio to 1000 because of the higher hexene incorporation compared to the polymerizations performed at low Al/Zr ration. T_m reduced from 139 to 124 °C for **5**/MAO system and from 138 to 127 °C for **6**/MAO system. Copolymerization with 1-hexene does not significantly affect the Mw or broaden the MMD under these conditions.

7.4   Outlook

Although the LCB-PEs synthesized here have very interesting material properties, they are fairly complicated to synthesize and thus too expensive to be used in pure form in the most industrial applications.

In the future, the further works in this field should combine interesting material properties with easy and cheap synthetic method. Therefore, using vinyl chloride or any other chain transfer reagent to generate long chain branches and re-insert into the growing is very promising. The problem by using vinyl chloride is the reduction in catalyst activity due to the inactive Zr-Cl species generated by β-Cl elimination. A desirable chain transfer reagent would not deactivate the catalyst, such as $ZnEt_2$ used by Dow for their chain shuttling polymerizations. The Dow technology produces block copolymers, not the desirable LCB-PEs. The chain transfer reagent should be in the middle for these two extremes of reactivity, one which would not transfer too quickly to produce block structures or deactivate the catalyst. This finding could allow for the application of this technology to other polymerization systems, such as industrially relevant iPP.

Tp complexes represent an area of broad horizon. These systems allow for subtle steric and electronic tuning for polymerization reactivity enhancement. One possible area of expansion would be the use of BpCp systems, where one of the pyrazole rings has been replaced by a hydride. These systems would have different properties than the parent Tp systems, yet retain the rigidity necessary for competent catalysis.

8 EXPERIMENTAL PART

8.1 General Considerations

All manipulations were performed using glovebox or standard Schlenk techniques under purified argon or nitrogen atmosphere.

8.2 Chemicals

Gases

Ethylene (99.8%) was provided by Linde and purified by passage through columns of BASF R3-11 catalyst and 4 Å molecular sieves for the polymerizations in Hamburg. Polymer grade ethylene was obtained from Matheson for polymerizations in Chicago. Propylene (99.8%) was provided by Gerling, Holz & Co. and was purified by passage through columns of BASF R3-11 catalyst and 4 Å molecular sieves. Vinyl chloride was provided by Aldrich and used as recieved. Argon was purchased from Linde and purified by using Oxisorb of Messer-Griesheim. Nitrogen was purified by passage through columns containing activated molecular sieves and Q-5 oxygen scavenger.

Solvents

Pentane, hexanes, toluene and benzene were purified by passage through columns of activated alumina and BASF R3-11 oxygen scavenger. Polar sovents THF and CH_2Cl_2 were also purified by passage through two columns of activated alumina. THF-d_8 was stored over Na/benzophenone ketyl. $CDCl_3$ and CH_2Cl_2 was stored over P_2O_5.

Methylaluminoxane

MAO was provided by Akzo Nobel in Hamburg and purified by condensation in Hamburg, and by Amberlee as a 10% solution in toluene for polymerizations in Chicago, and used as received.

8.3   Synthesis of Ligands and Catalysis

Preparation of 9-(1,3-cyclopentadien-1-yldiphenylmethyl)-2,7-bis(1,1dimethylethyl)-9H-fluorene and isomer [Ph₂C(2,7-tert-Bu2Flu)(Cp)]

6,6-diphenylfulvene
M = 230.31 g/mol

2,7-di-*tert*-butylfluorene
M = 278.44 g/mol

butyl lithium
M = 64.06 g/mol

9-(1,3-cyclopentadien-1-yldiphenylmethyl)-2,7-*bis*(1,1-dimethylethyl)-9*H*-fluorene and isomer
M = 508.75 g/mol
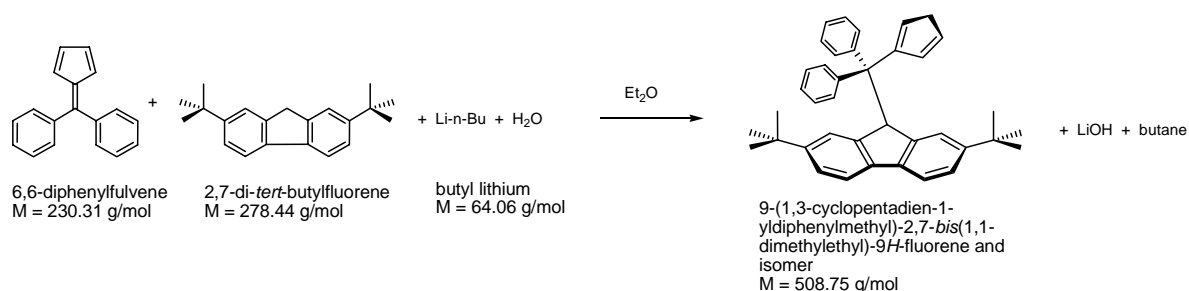
2,7-di-*tert*-butylfluorene [3.63 g, 13.0 mmol] was dissolved in 58 ml diethyl ether and 5.55 g of *n*-butyllithium (≡ 0.833 g, 13.0 mmol, 1.6 M in hexane) was added dropwise. The yellow solution was stirred for 4 h and 6,6-diphenylfulvene [3.00 g, 13.0 mmol] was added and stirred for 18 hours. The reaction mixture was quenched with 60 ml of water and the organic layer was separated from the aqueous phase. The aqueous layer was extracted 3 times with diethyl ether and all organic layers were combined. The organic layer was dried over sodium sulphate, and diethyl ether was removed under vacuum until the product precipitated. The product was crystallized at − 30 °C and washed with cold diethyl ether to yield 4.15 g (8.16 mmol, 63 %) as colorless crystals of 9-(1,3-cyclopentadien-1-yldiphenylmethyl)-2,7-*bis*(1,1-dimethylethyl)-9*H*-fluorene and its isomers.

¹H-NMR (400 MHz, CDCl₃): δ = 1.06/1.10 (s, 18 H, *tert*-butyl), 2.81/2.90 (m, 2H, CH₂Cp), 5.36/5.41 (s, 1H, CH$_{Flu}$), 6.14-6.45 (m, 3 H, H$_{Cp}$), 7.03-7.28 (m, 16 H$_{Ar}$) ppm.

¹³C-NMR (100 MHz, CDCl₃): δ = 31.8 (C(**CH₃**)₃), 35.0, (**C**(CH₃)₃), 59.4, 118.4, 123.8, 124.8, 126.4, 127.5, 130.3, 136.0, 139,9, 145.1, 148.8 ppm.

Preparation of dichloro[η^{10}-2,4-cyclopentadien-1-yliden(diphenylmethylen)[2,7-*bis*(1,1-dimethylethyl-9*H*-fluoren-9-yliden]zirconium

[{Ph$_2$C(2,7-*tert*-Bu$_2$Flu)(Cp)}ZrCl$_2$]

9-(1,3-cyclopentadien-1-yldiphenylmethyl)-2,7-*bis*(1,1-dimethylethyl)-9*H*-fluorene and isomer
M = 508.75 g/mol

butyl lithium
M = 64.06 g/mol

zirconium tetrachloride
M = 233.03 g/mol

dichloro[eta^{10}-2,4-cyclopentadien-1-yliden(diphenylmethylen)[2,7-*bis*(1,1-dimethylethyl-9*H*-fluoren-9-yliden]zirconium
M = 668.68 g/mol
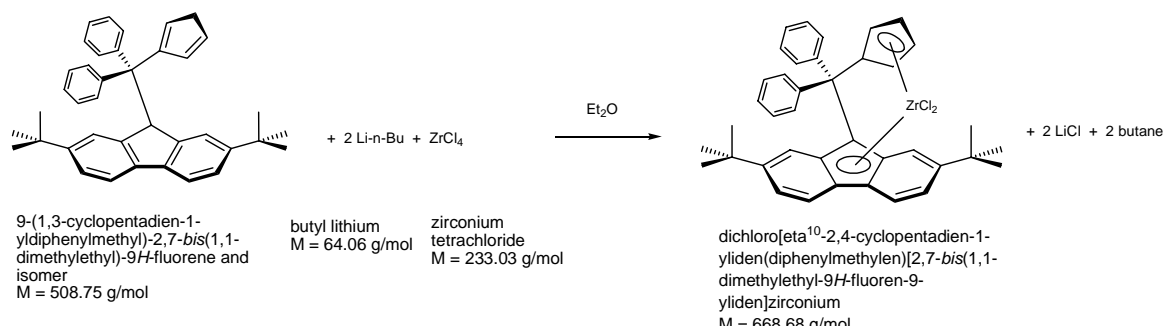
9-(1,3-cyclopentadien-1-yldiphenylmethyl)-2,7-*bis*(1,1-dimethylethyl)-9*H*-fluorene [2.42 g, 4.76 mmol] was dissolved in 100 ml diethyl ether and 4.06 g of *n*-butyllithium (≡ 0.609 g, 9.52 mmol, 1.6 M in hexane) was added dropwise. The orange solution was stirred for 16 h and zirconium tetrachloride [1.11 g, 4.76 mmol] was added. After 4 h the reaction mixture was filtered over sodium sulfate to aid removal of lithium chloride. The diethyl ether was removed under vacuum until the product precipitated. The product was crystallized from diethyl ether at − 30 °C and washed with ice-cold diethyl ether to yield 1.24 g (1.86 mmol, 39 %) as orange-red crystals of dichloro[η^{10}-2,4-cyclopentadien-1-yliden(diphenylmethylen)[2,7-*bis*(1,1-dimethylethyl-9*H*-fluoren-9-yliden]zirconium.

^{1}H-NMR (400 MHz, CDCl$_3$): δ (^{1}H) = 1.07 (s, 18 H, *tert*-butyl), 5.71 (m, 2 H, α-C$_5$H$_4$), 6.37 (m, 4 H, β-C$_5$H$_4$), 7.21 – 8.09 (m, 14 H, H$_{Ar}$) ppm.

^{13}C-NMR (100 MHz, CDCl$_3$): δ(^{13}C) = 30.6 (C(**C**H$_3$)$_3$), 34.7 (**C**(CH$_3$)$_3$), 58.2 (Ph**C**Ph), 102.6, 110.2, 118.3, 119.8, 120.7, 121.5, 124.0, 124.6, 126.5, 127.1, 128.9, 129.0, 129.4, 144.6, 150.7 ppm.

Synthesis of Potassium Hydrotris(3-methylpyrazol-1-yl)borate:
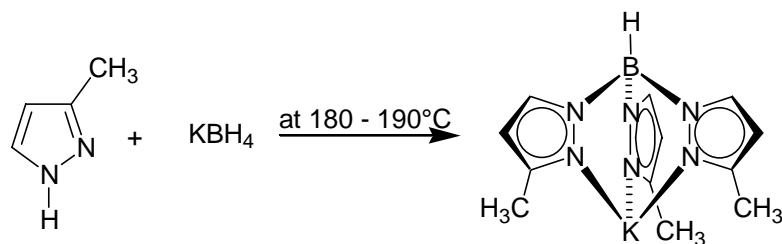
A mixture of 3-methylpyrazole (5 g, 60.9 mmol) and of potassium borohydride (1 g, 18.5 mmol) was heated to 180-190 °C for 4 h by the method of McCurdy (W.H, *Inorg. Chem.* **1975**, 14, 2292). The clear melt was obtained and washed with toluene and hexane several times. The colourless salt was dissolved in hot THF and crystallized by adding toluene.
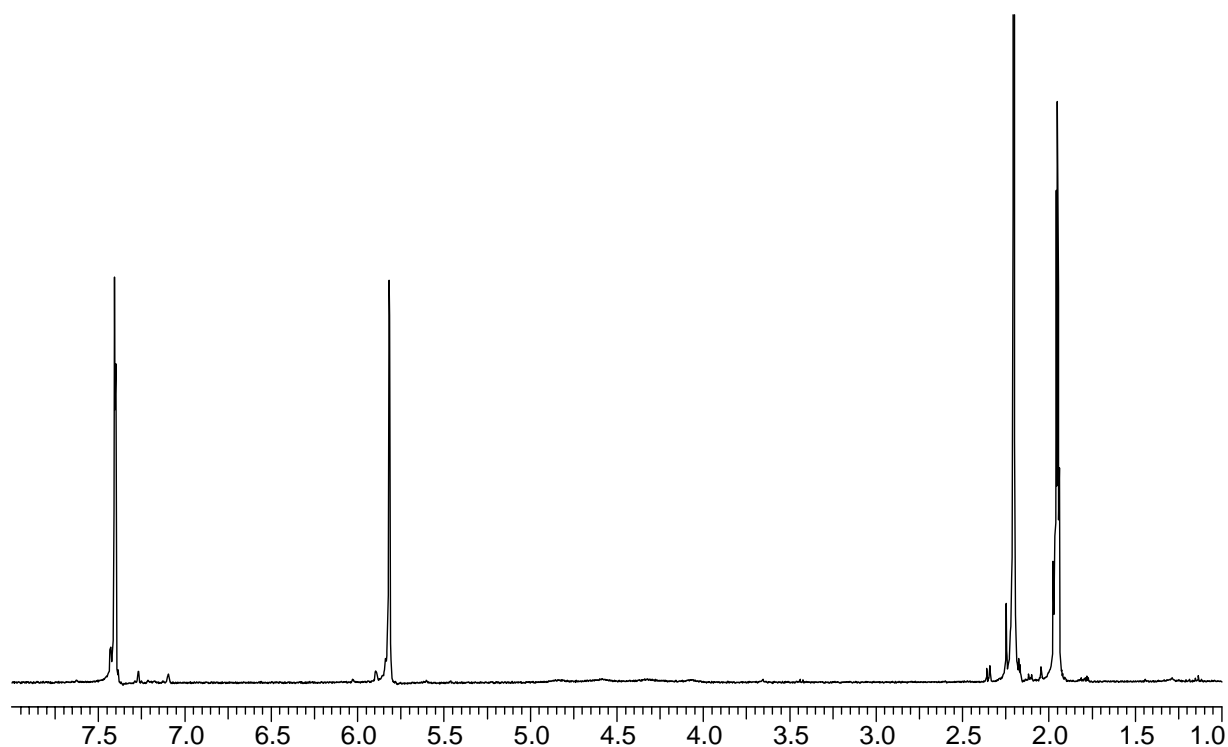
^{1}H NMR (400 MHz, CDH$_2$CN): $\delta\,(^1\text{H}) = 7.42$ (1 H, d, $J = 2.0$), 5.78 (1 H, d, $J = 2.0$) $\delta\,(^1\text{H})$ 2.22 (3 H, s)

General Procedure for the Synthesis of Tp´CpZrCl₂ Complexes
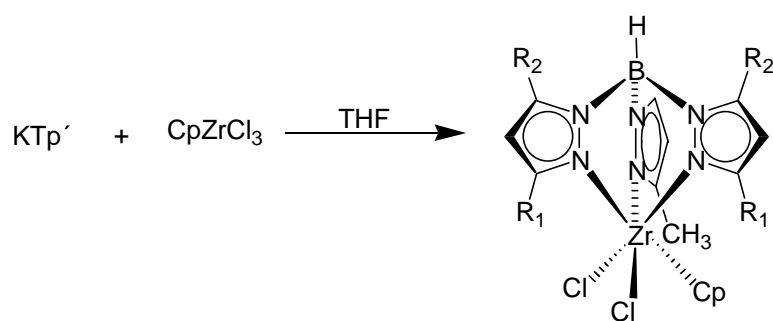
Figure 8.1   The general reaction for the synthesis of Tp´CpZrCl₂ complexes

The complexes were prepared reaction of $CpZrCl_3$ with appropriate tris(pyrazolyl) borate. A Schlenk flask was charged with equivalent amount of $KTp´$ and $CpZrCl_3$. THF was added at – 78 °C by vacuum transfer and the resulting solution was stirred overnight, gradually warming to room temperature. The solution was filtered through celite and dried under vacuum. The crude product was purified by either washing several times with toluene, or was re-crystallized from CH_2Cl_2.

The products were isolated as white crystals, based on the pure product the yield is approximately 30 %.

[Hydrotris(3-methylpyrazolyl)borato]dichlorocyclopentadienyl-zirconium:

ppm

ppm
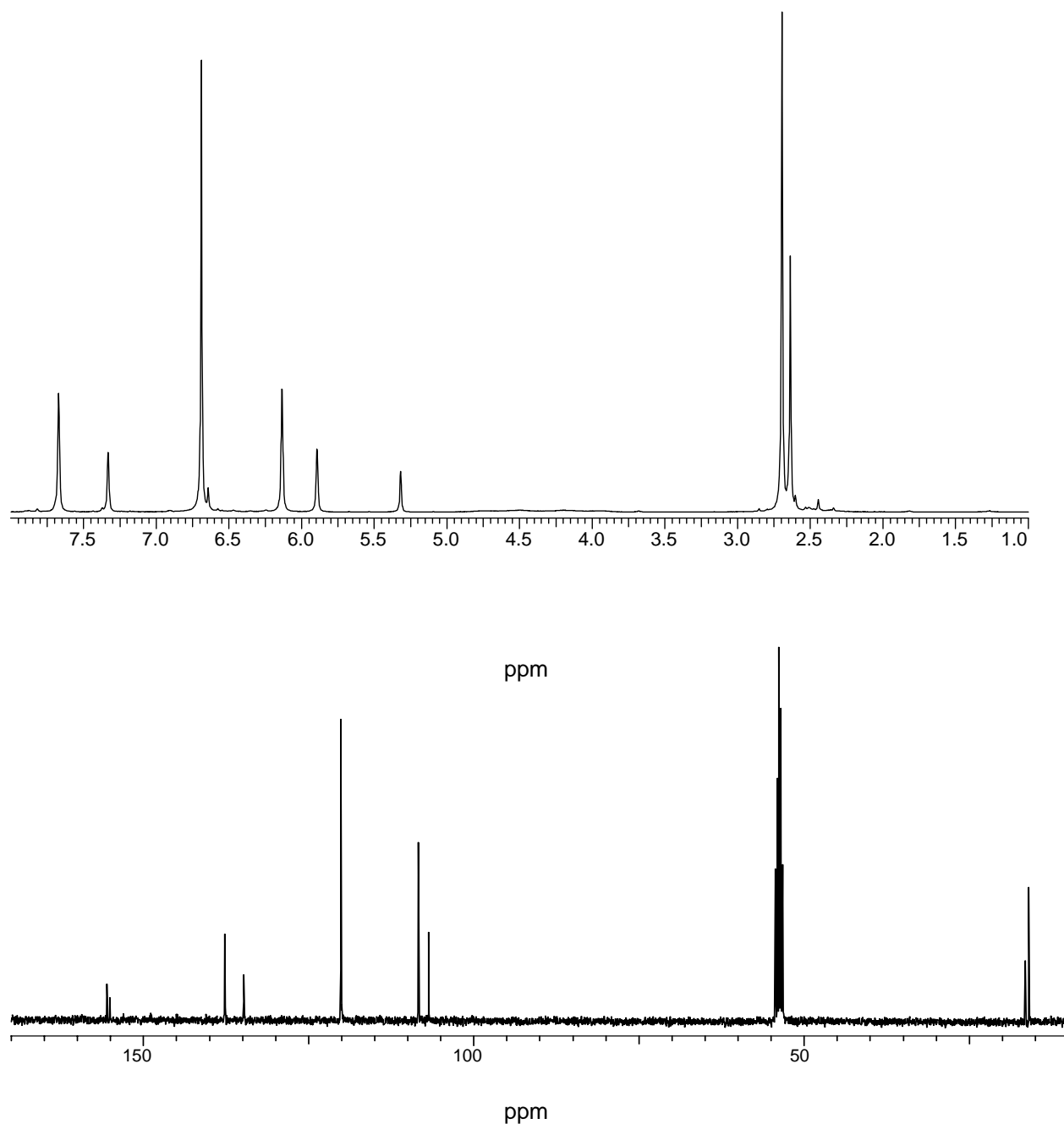
Figure 8.2   [1]H and ^{13}C spectra of cyclopentadienyl hydrotris(3-methylpyrazol-1-yl)borate zirconium dichloride

^{1}H NMR (400 MHz, CD₂Cl₂) δ (^{1}H) = 7.63 (2 H, s), 7.29 (1 H), 6.65 (5H, s), 6.10 (2 H, s), 5.86 (1 H, s), 2.66 (3 H, s), 2.60 (3 H, s)

^{13}C NMR (400 MHz, CD₂Cl₂) δ (^{13}C) = 155.54 (pz C-5), 155.10 (pz C-5), 137.7 (pz C-3), 134.82 (pz C-3), 120.14 (Cp), 108.40 (pz C-4), 106.85 (pz C-4), 16.55 (C-Me), 16.03 (C-Me)

105

[Hydrotris(3,5-dimethylpyrazolyl)borato]dichlorocyclopentadienyl-zirconium:
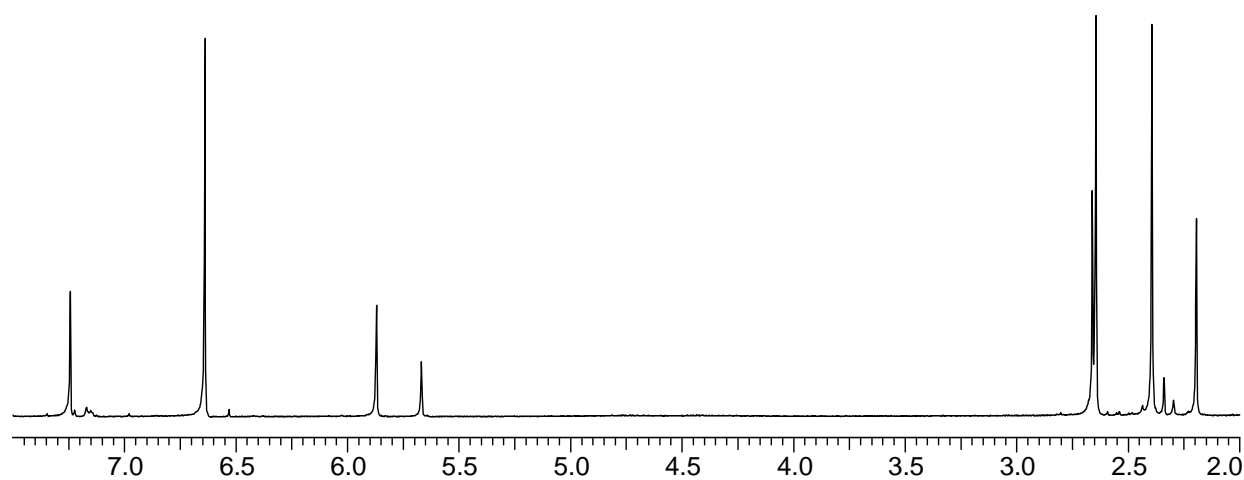
Figure 8.3 ^{1}H spectrum of [hydrotris(3,5-dimethylpyrazol-1-yl)borato]dichloro cyclopentadienyl-zirconium

^{1}H NMR (400 MHz, CDCl₃) δ (^{1}H) = 6.64 (5 H, s), 5.88 (2 H), 5.68 (1H, s), 2.68 (9 H, s), 2.45 (6 H, s), 2.25 (3 H, s)

8.4   Polymerization Systems

8.4.1 Reactor

All the long chain branched polyolefin polymerization in Hamburg were performed in a 1L glass reactor from Firma Buchi. (Figure 8.4).
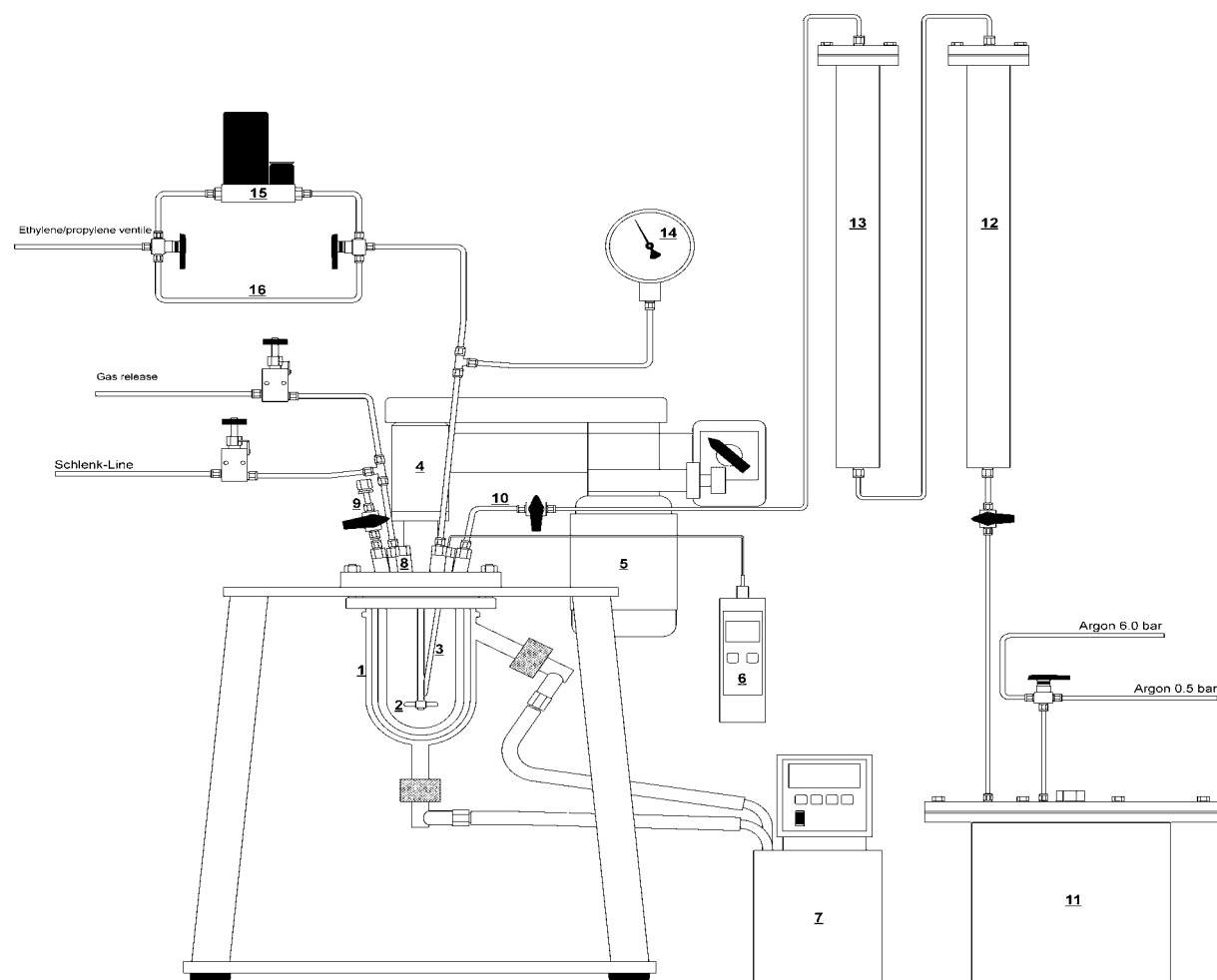
Figure 8.4   Glass reactor from Firma Buchi   1) temperature jacket and thermostate connection 2) stirer 3) autoclave 4&5) stirrer motor 6) digital thermometer 7) thermostate 9) ventile with septum 10) toluene ventile 11) toluene tank 12) a column of BASF R3-11 catalyst 13) a coloumn with 4 Å molecular sieves 14) manometer 15) mass-flow control 16) bypass

8.4.2 Synthesis of EP-Comonomers

The 1l reactor was heated up to 90 °C and flushed with Argon several times. Dry and powdered MAO was introduced to the reactor. The reactor was loaded with 400 mL toluene. The solution was then saturated with propylene and ethylene. The ethylene pressure was kept stable by mass-flow control. The reaction was initiated by injection of the desired volume of a stock solution of catalyst A into the reactor. The reaction was quenched after 2 hours by addition of 10 ml ethanol. Then the reactor was emptied and washed with toluene and ethanol. 100 ml of dilute hydrochloric acid was given to the reaction solution and the mixture was stirred overnight. The organic phase was separated and washed three times with water. The organic phase was concetrated under vacuum and the waxy product was dried in the vacuum oven overnight at 40 °C.

8.4.3 Synthesis of long chain branched polyethylene

The 1l reactor was heated together with EP-comonomers at 60 °C for 1.5 h and 400 mg of dry and powdered cocatalyst MAO was introduced to the reactor. The reactor was filled with 200 ml of dry toluene. Hydrogen gas was fed to the reactor for 2 min and the solution was saturated with ethylene with stable pressure by mass-flow control. The reaction was initiated by injection of the desired volume of a solution of fluorenyl catalyst into the reactor. The copolymerisation reaction was quenched after 2 hours by addition of 10 ml ethanol. The reactor was emptied and washed with toluene and ethanol. 100 ml of dilute hydrochloric acid was given to the reaction solution and the mixture was stirred overnight. The polymer solution was strained by suction filtration and washed three times with ethanol. The product was dried under vacuum in an oven overnight at 40 °C.

8.4.4 Purification of long chain branched polyethylene

Soxhlet-Extraction was used to purify bimodal long chain branched polyethylene. The residual ethylene/propylene comonomers with low molar mass were separated from the LCB-PE with high molar mass. In contrast to LCB-PE the comonomers are soluable in toluene. Toluene was put into a flask. The flask was heated and the toluene gas rised up through condenser. Then the condensed solvent dropped into the Soxhlet tube and perfused the product in the paper thimble. The hot toluene extracted ethylene/propylene comonomers from the product. When the level of solvent was higher than the U-shaped sidearm, solvent with dissolved low molar mass fraction was drained into the flask.

8.5   Analytical Methods

8.5.1 NMR-Spectroscopy

Polymer samples were measured by Bruker Avance-Ultrashield-400-Spectrometer at 100 °C according to following parameters at University of Hamburg :

Tabel 8.1   The parameters of different ^{13}C-NMR measurements

Spectrum	1H-broad band	DEPT	IGated
Pulse program	Waltz16	dept135	IGated100
Measurement frequency	100.63 MHz	100.63 MHz	100.63 MHz
Number of scans	1024-4096	1024	4096
Pulse angle	60°	135°	60 °
Relaxation time	5 s	5 s	10 s
Sweep-width	25126 Hz	23980 Hz	25126 Hz

In each case, 100-200 mg of product was dissolved in hexachlorobutadiene in a 10 mm tube. 1,1, 2,2-tetrachloroethane-d_2 was used as a lock solvent and reference substance.

In addition to that, all the NMR spectra of air sensitive compounds were recorded in Teflon-valved NMR tubes on Bruker DRX-400 or 500 spectrometers at room temperature at University of Chicago. ^{1}H and ^{13}C chemical shifts were determined by reference to the residual solvent peaks. $Cl_2DCCDCl_2$, $CDCl_3$ and CD_2Cl_2 were distilled from CaH_2 or P_2O_5.

8.5.2 Gel Permeation Chromatography

Measurements in Hamburg for the molar mass and polydispersity of synthetic polymers were determined using a Waters GPC 2000 at 150 ^{o}C containing an alliance system equipped with a refractive index detector and three columns. The particle size for the columns was 10 μm, and pore sizes were 10^3 Å, 10^4 Å and 10^6Å. 1,2,4-Trichlorobenzene was used as a solvent, with 1% ofa 2,6-Di-*tert*-butyl-4-methyl phenol as a stabilizer. Polystyrene, polyethylene, and polypropylene standards were used for the calibration.

Measurements in Chicago were performed on a Polymer Laboratories PL-GPC 220 using 1, 2, 4-trichlorobenzene solvent stabilizied with 125 ppm BHT at 150 °C. A set of three PL gel 10 μm Mixed-B or Mixed-B LS coloums were used.

8.5.3 Melt Rheology

Rheological measurements were carried out at the University of Erlangen, in the research group of Prof. Münstedt. Rheological characterization was performed with a Bohlin Gemini (Malvern) using 25 mm parallel plate geometry. The samples were stabilized with 0.5 wt.% Irganox 1010$^®$ and 0.5 wt.% Irgafos 168$^®$ (Ciba), and compression molded in 25 mm discs with a height of 1 mm at 180°C in vacuo. Activation energies were determined from temperature dependence (140 to 240 °C) in the proximity of the terminal regime, and measured every 20 ^{o}C.

8.5.4 Size Exclusion Chromotography with Coupled Multi-Angle Laser Light Scattering (SEC-MALLS)

All the measurements were performed by Dr. J. Kaschta at the University of Erlangen with the instrumental setup is shown in Figure 8.5.
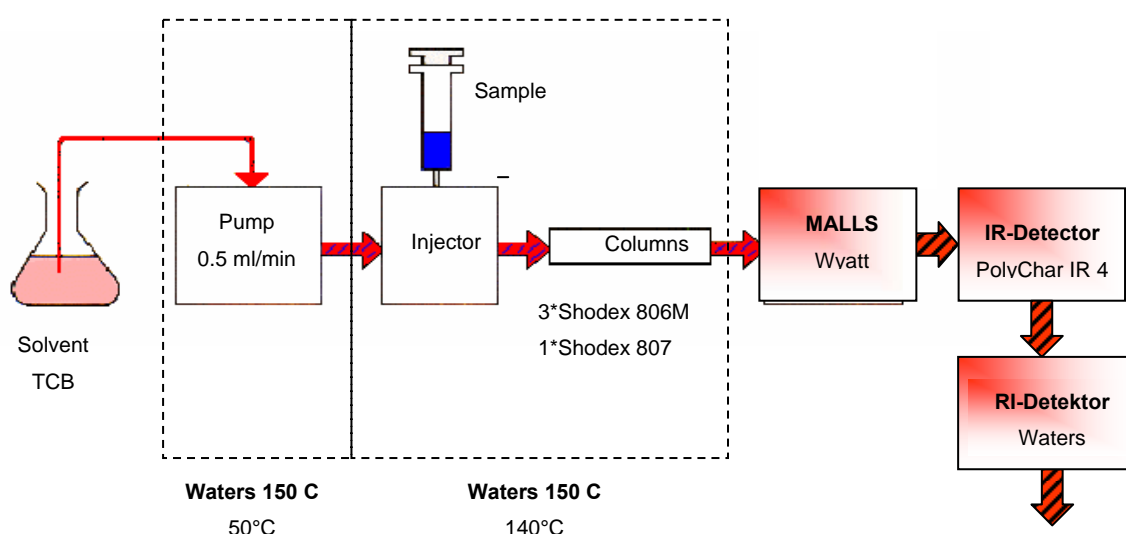
Figure 8.5 The schematic of the SEC-MALLS used at the University of Erlangen

Molecular characterization was carried out on a Waters 150C, equipped with a refractive index (RI) detector and an infrared (IR) detector (PolyChar, IR4) at 140°C for the column and sample compartment using 1,2,4-trichlorobenzene (TCB) as the solvent. High temperature SEC was coupled with a multi-angle light scattering apparatus (Wyatt, DAWN EOS), which was also operated at 140°C. The samples (2 g/l) were dissolved in TCB at 160°C for three hours prior to the analysis. Irganox 1035 (Ciba SC) was added to the solution in a concentration of 1 g/l to avoid degradation of the polymer during analysis.

The flow rate was 0.5 ml/min and the sample was injected in 300 µl aliquots onto a set of 4 SEC-columns (3 Shodex columns UT 806, 1 Shodex UT807). Calibration of the SEC was performed with narrow MMD polystyrene. Mark Houwink constants for the universal calibrations were K=$1.21 \cdot 10^{-4}$ ml/g and a=0.707 for PS and K=$4.06 \cdot 10^{-4}$ ml/g and a= 0.725 for PE.

8.5.6 Differential Scanning Calorimetry

The melting and glass transition temperatures of polymers were measured by DSC. In Hamburg measurements were carried out on a Mettler Toledo DSC 821°. Indium with a melting point of 156.61 °C was used as a calibration standard. Aluminium pans were used and the mass of samples for the measurements was about 5 mg. The heating rate was 10°C/min or 20°C/min and the temperature range from -100 °C to 200 °C.

9 REFERENCES

1   Fawcett, E. W.; Gibson, R. U.; Perrin, M. W.; Paton, J. G.; Williams, E. G. (ICI) GB-Patent 471590, **1936** [*Chem. Abstr.* **1938**, *32*, 1362]

2   Andresen, A.; Cordes, H. G.; Herwig, J.; Kaminsky, W.; Merck, A.; Mottweiler, R.; Pein, J.; Sinn, H.; Vollmer, H.-J. *Angew. Chem.* **1976**, *88*, 679-680

3   Ziegler, K. *Angew. Chem.* **1952**, *64*, 323-329

4   Ziegler, K.; Breil, H.; Holzkamp, E.; Martin, H. DE 973626, **1953** [*Chem. Abstr.* **1960**, *54*, 14794]

5   Ziegler, K.; Holzkamp, E.; Breil, H.; Martin, H. *Angew. Chem.* **1955**, *67*, 541-547

6   Natta, G. *Angew. Chem.* **1956**, *68*, 393-403

7   Huggins, M. L.; Natta, G.; Desreux, V.; Mark, H. *J. Polymer Sci.* **1962**, *56*, 153-161

8   Natta, G.; Pino. P.; Mazzanti, G.; Giannini, U. *J. Am. Chem. Soc.* **1957**, *79*, 2975-2976

9   Natta, G.;Pino, P.;Mazzanti, G.; Lanzo, R. *Chim. Ind.* **1957**, *39*, 1032-1033

10 Breslow, D. S.; Newburg, N. R. *J. Am. Chem. Soc.* **1957**, *79*, 5073-5074.

11 Breslow, D. S. (Hercules Powder Co.) US-Patent 2827446, **1958** [*Chem. Abstr.* **1959**, *53*, 9854]

12 Reichert, K. H.; Meyer, K. R. *Makromol. Chem.* **1973**, *169*, 163-176

13 Long, W. P.; Breslow, D. S. *Justus Liebigs Ann. Chem.* **1975**, 463-469

14 Sinn, H.; Kaminsky, W.; Vollmer, H.-J.; Woldt, R. *Angew. Chem.* **1980**, *92*, 39

15 Sinn, H.; Kaminsky, W. *Adv. Organomet. Chem.* **1980**, *18*, 99-149

16 Wild, F. R.; Zsolnai, L.; Huttner, G.; Brintzinger, H. H. *J. Organomet. Chem.* **1982**, *232*, 233-247

17 Ewen, J. A. *J. Am. Chem. Soc.* **1984**, *106*, 6355-6364

18 Kaminsky, W.; Kuelper, K.; Brintzinger, H. H.; Wild, F. R. W. P. *Angew. Chem.* **1985**, *97*, 507-508

19 Ewen, J. A.; Jones, R. L.; Razavi, A.; Ferrara, J. D. *J. Am. Chem. Soc.* 1988, *100*, 6255-6256

20 Sinn, H.; Kaminsky, W.; Vollmer, H.-J.; Woldt, R. *Angew. Chem.* **1980**, *92*, 39

21 Sinn, H.; Kaminsky, W. *Adv. Organomet. Chem.* **1980**, *18*, 99-149

22 Sinn, H. *Macromol. Symp.* **1995**, *97*, 27-52.

23 Mason, M. R.; Smith, J. M.; Bott, S. G.; Barron, A. R. *J. Am. Chem. Soc.* **1993**, *115*, 4971-4984

24 Gasman, P.G; Callstorm, M. R. *J. Am. Chem. Soc.* **1987**, *109*, 7875

25 Watson, P.L.; Parshall, G. W. *Acc. Chem. Res.,* **1985**, *18*, 51

26 Sishta, C.; Hathorn, R. M.; Marks, T. J., *J. Am. Che. Soc.* **1992**, *114*, 1112

27 Cam, D.; Giannini U. *Makromol. Chem.* **1992**, *193*, 1049

28 Tritto, I.; Sacchi, M. C.; Li, S. *MRC* **1994**, *15*, 217

29 Jordan, R. F.; Bajgur, C. S.; Willet, R.; Scott, B. *J. Am. Chem. Soc.* **1986**, *108*, 7410

30 Chen, E. Y. X.; Marks, T.J. *Chem. Rev.* **2000**, *100*, 1391-1434

31 Cossee, P. *Tetrahedron Lett.* **1960**,12-16

32 Cossee, P. *J. Catal.* **1964**, *3*, 80-88

33 Cossee, P. *Recl. Trav. Chim. Pays-Bas* **1966**, *8*, 1151-1160

34 Arlman, E. J. *J. Catal.* **1966**, *5*, 178-189

35 Brookhart, M.; Green, M. L. H.; Wong, L. L. *Progress in Inorganic Chemistry* **1988**, *36*, 1-124

36 Brookhart, M.; Green, M. L. H. *Journal of Organometallic Chemistry* **1983**, *250 (1)*, 395-408

37 Shiono, T.; Soga, K. *Macromolecules* **1992**, *25*, 3356-3561

38 Kaminsky, W.; Kricheldorf, R. *Handbook of Polymer Science Part A*, Marcel Dekker Inc. **1992**

39 Farina, M. *Top. Stereochemistry*, **1987**, 17-111

40 Ewen, J. A. *J. Am. Chem. Soc.* **1984**, *106*, 6355-6364

41 J., Scheirs; Kaminsky, W. *Metallocene-Based Polyolefins Volume One* Wiley **2000**

42 Thostenson, ET. ; Ren, Z.; Chou, T-W. *Compos Sci Technol*, **2001**, *61*, 912-1899

43 Mülhaupt R., *Macromol. Chem. Phys.* **2003**, 204, 289

44 Wolfenberger, A., Gahleitner, M., *Kunststoffe,* **2004**, 62

45 Arriola, J. D.; Carnahan, M. E.; Husted, D. P.; Kuhlman, R. L; Wenzel, T.T. *Science*, **2006**, *312*, 714-718

46 Vega, J. F. *Macromolecules* **1996**, *29*, 960-965

47 Lohse, D. J. *Macromolecules* **2002**, *35*, 3066-3075

48 Imuta, J.; Todo, A.; Tsutsui, T.; Hachimoei, T.; Kashiwa, N. *Bull. Chem. Soc. Jpn.* **2004**, *77(4),* 607-615

49 Fleury, G.; Schlatter, G.; Muller, R. *Rheol. Acta*, **2004**, *44,* 174-187

50 Piel, C.; Stadler, F.; Kaschta, J.; Rulhoff, S.; Münstedt, H.; Kaminsky W. *Macromol. Chem. Phys.* **2006**, *207(1)*, 26-38

51 Kaminsky, W.; Piel, C.; Scharlach K. *Macromol. Symp.* **2005**, *226(1)*, 25-34

52 Lai, S.-Y.; Wilson, J.R.; Knight, G.W.; Stevens, J.C.; Chum, P.-W.S. U.S. Patent WO 9308221 (**1993**), Dow Chemical Co

53 Brant, P.; Canich, J. A. M.; Dias, A. J.; Bamberger, R. L.; Licciardi, G. F.; Henrichs, P. M.Int. Pat. Appl. WO 94/07930 (**1994**), Exxon Chemical

54 Beigzadeh, D.; Soares, J. B. P.; Hamielec, A. E. *Polym. React. Eng.* **1997**, *5,(3),* 141-180

55 Kokko E., Malmberg A., Lehmus P., Löfgren B. Seppälä J.V, *J. Polym. Sci., Part A: Polym. Chem* **2000**, *38(2),* 376-388

56 Woo, T. K.; Margl, P.M; Ziegler, T.; Blochl, P. E. *Organometallics* **1997**, *16(15),* 3454-3468

57 Kolodka, E.; Wang, W. J. *Polymer* **2002**, *41(11),* 3985-3991

58 Lehmus, P.; Kokko, E.; Härkki, O.; Leino, R.; Luttikhedde, H.J.G.; Näsman, J.; Seppälä, J.V. *Macromolecules* **1999**, *32(11)*, 3547-3552

59 Stadler,J. F.; Piel, C.; Kaminsky,W.; Münstedt, H. *Macromolecular Symposia* **2006,** *236, (1),* 209-218

60 Ruymbeke, E.; Stéphenne, V.; Daoust, D.; Godard, P.; Keunings, R.; Bailly, C. *Journal of Rheology* **2005,** 49, *(6)*, 1503-1520

61 Trinkle, S.; Walter, P.; Friedrich, C. *Rheologica Acta* **2002,** *41*, 1-2, 103-113

62 Auhl, D.; Stange, J.; Munstedt, H.; Krause, B.; Voigt ,D.; Lederer, A.; Lappan, U.; Lunkwitz, K. *Macromolecules* **2004,** *37, (25),* 9465-9472

63 Münstedt, H. *Rheologica Acta* **1979,** *18*, 492- 504

64 Münstedt, H.; Gabriel, C.; Auhl, D. *Abstracts of the Papers of American Chemical Society* **2003,** 226, U382-U382

65 Gabriel, C.; B. Kokko; Löfgren B.; Seppälä, J.; Münstedt, H. *Polymer* **2001**, *43*, 24, 6383-6390

66 Auhl, D.; Stange, J.; Münstedt, H.; Krause, B.; Voigt, D.; Lederer, A.; Lappan, U.; Lunkwitz, K. *Macromolecules* **2004,** *37, (25)*, 9465-9472

67 Wood-Adams, P. M.; Costeux, S. *Macromolecules* **2001,** *34* (18), 6281-6290

68 Kokko, E.; Lehmus, P.; Malmberg A.,Löfgren B. Seppälä J.V. *Polyethylene via Metallocene-Catalysis: Comparison of Catalyst.* Springer: **2001**, 335-345

69 Kraus, G.; Gruver, J. T. *Journal of Polymer Science Part A: General Papers* **1965,** *3*, 105-122

70 Fujimoto, T.; Narukawa, H.; Nagasawa, M. *Macromolecules* **1970,** *3*, 1 57-64

71 Gabriel, C.; Lilge, D. *Rheologica Acta* **2006,** *45*, 992-1002

72 Stadler, F. J.; Gabriel, C.; Münstedt, H. *Macromolecular Chemistry and Physics* **2007,** DOI: 10.1002/macp.200700267

73 Vega, J. F.; Santamaria, A.; Munoz-Escalona, A.; Lafuente, P. *Macromolecules* **1998,** 31 (11), 3639-3647

74 Laun, H. M.; Münstedt, H. *Rheologica Acta* **1978,** *17*, 415-425

75 Agarwal, P. K.; Plazek, D. J. *Journal of Applied Polymer Science* **1977,** *21* (12), 3251-3260

76 Plazek, D. J.; O'Rourke, V. M.; Choy, I. C. *Proc. IUPAC, I. U. P. A. C., Macromol. Symp., 28th* **1982**, 852

77 Rulhoff, S.; Kaminsky, W., *Macromolecular Symposia* **2006**, *236*, 161-167

78 Wang, Wen-Jun; Zhu, Shiping; Park, Shin-Joon, Macromolecules **2000**, *33,(16)*, 5770-5776

79 Kokko Esa, Pietikainen Pirjo, Koivunen Jari, Seppala Jukka V., *Journal of Polymer Science, Part A: Polymer Chemistry* **2001**, *39*, 3805-3817

80 Weng, Weiqing; Markel, Eric J.; Dekmezian Armenag H. *Macromolecular Rapid Communications* **2001**, *22,* 1488-1492

81 Resconi, L.; Piemontesi, F.; Franciscono, G.; Abis, L;. Fiorani, T. *J. Am. Chem. Soc.* **1992**, *114*, 1025-1032

82 Repo, T.; Jany, G.; Hakala, K.; Klinga, M.; Polamo, M.; Leskela, M.; B. Rieger *J. Organomet. Chem.* **1997**, *549*, 177

83 Arikan, B.; Kaminsky, W. *Designed Monomers and Polymers* **2005**, *8,* (6), 589-600

84 Randall, J.C. *J. Macromol. Sci.*, **1989**, *C29*, 201-317

85 Kaminsky, W.; Ahlers, A.; Lindenhof, N. Möller *Angew. Chem. Int. Ed. Eng.* **1991**, *113*, 3623-3625

86 Stadler, Florian J.; Piel, Christian; Klimke, Katja; Kaschta, Joachim; Parkinson, Matthew; Wilhelm, Manfred; Kaminsky, Walter; Muenstedt, H. *Macromolecules* **2006**, *39* (4), 1474-1482.

87 Sperber, O.; Kaminsky, W. *Macromolecules* **2003**, *36, (*24), 9014-9019.

88 Kong, J.; Fan, X.; Jia, M. *J. Appl. Polym. Sci.* **2004**, *93*, 2542-2549

89 Chu, K. J.; Soares, B. P.; Penlidis, A. *Macromolecular Chemistry and Physic* **2000**, *201*, 552-557

90 Wang , W. J.; Kharchenko, S.; Migler. K.; Zhu S. P. *Polymer* **2004**, *45,* (19), 6495-6505

91 Zimm, B. H. M.; Stockmayer, W. H. *Journal of Chemical Physics* **1949**, *17, (12)*, 1301-1314

92 Bersted, B. H. *J. App. Pol. Sci.* **1985**, *30*, 3751

93 Carella, J. M.; Gotro, J. T.; Graessley W.W, *Macromolecules* **1986**, *19*, 659

94 Raju, V. R.; Rachapudy, H.; Graessley, W.W. *J. Polym. Sci. Polym. Phys. Ed.* 1979, *17*, 1223

95 Graessley, WW.; Edward, S. F. *Polymer* **1981**, *22*, 10, 1329-34

96 Bersted, B. H.; Slee, J. D.; Richter, A. *J. App. Pol. Sci.* **1981**, *26*, 1001-1014

97 Gabriel, C.; Münstedt, H. *Rheol. Acta* **2002**, *41*, 232

98 Gabriel, C.; Münstedt H., *Rheol. Acta* **1999**, *38*, 393

99 Stadler, F. J.; Piel, C.; Kaschta, J.; Rulhoff, S.; Kaminsky, W.; Münstedt, H. *Rheologica Acta* **2006,** *45, (5),* 755 - 764.

100 Stadler, F. J.; Piel, C.; Klimke, K.; Kaschta, J.; Parkinson, M.; Wilhelm, M.; Kaminsky, W.; Münstedt, H. *Macromolecules* **2006,** *39, (4),* 1474 – 1482

101 Trinkle, S.; Walter, P.; Friedrich, C. *Rheologica Acta* **2002,** 41, (1-2), 103-113

102 Stadler, F. J., *Molecular Structure and Rheological Properties of Linear and Long-Chain Branched Ethene-/a-Olefin Copolymers*. Sierke-Verlag: Göttingen, **2007**

103 Gaynor, S. G.; *Macromolecules* **2003**, *36*, 4692-4698

104 Stockland, R. A.; Foley, S. R.; Jordan, R. F. *Journal of the American Chemical Society* **2003**, *125*, (3), 796-809

105 Brant, P.; Ruff, C. J.; Sun, T. *Macromolecules* **2005,** *38*, 7181-7183

106 Zambelli, A.; Locatelli, P. *Macromolecules* **1975**, *8*, 687

107 Ruymbeke, E. van; Stéphenne, V.; Daoust, D.; Godard, P.; Keunings, R.; Bailly, C. *Journal of Rheology* **2005,** *49*, 1503-1520.

108 Stadler, F. J.; Piel, C.; Kaminsky, W.; Münstedt, H. *Macromolecular Symposia* **2006,** *236*, 209-218.

109 Costeux, S.; Wood-Adams, P.; Beigzadeh, D. *Macromolecules* **2002,** *35*, 2514-2528

110 Read, D. J.; McLeish, T. C. B. *Macromolecules* **2001,** *34*, 1928-1945.

111 Stadler, F. J. Personal Communication

112 Auhl, D.; Stange, J.; Münstedt, H.; Krause, B.; Voigt, D.; Lederer, A.; Lappan, U.; Lunkwitz, K. *Macromolecules* **2004,** *37*, 9465-9472

113 Gabriel, C.; Kokko, E.; Löfgren, B.; Seppälä, J.; Münstedt, H. *Polymer* **2002,** *43*, 6383-6390

114 Seppälä, J.; Kokko, E;. Malmberg, A.; Löfgren, B. *Polymer* **2003,** *226*, U382-U382.

115 Laun, H. M. *Progress in Colloid Polymer Science* **1987,** *75*, 111-139

116 Rojo, E.; Munoz, M. E.; Santamaria, A.; Pena, B. *Macromolecular Rapid Communications* **2004,** *25*, 1314-1318

117 Hingmann, R. B.; Marczinke, L. *Journal of Rheology* **1994,** *38*, 573-587

118 Reger, D. L.; Mahtab, R. J.; Baxter, C.; Lebioda, L. *Inorg. Chem.* **1986**, *25*, 2046-2048

119 Lee, H.; Jordan, R. F. *J. Am. Chem. Soc.* **2005**, *127*, 9384-9385

120 Michiue, K.; Jordan, R. F. *Organometallics* **2004**, *23*, 460-470

121 Michiue, K.;Jordan, R. F. *Organometallics* **2003**, *23*, 9707-9709

122 Murtuza, S.; Casagrande, O. L. Jr.; Jordan, R. F. *Organometallics* **2002**, 21, 1882-1890

123 Galland, G. B.; Mauler, R. S.; Demenezes, S. C.; Qiijada, R. *Polymer Bulletin* **1995**, *34*, 599-604

124 Galland, G. B.; de Souza R.F.; Mauler, R. S.; Nunes F. F. *Macromolecules* **1999**, *32*, 1620-1625

125 Arikan, B.; Stadler, F. J.; Kaschta, J.; Münstedt, H.; Kaminsky, W. *Macromolecular Rapid Communications* **2007,** *28*, 1472-1478

126 Fetters, L. J.; Lohse, D. J.; Colby, R. H. Chain Dimensions and Entanglement Spacings. In *Physical Properties of Polymers, 2nd Ed.*, Mark, J. E., Ed. Springer: Heidelberg, **2007**

127 Nakazawa, H. *Journal of Molecular Catalysis A: Chemical 132* **1998**, 33-41

128 Wang, H.; Yi-Chun Chen, T.; Shu-Hua Chan, M.L.; Tsai, S. M. US Patent 5519099, **1996**

10 APPENDIX

10.1 Dispose of Chemicals

All the chemicals used in this work are listed in table 10. They were disposed carefully according to their classification in the appropriate containers.

Table 10   Hazardous chemicals used in work and their security data.

Chemical Substance	Classification	Risk Phrases	Safety Phrases
Acetone	Xi, F	11-36-66-67	9-16-26
Decalin	Xn	47-20/22/38/40/48	43-36/37
Ethanol	F	11	7-16
Ethylene	F^+	12	9-16-33
Hexachloro butadien	T	21-25-40	36/37/29-45
iso-propanole	F	11	7-16
Methylaluminoxan	F, C, Xn	14/15-17-35	16-23-30-36-43
Hydrogen chloride	C	35-37	7/9-26-44
Toluene	F, Xn	47-11-20	53-16-25-29-33
Propylene	F	13	9-16-33
Acetone	F	11	9-16-23-33
Decaline	Xn	47-20/22/38/40/48	43-36/37
Hydrogen	F^+	12	2-9-16-33
1,2,3-trichlorobenzene	Xn, N	22-38-50/53	2-23-37/39-60-61
n-butyllithium	F, C, N	14/15-17-34-48/20-62	6.1-26-33-36/37/39-45
zirconium tetrachloride	C	14-20-/21/22-34	26-36/37/38-45
THF	F, Xi	11-19-36/37	16-29-33
Chloroform	Xn	22-38-40-48/20/22	36/37
1-Hexene	F	11	9-16-23.2-29-33
n-Hexane	F, Xn, N	11-38-48/20-51/53-62-65-67	9-16-29-33-36/37-61-62
Dichlormethane	Xn	40	23.2-24/25-36/37
Vinyl Chloride	T, F^+	13-20-21-22-45	9-16-44-53

10.2 Publications

Papers

1.   Arikan, B.; Kaminsky, W. *Designed Monomers and Polymers* **2005**, *8* (6), 589-600

2.   Kiesewetter, J.; Arikan, B.; Kaminsky, W. *Polymer* **2006**, *47*, 3302-3314.

3.   Arikan, B.; Stadler, J. F.; Kaschta*,* J.; Münstedt, H.; Kaminsky W. *MRC* **2007,** *28,* 1472-1478.

Posters

S. Rulhoff; C. Piel; B. Arikan; W. Kaminsky; *Short and Long Chain Branched Polyolefins of Defined Microstructure by Metallocene/MAO catalysts*; Makromolekulares Kolloquium, Freiburg, Germany; **2005**.

C. Piel; S. Rulhoff; B. Arikan; W. Kaminsky; *Definiert langkettenverzweigte Polyolefine durch Copolymerisation mit Metallocen Katalysatoren*; Hamburger Makromolekulares Symposium, Hamburg, Germany; **2005**.

Presentations

W. Kaminsky, B. Arikan, S. Rulhoff; *Tailored long chain branched polyolefins by metallocene catalysis*, 1st European Chemistry Congress, Budapest, Hungary, **2006.**

Acknowledgements

This work was carried out in the period of May 2005 to January 2008 in the research group of Prof. Dr. Walter Kaminsky at the Institute of Technical and Macromolecular Chemistry of the Hamburg University.

I am deeply thankful to my advisor, Prof. Dr. Walter Kaminsky not only for giving me the interesting topic but also for the continuing encouragement and freedom during the preparation of this thesis and my enrolment at the Hamburg University as well. I am also grateful to my whole work group for giving me their scientific help, enthusiasm and friendship. Special thanks to Stefanie Derlin, Andreas Funck, Dr. Ignacio Javier Nuñez Zorriqueta, Dr. Matthias Donner, and Dr. Sascha Rulhoff not only working together in the lab but also their friendship during this work. Mr. Horbaschk for giving me unforgettable life experiences during my time in the lab. Particularly, Andreas Funck for helping me in this thesis.

I also want to thank Prof. Dr. R. F. Jordan for accepting me in his group at University of Chicago and giving me an opportunity to broaden my knowledge in chemistry.

Of course, I'd like to thank Dr. Florian J. Stadler Dr. Jochen Kaschta and Prof. Dr. H. Münstedt for the measurements and for our great cooperation. Especially, Dr. Florian J. Stadler for helping me to correct this thesis as well.

I must express my deeply thankful to Matt Conley for his enormous support and endless patience for the correction of this thesis no matter how far we are apart. And finally, my parents and my sisters for always believing in me.

Curriculum Vitae

■ Personal Information

Name: Burçak Arıkan

Date of birth: 27.08.1979

Marital status: Single

Gender: Female

Nationality: Turkish

■ Education and Training

05/2005 – 01/2008	Ph.D. Thesis in Chemistry
	Degree thesis: "Synthesis of long/short chain branched polyolefins with defined structure by metallocene/MAO system"
	Research group of Prof. Dr. W. Kaminsky,
	Institute of Technical and Macromolecular Chemistry, Hamburg
05/2005 - 12/2006	**Project** with the research group of Prof. Dr. H. Münstedt,
	Friedrich-Alexander-University Erlangen, Nürnberg
01/2007 – 07/2007	**Project** with the research group of Prof. Dr. R. F. Jordan
	Department of Chemistry, University of Chicago, USA
11/2001 - 03/2005	"Diplom" degree in Chemistry (equivalent of Master of Science)
11/2001 - 07/2004	**Studies of Chemistry**, University of Hamburg
09/1997 - 06/2001	**Bachelor Degrees in Chemistry**
	Middle East Technical University, Ankara, Turkey
09/1993 - 06/1996	Atakent High School, Izmir, Turkey

■ Scholarship

10/2005 – 10/2007	PhD Grant of University of Hamburg based on the Hamburg Law of Funding for Young Academics and Artists
11/2001- 04/2005	Scholarship of International Centre of Graduate Study (ICGS) University of Hamburg
08/2003 - 08/2004	One year scholarship for outstanding international students "Leistungsstipendium für ausländische Studenten Abteilung Internationale Betreuung und Förderung" University of Hamburg

■ Work Experiences

05/2005 onwards	**Research Assistant** in research group of Prof. Dr. W. Kaminsky Responsible for the NMR measurements (Bruker Ultrashield 400)
12/2002 - 09/2003	**Student Assistant** in research group of Prof. Dr. H.-U. Moritz Institute of Technical and Macromolecular Chemistry, Hamburg
04/2002 - 09/2002	**Student Assistant** in research group of Prof. Dr. S. Förster Institute of Technical and Macromolecular Chemistry, Hamburg
07/2000 - 09/2000	Internship, Henkel KGaA, Izmir, Turkey

■ Personal Skills

Languages	Turkish - Native speaker
	English - Fluent
	German - Good
Computer skills	MS Office, Corel Draw, Adobe Photoshop
	CAS SciFinder Scholar 2004 (Chemical Abstracts Database)

Declaration

I declare to have developed the results presented in this thesis myself, and with the help of no other than the cited references and resources.

This work has not been presented to any inspecting authority in the same or a similar form before.

Burçak Arıkan

Erklärung

Der Verfasser erklärt, die vorliegende Arbeit selbständig und ohne fremde Hilfe verfasst zu haben. Andere als die angegebenen Hilfsmittel und Quellen wurden nicht benutzt und die benutzten wörtlich oder inhaltlich entnommen Stellen sind als solche kenntlich gemacht.

Diese Arbeit hat in gleicher oder ähnlicher Form noch keiner Prüfungsbehörde vorgelegen.

Burçak Arıkan